Avian wing morphology: intra- and inter- specific effects on take-off performance and muscle function in controlling wing shape over the course of the wing stroke.

Laura Ann McFarlane

Submitted in accordance with the requirements for the degree of

Doctor of Philosophy

The University of Leeds

Faculty of Biological Sciences

School of Biomedical Sciences

September 2014

Intellectual property statements

The candidate confirms that the work submitted is her own and that appropriate credit has been given where reference has been made to the work of others.

Declaration

Collaboration and assistance has been involved within this thesis. Marion Kaufmann filmed, determined the x, y and z coordinates and calculated some of the wing beat kinematic variables for thirty one out of the one hundred and eighty nine birds used in chapter 4. The raw electromyography (EMG) and sonomicrometry data required to determine the; cycle duration, cycle frequency, EMG duration, phase duration and muscle strain, were provided by Dr. Angela Berg Robertson (University of Houston) and Prof. Andrew Biewener (Harvard University) (Chapter 5). Throughout the thesis, Graham Askew as provided assistance in the initial set-up, muscle dissections, Testpoint virtual instruments, and Mathcad files which were modified and used.

Acknowledgements

I would firstly like to thank my supervisor, Dr Graham Askew, for his support, advice, encouragement and humour, throughout my PhD. Prof. John Altringham also provided constructive criticism and good advice on chapters 3 and 4. The catching of the majority of the birds used in this thesis would not have been possible without Chris Wright, and I'd also like to thank him for his enthusiasm, knowledge and for giving up his time, as well as for allowing me to pursue my interest in birds and introducing me to the BTO ringing scheme. Thanks also to all the other BTO ringers who have provided birds for me to film and photograph.

During my PhD I have been lucky enough to meet some great people and new friends. My lab group, past and present, have provided support and stimulating discussions on work and non-work relating topics! They have made the lab a really enjoyable place to be, so thank you! I have also made some great friends outside of the lab, on the Edge football pitch and in Miall and Manton social spaces. We have enjoyed many lunches and "Fav Friday's" together, so thanks for keeping me sane during the trials and tribulations of my PhD!

Thanks to Mr Reilly for telling me I could do physics and Mr and Mrs Griffiths for changing my career path to biology. Finally, thanks mum for your support and I hope you'd have been proud dad.

Abstract

Take-off is how a bird initiates flight and is important for predator evasion and therefore survival. A birds' take-off ability is affected by the mechanical power available from the flight muscles, the size and shape of the wings, the mechanical control of the wings and therefore the wing beat kinematics, and the body weight that needs to be supported. How a birds' body weight, size, shape and dynamic motions of their wings interact with the air flow during flight, will determine flight performance and trade-offs in wing morphology are likely due to different morphologies being optimal for different types of flight, impacting on the ecology and behaviour of birds.

Understanding the power required to overcome drag and support an animals' body weight during flight is only one side of the flight equation. The mechanical performance of the flight muscles determine the power available for creating thrust and lift, by powering the wing stroke, as well as controlling the shape and the postural position of the wings. The mechanical work and power output has been found to vary with flight speed when studying the main depressor and pronator muscle, the pectoralis. However, the mechanical performance in terms of work and power production, and therefore the mechanical function, is not known for the intrinsic wing muscles. The shape and position of the wings during the wing beat are determined by the muscles of the wing, affecting the wing beat kinematics and flight performance. Whether the mechanical function of the wing muscles varies with flight type is also unknown.

Determining the aerodynamic power required and the muscular power available for different types of flight, were examined separately. The effects of intra- and interspecific variation in wing morphology and wing beat kinematics on take-off performance were examined. Two high-speed digital cameras were used to track the position of a birds' centre of mass and wing positions spatially and temporally as they took off to determine flight velocities, accelerations and wing beat kinematics so as to calculate the aerodynamic power required. The relationship between the power used to increase the rate of the potential and kinetic energy of a birds' bodies' centre of mass and the birds' wing morphology and wing beat kinematics were tested. The effects of phylogeny were included in inter-specific comparisons. The mechanical function of

two intrinsic wing muscles; the biceps brachii and the scapulotriceps, were investigated *in vitro* using the work-loop technique. The muscles were stimulated with strain and activity patterns that had previously been measured *in vivo* during take-off, level and landing flight. This meant that the mechanical work and power output, and therefore the muscle function, could be determined. Whether the biceps and scapulotriceps mechanical function varied relative to flight mode was also investigated.

Body mass did not influence take-off performance intra-specifically but some wing morphological and kinematic traits did scale isometrically inter-specifically. However, when examining take-off performance both within and between species; large, broad wings favoured improved take-off ability by reducing the power needed to generate lift. Short wings were also beneficial as this correlated with higher wing beat frequencies which improved take-off. Larger species had lower induced power requirements than expected for their size and therefore could devote more energy to moving their body's centre of mass. Even when differences due to phylogeny were accounted for, wing morphology was important for take-off performance and affected the wing beat kinematics, altering the aerodynamic forces generated and loads acting upon the wings, impacting on take-off performance.

The biceps brachii and scapulotriceps co-contract and are involved in the postural position of the elbow, flexing and extending the elbow respectively during muscle shortening and therefore affecting the wing shape during the wing beat cycle. Both muscles also act as elbow stabilisers and decelerators during active lengthening of the muscles, doing negative work. Net work is near zero for the biceps and positive for the scapulotriceps. The work done by the biceps is less than the work done onto the scapulortriceps, suggesting the involvement of other muscles or wing inertia in providing the energy recovered by the scapulotriceps when lengthening. The mechanical power output of these muscles is stereotypical, regardless of mode of flight.

1 Table of contents

Table of figures

Chapter 1

Chapter 2

Chapter 3

Chapter 4

Chapter 5

List of tables

Chapter 3

Chapter 4

Chapter 5

List of abbreviations

AR	aspect ratio
b	total wing span
c, d, e	x, y, z coordinates of the wing root
$C_{D,\,par}$	parasite drag coefficient of the body
$C_{D,\,pro}$	profile drag coefficient of the wing
CoM	centre of mass of the body
$D\%$	Relative downstroke duration
$E_{K,\,ext}$	kinetic energy of the CoM
EMG	electromyography
E_P	potential energy of the CoM
f	Wing beat frequency
g	gravitational acceleration
h, i, j	x, y, z coordinates of the wing tip
k	induced velocity correction factor
L	muscle length
L_m	muscle mean length
L_{max}, L_{min}	maximum and minimum muscle length

L_0	muscle operating length
L_R	muscle resting length
l_w	length of one wing
M_b	body mass
$M_b g$	body weight
M_m	muscle mass
P_{aero}	total aerodynamic power
P_{CoM}	take-off power to change the potential and kinetic energy of the body's CoM
P_{E_P}	power to change the potential energy of the body's CoM
P_{ind}	induced power
$P_{ind'}$	induced power required to create the induced velocity
P_{mech}	muscle-mass specific mechanical power
$P_{E_{K,ext}}$	power to change the kinetic energy of the body's CoM
P_{par}	parasite power
P_{pro}	profile power
rWL	relative wing loading
S	total wing area
S_b	body frontal area
S_w	area of one wing

$S\%$	relative downstroke duration
t	time
$t_{relax_{90}}$	time taken for isometric peak force to reduce by 90%
$\Delta\, t$	difference in time
v	velocity of the CoM
v_{max} , v_{min}	maximum and minimum v of the CoM
V_R	resultant velocity of the air passing over the wings
w	induced velocity
WL	wing loading
x, y, z	coordinates describing the three-dimensional position of the bird
$\dot{x}, \dot{y}, \dot{z}$	v of the CoM in the x, y and z directions, respectively
$\ddot{z}$	vertical acceleration of the CoM
ρ	air density
θ	angle of elevation
β	stroke plane angle
Φ	wing beat amplitude

1 General Introduction

1.1 Flight aerodynamics

To be able to fly, the wings of an organism need to generate lift so as to support their body weight, and thrust to oppose drag forces (Norberg, 1990; Pennycuick, 2008; Rayner, 1994). To create lift, birds, insects and bats have asymmetric wing profiles with a convex upper surface, so that there is a pressure difference above and below the wing (Altringham, 1996; Norberg, 2002). How lift forms is explained by the Bernoulli Principle, the velocity of the air that flows over the wing is greater than that flowing below the wing (Norberg, 2002). The force that follows the direction of the air flow is the drag and the force that acts at a right angle to this is the lift (Figure 1-1 A and B). The shape of the wing therefore creates the pressure differences required to generate the lift, drag and net aerodynamic force (Altringham, 1996; Norberg, 1990) (Figure 1-1). The relative size and importance of these forces depends on the shape of a wing, the angle at which air is forced downwards, circulation of the vortex that is bound to the wing, and the Reynolds number that describes the inertial and viscous forces relative to each other that act along the mean wing chord (wing area relative to wing span) (Pennycuick, 2008; Norberg, 1990). A bound vortex is formed due to the pressure difference between the upper and lower surface of a wing. As the pressure difference reduces towards the wingtips, some of the air will flow upwards joining the air flowing above the wing due to the higher air pressure below the wing as opposed to above (Norberg, 1990).

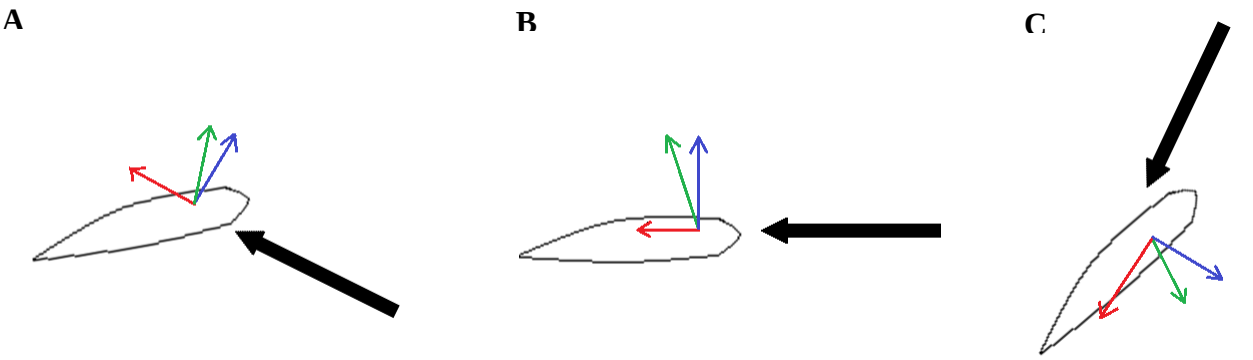

Figure 1-1 *Force relative to resultant velocity at the wing during a wing stroke. The resultant air velocity (bold arrow), lift (blue arrow), drag (red arrow) and net aerodynamic force (green arrow). Drag force is at approximately perpendicular to the lift force. (A) Early downstroke when the resultant velocity (V_R) meets the wing at the lower surface, resulting in a slightly forward directed lift and net aerodynamic force. (B) Mid downstroke when the V_R is horizontal relative to the leading edge of the wing. Lift is at a right angle to the V_R and the net aerodynamic force is directed slightly backwards. (C) Upstroke when the V_R meets the wing at the upper surface, resulting in negative lift and a downwards directed net aerodynamic force. Figure adapted from Norberg (1990).*

Volant organisms flap their wings to generate the aerodynamic forces required to stay airborne and move through the air, but power is needed to create the lift and thrust forces required to oppose gravity and drag. The aerodynamic force that can be generated during flapping flight is dependent on the resultant velocity of the wings (Askew et al., 2001; Ellington, 1984b) which reflects the flapping velocity and the induced velocity (Ellington, 1984b). The stroke plane angle, wing beat amplitude, wing beat frequency and the proportion of the wing stroke that is downstroke (Askew et al., 2001; Ellington, 1984a; Ellington, 1984b; Norberg, 1990) determine the resultant velocity so variation in wing beat kinematics can affect aerodynamic force and therefore flight power requirements. The stroke plane angle is the angular path of the wing tips relative to the horizontal whereas the wing beat amplitude describes the total angle swept by the wings during a wing beat (Norberg, 1990). The dynamic motion of the wings varies with flight speed during a wing stroke so as to maintain the optimal angle of attack, reduce wing area and therefore drag during the upstroke, and accelerate and increase the wing area during the downstroke (Norberg, 1990). The rotation of the wings at the shoulder, elbow and wrist during flapping flight can alter the flapping velocity, wing area, position relative to the body and the air flow, and therefore the lift to drag ratio. During the downstroke the net aerodynamic force is directed upwards and slightly backwards relative to flight direction, whereas during upstroke the net aerodynamic force is directed upwards and slightly forward. Therefore, the wing area needs to be reduced during the upstroke so that the force generated is not cancelled out by the net

direction of force created during the downstroke. These motions are likely controlled by the physiology and functioning of the wing musculature.

The resultant air flow varies in a chordwise direction along the wing and during different phases of the wing stroke and therefore the lift and thrust that can be generated, and the profile drag force that needs to be overcome (Ellington, 1984b), will vary dependent on wing beat phase (Norberg, 1990). During the downstroke (Figure 1-1 A and B), flapping velocity is greatest at the wing tips so the resultant velocity is directed behind the wings with lift being directed upwards and slightly forward, resulting in a forward thrust force (Figure 1-1B) (Norberg, 1990). The inner wing has a lower flapping velocity due to being closer to the wing root, and therefore the resultant velocity is either horizontal or slight below the leading edge of the wing resulting in a forward directed lift and drag force (Norberg, 1990). The lift and drag generated are therefore proportional to velocity^2 (Norberg, 1990) and the direction and size of the aerodynamic forces generated will depend on where the resultant velocity meets the wing (Figure 1-1). During the upstroke (Figure 1-1C) the resultant velocity is directed from above the wing due to the direction of the flapping velocity and therefore the lift force is downwards and can be described as negative lift (Norberg, 1990). Varying the wing beat kinematics so that the flapping velocity is nearer the horizontal during the upstroke, changing the stroke plane angle for example (Ellington, 1984a), will reduce the negative lift generated. Variation in the proportion of the wing stroke spent in downstroke relative to the upstroke can also affect the lift generated as greater downstroke ratio can increase the lift and thrust created, resulting in positive net lift.

1.1.1 *Aerodynamic power*

The induced power (P_{ind}) is the power needed to do muscular work to create a downwash, transferring kinetic energy by imparting a downward velocity onto the air, with this velocity termed as the induced velocity (w) (Askew et al., 2001; Pennycuick, 2008). Air needs to be forced downwards by the wings to create force to balance body weight and accelerate, transferring kinetic and potential energy to the centre of mass of the body so an organism is able

accelerate and climb (Askew et al., 2001). The rate at which energy is transferred to work is the induced power requirement (Usherwood et al., 2003). The profile power is the power required to overcome the drag of the wings as air flows over them and also due to the drag created by the flapping motion (Askew et al., 2001; Pennycuick, 2008). The parasite power is the power required to overcome the drag acting on the body (Pennycuick, 2008).

The original models used to estimate the power required to fly were derived from the aeronautics of fixed wing aircraft where a steady flow regime over the wings is assumed (Norberg, 2002). The P_{ind} is inversely related (Figure 1-2) to the flight velocity due to the minimal airflow over the wings (Pennycuick, 2008) so power is required from the flight muscles to flap the wings and generate the induced velocity. For forward flight at high flight velocities the Rankine-Froude momentum-jet theory can provide a reasonable estimate of the induced drag and is based on rotary wings of a helicopter (Norberg, 1990). Wings are swept over an area termed the actuator disc, forcing air downwards with an induced velocity that does not vary over the disc area (Norberg, 1990). The area of this "jet" below the wings reduces as it moves downwards creating the required pressure gradient (Norberg, 1990) to generate lift which is described by the Bernoulli Principle (see section 1.1.1). It is however unlikely that the w does not change over the actuator disc area so Ellington modified the classical actuator disc theory to account for this by multiplying the w by a correction factor (k) (Askew et al., 2001; Ellington, 1984b). This correction factor accounts for the circulation and periodicity of the wake, created by the flapping of the wings (Ellington, 1984b). The k usually used is based on values from the aeronautical industry as the actuator disc models used to determine k for helicopter rotors are what the bird flight literature have based their k values on, ranging from 1.1 for gliding flight to 1.3 for flapping flight where the aspect ratio of the model wing used was 6 (Spedding and McArthur, 2010). A k of 1.2 is equivalent to a span efficiency of 0.83 and values of k ranging from 1.12 to 1.2 are thought to be a good estimate as bird and bat wings are likely to be better able than model wings of similar Reynolds numbers at controlling the separation of the vortex from the boundary layer (Spedding and McArthur, 2010).

The parasite power (P_{par}) is the power required to overcome body drag and can be calculated if the body's frontal area and air density are known and a body drag coefficient is applied (Askew et al., 2001; Pennycuick et al., 1989). This drag coefficient relates to how streamlined the volant organism is and can vary depending on the species being examined (Askew and Ellerby, 2007). The profile power (P_{pro}) is the power required to overcome the drag of the wings and is determined from the air density, wing area, the resultant velocity that incorporates the induced, flapping and flight velocity, and a profile drag coefficient (Askew et al., 2001). Both P_{pro} and P_{par} show the opposite relationship between power required and flight speed to that seen for P_{ind}, as the requirement for both increases with flight velocity (Figure 1-2) due to the higher drag force as the air flow over the wings and body is greater (Rayner, 1999). Models that estimate the aerodynamic power requirement of flight can vary not just with flight speed but will also depend on the drag coefficient values. This can lead to disparities between indirect measures of the power needed for flight and direct measures such as the use of deltopectoral crest strain gauges to determine force (Biewener, 1998; Biewener et al., 1992; Dial and Biewener, 1993; Dial et al., 1997; Williamson et al., 2001), flow visualisation of the wake using particle image velocimetry methods (Muijres et al., 2011; Provini et al., 2012; Tian et al., 2006). It is therefore important to consider the values of the drag coefficient used as they influence the amount of power required to overcome the profile and parasite drag, and can also vary the relative contribution of P_{pro} and P_{par} to P_{aero}. At high flight speeds when the P_{pro} and P_{par} requirements are expected to be high, the value of the drag coefficients could lead to large over or under estimates. There have been some doubts raised by the low values often for used for $C_{D,pro}$ which assume a minimal or zero lift-drag coefficient (Rayner, 1979; Usherwood, 2009a). (Usherwood, 2009a) However, in flight birds wings are deformable and efficient aerofoils maintaining the optimal near-zero lift-drag coefficient (Rayner, 1979).

The total power required is the a combination of the total drag acting upon the animal and the resultant air velocity, which constitutes the forward, wing flapping and induced (see above) velocities experienced by the flier (Norberg, 1990). To determine the total aerodynamic power (P_{aero}) needed, the P_{ind}, P_{pro} and P_{par} drags need to be overcome by generating power. When

calculating the different power components it is important to consider flight velocity as air flows are often unsteady at slow speeds due to the prominent contribution of the wing flapping velocity to the resultant air velocity. The flight power-velocity curve is distinctly U-shaped (Askew and Ellerby, 2007; Morris and Askew, 2010a; Pennycuick, 2008; Rayner, 1979; Tobalske et al., 2010) in most instances (but see Chai et al., 1999; Dial et al., 1997) due to the differing relationships of induced, profile and parasite power with flight velocity (Figure 1-2).

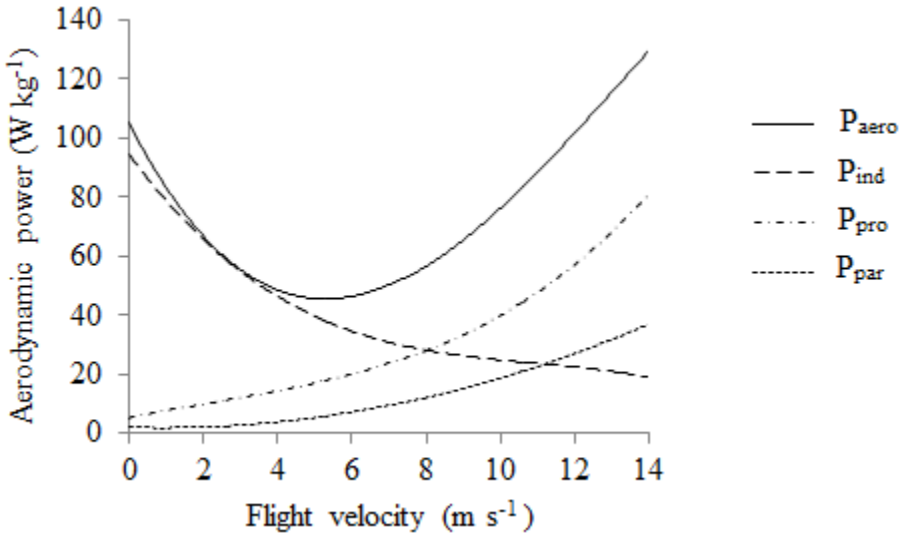

Figure 1-2 *Power curves showing the relationships between the power required and flight velocity. The total aerodynamic power requirement ($\boldsymbol{P_{aero}}$) is from zebra finches and is adapted from (Askew and Ellerby, 2007). The hypothetical relationships between induced ($\boldsymbol{P_{ind}}$), profile ($\boldsymbol{P_{pro}}$) and parasite ($\boldsymbol{P_{par}}$) power and flight velocity are also shown (Ellington, 1991).*

1.2 Wing morphology and flight performance

Wing shape and motions affect the instantaneous aerodynamic forces during a wing stroke (Hedenstrom, 2002), so to understand the aerodynamic requirements of flight the wing

morphology and wing beat kinematics need to be considered. Wing area is proportional to the amount of lift that can be generated (Norberg, 1990) so wings of a low wing loading; ratio of wing area to body weight, can produce more lift and reduce the P_{ind} requirement. During slow flight the P_{ind} requirement is high (Figure 1-2) so for species that regularly fly slowly, such as those that manoeuvre through cluttered habitats, natural selection is likely to favour large wing areas of low wing loading. It has been shown in Phylloscopus warblers in Siberia that warblers of low wing loading tended to forage near the ground in highly vegetated habitats (Forstmeier and Kessler, 2001). The turning radius also depends on the wing loading for a given lift coefficient and angle of the turn (Norberg, 1990), with lower wing loading reducing the turn radius and improving manoeuvrability. Take-off ability is also likely affected by wing loading due to slow initial flight velocity and therefore maximising lift and reducing the P_{ind} requirement will provide a selection pressure for low wing loading in species that regularly engage in take-off, such as perch and wait foragers (Norberg, 1990). However, for fast flight the profile drag is likely to dominate the flight requirement so low wing loading is no longer an advantage and may increase the profile drag as this is proportional to wing area (Pennycuick, 2008).

The size and shape of the wing is not just defined by the wing area but is also dependent on the wing span. Aspect ratio; ratio of wing span to wing area, and wings with a large wing span relative to their wing area have a high aspect ratio. Span efficiency should increase with higher aspect ratio (Pennycuick, 2008) and the induced power required to create the *w* should also be lower (Norberg, 1990; Warrick, 1998). Selection has acted on many species that fly long distances to have high aspect ratio wings to reduce the cost of flight by reducing the P_{ind} requirement (Norberg, 1990). Iberian blackcaps (*Sylvia atricapilla*) vary from North to South in terms of how long, narrow and pointed their wings are as Northern blackcaps are more migratory than their Southern con-specifics so selection has favoured longer wings (Telleria and Carbonell, 1999). For short bouts of flight activity, it has been shown in grouse that low aspect ratio wings can be accelerated faster improving vertical, burst take-off performance (Norberg, 1990). Reduced wing inertia and higher lift generation can also be associated with low aspect ratio (Warrick, 1998). Short, broad wings of large wing area and low span, low wing loading and

aspect ratio, is favoured in vegetated habitats where take-off is followed by short bursts of slow, manoeuvrable flight (Norberg, 1990). The link between ecology, flight style and wing morphology is clearly seen in both birds and in bats (Brewer and Hertel, 2007; Emrich et al., 2013; Marchetti et al., 1995; Norberg and Rayner, 1987; Vanhooydonck et al., 2009; Winkler and Preleuthner, 1999; Zhang et al., 2007). Norberg and Rayner (1987) demonstrated the close relationship between wing morphology and foraging habitat by studying the aspect ratio and wing loading of a number of bat species from varying foraging niches. They demonstrated ecological convergence in wing morphology relative to habitat choice and the related flight requirements (Norberg and Rayner, 1987).

1.2.1 *Intra-specific variation in wing morphology*

Wing morphology can vary intra-specifically due to differences between adults and juveniles (Fernandez and Lank, 2007; Heers et al., 2011; Perez-Tris and Telleria, 2001), males and females (Kullberg et al., 2002), or seasonally due to changes in body mass or wing area due to moult. In some passerines juveniles have been found to have shorter, broader wings which may improve their manoeuvrability and take-off ability, increasing their chances of surviving predation as their predation risk is likely to be higher due to their inexperience (Fernandez and Lank, 2007; Perez-Tris and Telleria, 2001). Differences in wing morphology due to age were not observed in migratory species possibly due to the trade-off that is likely to exist between optimising a wing morphology favourable for manoeuvrability compared to a morphology for flight efficiency (Perez-Tris and Telleria, 2001) as the former selects for short, broad wings whereas the latter selects for long, narrow wings. Males and females can vary in wing morphology due to the effect of increased body mass in gravid females increasing their wing loading (Kullberg et al., 2002; Lee et al., 1996), or due to differences in migratory distance (Nam et al., 2011; Perez-Tris and Telleria, 2001) or the need for males to be more manoeuvrable for sexual displays and territorial interactions (Fernandez and Lank, 2007). Sexual differences will often vary depending on the season as the importance of defending territories, sexual displays and changes in body mass in pregnant females, all relate to the breeding season.

Wing loading can increase due to increases in body mass and/or as a result of reduction in wing area. Prior to migration an individual will deposit more fat to be used as fuel during migration (Bednekoff and Houston, 1994) and this added body weight could affect flight performance as a higher body weight will require more lift to be generated and may increase the parasite drag and induced requirement. It has been shown in a sub-species of red knots (*Calidris canutus islandica*) that as body mass increases due to fuel loading prior to migration, the bird reduces pectoral mass which detrimentally affects manoeuvrability but reduces some of the cost of carrying a heavy load when migrating (Dietz et al., 2007). Increases in body mass are not always reflected by an increase in wing loading as the replacement of old feathers with new feathers during moult can improve performance by increasing wing length and improving feather efficiency, improving the transfer of momentum to the wake (Hedenstrom, 2003). The velocity of the air at the wing tips is also greater in more developed feathers (Heers et al., 2011).

Feather replacement can lead to gaps in the wing (Hedenstrom and Sunada, 1999; Lind, 2001; van den Hout et al., 2010) and reduction in wing area which can be reflected by an increase in wing loading (Chai et al., 1999; Hedenstrom, 2003; Senar et al., 2002b). The effect of gaps in the wing on performance is dependent on where the gaps are and whether they effect the distribution of lift (Hedenström, 1998). It has been suggested that central gaps in the wing are more detrimental to circulation of the bound vortex and lift generation than gaps at the wing tip, and that loss of feathers at the wing tips could even make the distribution of lift more elliptical and improve performance (Hedenstrom and Sunada, 1999). However, reduction in wing span decreases flight efficiency and therefore the importance of moult at the wing tips will depend on the need for economical flight. Reduction in wing area can actually increase aspect ratio if the wing span is unaffected. Studies have not always found a detrimental effect of moult on flight performance (Hedenstrom, 2003) which may be due to physiological or behavioural strategies used to compensate for reduction in wing area, as well as the benefits of feather renewal (Hedenstrom, 2003). Starlings (*Sturnus vulgaris*) (Swaddle and Witter, 1997), ruby-throated hummingbirds (*Archilochus colubris*) (Chai et al., 1999) and tree sparrows (*Passer montanus*) (Lind 2001), reduce their body mass without reducing their pectoral muscle mass during moult so as maintain flight performance. A reduction in body mass can also decrease wing loading

(Zimmer et al., 2010) and therefore lift generation. Williams and Swaddle (2003) also found that the starling altered its' wing beat kinematics as well as their wing shape during moult, increasing wing beat amplitude and deforming their wings to vary the angle of attack to improve lift generation.

1.2.2 *Wing morphology and wing beat kinematics*

An individual or species may be able to vary their wing beat kinematics (Crandell and Tobalske, 2011) within a narrow range (Pennycuick, 2008) so as to meet the differing flight power requirements. Variation in wing beat kinematics is likely to reflect differences in wing morphology. A long wing of high aspect ratio will have an increased moment of inertia reducing the wing acceleration that can be generated, and therefore a lower wing beat frequency (Warrick 1998). The area that can be swept out by a wing is also likely dependent on wing area and wing span and this may be reflected in the wing beat amplitude and stroke plane angle used by a bird during flight. Berg and Biewener (2008), found that pigeons varied their stroke plane angle during take-off and hypothesised that pigeons were forcing more air downwards and backwards to increase lift and thrust. The ability to change their body angle and consequently their stroke plane angle may improve take-off performance without needing to vary flight muscle mechanics (Biewener, 2011). Wing beat amplitude, frequency and proportion of the stroke dedicated to the downstroke, have all been suggested as potential mechanisms to improve take-off ability. Higher wing beat frequency and amplitude may increase lift generation (Askew et al., 2001; Hedenstrom, 2003; Williams and Swaddle, 2003), but may also point to variation in flight muscle mechanics by indicating higher muscle cycle frequencies and strain amplitudes respectively (Ellerby and Askew, 2007; Pennycuick, 2001; Robertson and Biewener, 2012), changing the amount of mechanical power that is available. Wing beat frequency is expected to scale with body mass as larger birds are predicted to have lower wing beat frequencies (Jackson and Dial, 2011; Pennycuick, 2008). It is therefore important to consider whether variation in frequency is due to geometric similarity and/or dynamic similarity (similarity in motion due to the scaling of lengths by the same factor as well as forces by a scalar) (Alexander, 2003;

Alexander, 2005), before assuming an adaptation to locomotive ability. The downstroke is the power stroke for forward flight (Norberg, 1990) so by increasing the proportion of the wing stroke in downstroke may reflects asymmetry in the strain trajectory so more of the muscle cycle may be dedicated to shortening and performing positive work. This has been observed during take-off and slow flight in some birds (Askew et al., 2001; Ellerby and Askew, 2007), and also in scallops swimming (Marsh et al., 1992) and frog vocalisations (Girgenrath and Marsh, 1997). The importance of muscle mechanics on flight performance in the context of the wing musculature will be discussed below (section 1.3).

1.3 Muscle power available

The mechanical power available from the skeletal muscles is the rate at which mechanical work is performed (Josephson, 1993) i.e. the rate at which muscles do work by shortening against a load (Josephson, 1985). The power available from the muscles acts as a constraint on locomotive performance as muscles can only produce so much power due to their physiology and structure. Mechanical work is the muscle fibre strain multiplied by average fibre operating length, relative to the force generated over time (Biewener, 2011). The strain is the ratio of muscle length change relative to the initial (resting) length (Pennycuick, 2008). The intrinsic properties of a muscle determine the power output with some skeletal muscles designed to generate high power outputs, such as are required for short, high intensity bursts of activity, compared to muscles that support sustained, lower intensity activities or contract mainly isometrically to provide postural support. The pectoralis pronates and depresses the wing during the downstroke and is responsible for providing the majority of the power required to fly by shortening over a large part of their muscle fibre length, outputting a large amount of mechanical work (Biewener, 2011). This muscle needs to be able to generate a high power output due to its role in depressing and pronating the wing and in the blue-breasted quail can produce 400 W kg^{-1} (Askew and Marsh, 2001). This compares to the fast glycolytic part of the iliofibularis, which is a hindlimb muscle, that can generate 154 W kg^{-1} at 42^{o}C during locomotion in the desert iguana (*Dipsosaurus dorsalis*) (Swoap et al., 1993). These muscles all need to be able to output high

amounts of mechanical power due to their role in demanding locomotive tasks such as flight or sprint performance. High muscle strains and being able to shorten over a large part of a muscle fibres length, therefore performing more work, can increase power output and is seen in the pectoralis (Biewener, 2011). By remaining active for longer, either during the stretch phase or during isometric contractions, the work done during the following shortening phase can be maximised (Askew and Marsh, 1998; Biewener, 2011). Active lengthening may increase mechanical work output over a cycle potentially due to the cross-bridges between fibres remaining attached for longer as active stretch holds the cross-bridges in an area of low detachment rate (Askew and Marsh, 1998). Asymmetrical length cycles can increase the mechanical power output as more of the cycle is spent short (Holt and Askew, 2012). This has been observed in mouse soleus muscle (Askew and Marsh, 1997), the pectoralis (Askew and Marsh, 2002; Ellerby and Askew, 2007), swimming scallops (Marsh et al., 1992) and frog vocalisations (Gigenrath and Marsh, 1997).

1.3.1 *Muscle power for flight*

Flight is energetically demanding and therefore muscle efficiency will limit mechanical power output over time. If the power required to meet the aerodynamic requirements exceeds that available from the flight muscles then flight will be unsustainable. The pectoralis power required for flight varies as a function of flight velocity, as has been described above (section 1.1.1; Figure 1-2). A bird that can not only maintain its position horizontally while flying at the minimum power speed (Norberg, 1990, Pennycuick, 2008) but can also continue to accelerate and climb, has a positive power margin in that not all of the available mechanical power from the flight muscles are required for basic weight support so there is additional muscle power that can be used for improving flight performance (Norberg, 1990). If it is assumed that stress and strain are invariant with body mass (Tobalske, 1996), (but see Altshuler et al., 2010b; Carr et al., 2011; Jackson and Dial, 2011), the wing beat frequency determines the upper and lower limits of the muscular power available (Pennycuick, 2008). To achieve a positive power margin then either more power needs to be made available from the muscles, recruiting anaerobic muscle for short

term activity for example, or the power requirements of the flight mode needs to be reduced. The sections above (section 1.2) describes how variation in wing morphology and wing beat kinematics can alter the power requirements of flight; primarily by increasing the lift and thrust, and reducing the drag generating capacity of the wings and body, so that less power is required from the muscles to meet the aerodynamic power requirements. The flight muscles can also modulate the power available depending on the needs of the animal, by use of: intermittent flight strategies (Ellerby and Askew, 2007; Morris and Askew, 2010b; Pennycuick, 2001; Tobalske, 1996), or by altering muscle strain trajectory (Ellerby and Askew, 2007; Girgenrath and Marsh, 1997; Morris and Askew, 2010b; Robertson and Biewener, 2012), cycle frequency (Morris and Askew, 2010b), recruiting more muscle fibres (Pennycuick, 2001; Rayner, 1994) and/or increasing the intensity of muscle activation (Dial, 1992; Robertson and Biewener, 2012).

1.3.2 *Studying mechanical function in vivo*

To determine the mechanical function of skeletal muscles, measures of muscle strain and activity can be made *in vivo*. This can include attaching strain gauges to the tendon or bone the muscle attaches to, so as to directly measure the force produced during a locomotive task (Biewener, 1998; Biewener et al., 1992; Dial and Biewener, 1993; Dial et al., 1997; Jackson and Dial, 2011; Tobalske and Biewener, 2008). In birds the strain gauges are usually attached to the dorsal surface of the delto-pectoral crest (DPC) of the proximal humerus as the main depressor muscle, the pectoralis, attaches to the ventral surface of the DPC so tensile strain applied by the muscle to the dorsal DPC is recorded (Biewener, 1998). A DPC strain gauge can only be used if the DPC shape and size makes it possible for the gauge to be attached. The insertion and action of the pectoralis on the DPC can vary inter-specifically, making it difficult to determine the forces being measured. This problem was highlighted in a study by Tobalske and Dial (2000) that attempted to attach DPC strain gauges in the ring-necked pheasant, *Phasianus colchicus*. The size and shape of the DPC made attachment difficult and the pectoralis attached nearer shaft of the humerus so pectoralis force was acting further down the bone than the DPC (Tobalske and

Dial, 2000). This was visible in recordings as both tensile and compressive strains were measured (Tobalske and Dial, 2000). Power output measured using DPC strain gauges can also vary from those measured *in vitro* (see section 1.2.2). This is likely due to how dominant the P_{ind} requirement is within the calculation as under or over estimates could account for the discrepancies seen (Askew et al., 01).

Sonomicrometry can be used to determine the strain trajectory of a muscle during locomotion or with limb kinematics so muscle strain patterns can be correlated with the motions of a limb (Askew et al., 01). Piezoelectric transmitter and receiver crystals are implanted into the muscle under study. The time it takes for the ultrasonic sound wave to pass between the transmitter and receiver crystal, together with the speed of sound within the muscle, gives the distance between the crystals and therefore, during locomotion, the length changes of the muscle can be measured (Askew et al., 01; Askew and Marsh, 2001). Knowledge of the length trajectories of a muscle allow strain and strain amplitude to be calculated. Length changes in the pectoralis (Askew and Marsh, 2001; Ellerby and Askew, 2007; Biewener et al., 1998) and supracoracoideus (Tobalske and Biewener, 2008) have been measured and can indicate the amount of power that will be output as changes in the rate of lengthening and shortening with asymmetrical strain trajectories can enhance power output if more of the cycle is spent shortening and performing positive work (Askew and Marsh, 2001).

To elucidate muscle function the activity pattern in terms of the onset, offset and magnitude of activation, need to be determined. This commonly involves the use of electromyography (EMG) where two electrodes are inserted into the muscle so as to measure muscle activity. Within birds the flight muscle activity has been examined during the wing stroke cycle by filming a bird in flight while recording muscle activity using EMG (Dial et al., 1991; Hedrick and Biewener, 2007). This has led to an understanding of which muscles are active, for how long and at what intensity during different phases of a wing stroke, whereas previously the mechanical function of flight muscles was based on anatomy and external measurements (Dial et al., 1991). When done in conjunction with sonomicrometry the electrodes are placed near the site of the crystal insertions. By combining information from sonomicrometry, EMG and limb kinematics, the

strain trajectories, muscle activation duration and intensity can be correlated with limb motion during a locomotive task and can indicate the amount of power a muscle will output (Askew and Marsh, 2001). This information can be used to hypothesise muscle function in terms of when work is being performed during a muscle cycle and locomotive task, and what effect this has on motion.

1.3.3 *Studying mechanical function in vitro*

The force produced by an active muscle during cyclical length change can be measure *in vitro* using the work loop technique (Josephson, 1985). The whole muscle, muscle fibre bundles or single muscle fibres are removed from the organism and are stimulated with the desired length change and activity pattern. If the muscle strain trajectory and activity have been measured *in vivo*, then this pattern of activation and length change can be used to stimulate the muscle *in vitro* (Askew and Ellerby, 2007). An understanding of when a muscle is active and at what intensity, as well as the strain trajectory during a muscle cycle suggests when and at what intensity work is being performed and the likely power output profile during a cycle. Without a measure of the actual forces generated and the work being done by a muscle or onto a muscle, the mechanical power output and therefore the mechanical performance can not be determined. To elucidate the function of a muscle during different locomotive tasks therefore requires the muscle activity, strain trajectory, force and mechanical work profiles to be known.

A muscle performs positive work to shorten (Figure 1-3A), whereas when a muscle is lengthened then work is done on the muscle, termed negative work (Figure 1-2B), due to the action of another muscle or external forces such as wing inertia during flapping flight. The net mechanical work is therefore the positive work minus the negative work (Figure 1-3C), The mechanical work of the muscle is determined by the area within the work loop (Figure 1-3C), and the mechanical power output is the mechanical work multiplied by the cycle frequency (Jackson and Dial, 2011; Pennycuick, 2008). This means the muscle-mass specific power available from a muscle during a locomotive activity can be calculated. A sinusoidal length change cycle is usually used when stimulating the muscle, but sawtooth cycles can be used to measure forces

generated by the muscle when it undergoes asymmetrical length changes where the proportion of the cycle spent shortening is varied (Askew and Marsh, 1997). The use of asymmetrical length trajectories have been shown in mouse soleus and extensor digitorum longus muscles to increase the mechanical power output if more of the cycle is spent shortening (Askew and Marsh, 1997). This is because power output is maximised by increasing muscle strain, operating at a cycle frequency that allows a muscle time to activate more rapidly and fully before deactivating and relaxing before the next cycle (Askew and Marsh, 1998; Josephson, 1993).

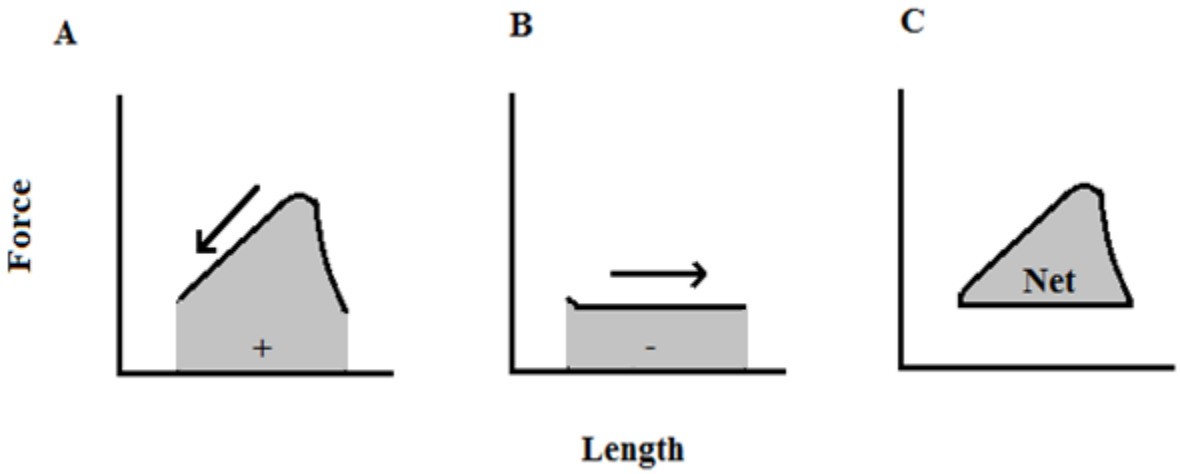

Figure 1-3 *Work-Loops. (A) the positive work (shaded area) done by a muscle to shorten, (B) the negative work (shaded area) done onto a muscle to lengthen it and (C) the net work done by a muscle (shaded area). The bold lines represent when the muscle is active and the arrows show in which direction force is produced as the muscle changes length. Figure adapted from Josephson (1985).*

1.3.4 *Wing muscle mechanics and mode of flight*

The mechanical function and power output during flight have been studied in the main pectoral muscles (see section 1.2.1) that power flapping flight and constitute between approximately 8 and 24% of a birds total body mass (Norberg, 1990). Far less is known about the mechanical

performance and functions of the intrinsic wing muscles (Robertson and Biewener, 2012; Welch and Altshuler, 2009). These muscles are likely involved in controlling the wing shape and position (Biewener, 2011; Robertson and Biewener, 2012) and therefore impact upon the lift and thrust that can be generated, and on the power that will be required to oppose induced and profile drag forces.

Research into the wing muscles have identified the activity patterns relative to the wingstroke during flight (Dial et al., 1991), and the strain trajectories and muscle activity during different modes of flight, such as take-off, mid-flight, landing (Robertson and Biewener, 2012), and manoeuvring flight (Hedrick and Biewener, 2007). An understanding of the activity patterns during the wing stroke of different intrinsic wing muscles demonstrated which muscles were associated with different wing motions (Dial et al., 1991). The addition of sonomicrometry data to muscle activity patterns within a wing stroke and across different modes of flight demonstrated the similarities and differences in muscle function relative to muscle activity and strain profile across different modes of flight and suggest when force, work and power are being output (Robertson and Biewener, 2012). There is also some information on the fibre type of some of the wing muscles in different species of bird that have varying ecologies and flight style uses (Welch and Altshuler, 2009). This has led to the suggestion that inter-specific variation in fibre composition within the wing muscles may be due to optimisation for different flight modes, with species that are predominantly gliders having slow or tonic fibres as repeated isometric twitches are required to maintain an outstretched wing posture (Welch and Altshuler, 2009).

Previous studies of intrinsic wing muscles have improved our knowledge of muscle function but have left some key questions still unanswered. Activity patterns identify onset and offset of muscle activity and this can be associated with general limb movements but do not fully explain the contribution of a muscle on controlling and moving joints (Dial et al., 1991). The force profile is required as this indicates muscle kinetics in terms of how long it takes force to develop and to decay (Dial et al., 1991). Measurements of strain trajectory indicate when work is being performed and in combination with muscle activity the timing of force development can be estimated (Robertson and Biewener, 2012). However, without analysis of the force produced

and the mechanical work done by these muscles during different locomotive tasks it is difficult to elucidate muscle function and whether function is stereotypical across flight types or varies relative to the task being performed. The net mechanical power output of the muscles is indicative of muscle performance and suggests whether a muscle is functioning primarily to generate the high power required for demanding tasks, such as wing depression and pronation by the pectoralis, or if power output is mimimal this may suggest the role of the muscle is primarily control of shape and posture.

1.4 Summary

This thesis examines the aerodynamic requirements of take-off flight both intra- (chapter 3) and inter-specifically (chapter 4) so as to address how variation in wing morphology can affect take-off performance. The effect of intra-specific variation in wing morphology due to seasonal changes in body mass and wing area due to moult were examined to see how these differences were reflected in performance (chapter 3). Species also vary in size, phylogeny and ecology, so the relationship between take-off performance and inter-specific variation in wing morphology was also examined (chapter 4). As a range of species were studied, take-off performance could be viewed in an ecological and evolutionary context. The kinematic and aerodynamic analysis used to quantify take-off performance both intra- and inter-specifically is also explained (chapter 2).

The second key aim of this thesis is to determine the mechanical function of two intrinsic wing muscles; the biceps brachii and scapulotriceps, and to see if function varies relative to flight mode (chapter 5). This is the first study to analyse the mechanical work and power output of bird wing muscles where the muscles have been stimulated *in vitro* with the strain trajectories and activity patterns measured *in vivo* during different types of flight. By understanding the function of muscles within the wing will aid understanding of the postural and shape control of the wings during a wing stroke, and whether this varies with the differing aerodynamic power requirements of different modes of flight.

2 Measuring take-off: video analysis, kinematics and power calculations

Flight studies of invertebrates and vertebrates, both in the laboratory and the field, involves tracking an animal's position temporally within a calibrated three-dimensional space, using multiple high speed cameras (Askew et al., 2001; Berg and Biewener, 2008; Berg and Biewener, 2010; Fernandez et al., 2012; Hedrick and Biewener, 2007; Iriarte-Diaz et al., 2012; Iriarte-Diaz et al., 2011; Iriarte-Diaz and Swartz, 2008; Park et al., 2001) or a single camera and mirrors (Altshuler and Dudley, 2003; Altshuler et al., 2010a; Dillon and Dudley, 2004; Morris and Askew, 2010a). Reconstructing the spatial and temporal position of a bird allows the velocity, acceleration the x, y, z coordinates can then be used to calculate the; velocity, acceleration, thrust and angle of elevation of the flight, within a specific flight volume, through time. To reconstruct the position of an object three-dimensionally involves aligning the image plane viewed by camera, with the object plane that consists of three-dimensional spatial coordinates (Hatze, 1988), mapping its actual location at any one time. Calibration involves constructing a camera model using direct linear transformation (DLT) and then using the coefficients created and the coordinates of the object to determine its three dimensional position (Hedrick, 2008). Flight volumes can also be calibrated by using a bundle adjustment procedure but this technique is more sensitive to noise (Hedrick, 2008) and position of the cameras as the position and orientation of these also need to be accurately reconstructed spatially so as construct an accurate three-dimensional coordinate frame as this is determined relative to the cameras (Triggs et al., 2000). As bundle adjustment uses the maximum likelihood in the construction of the coordinate frame, this method can also be computationally intensive (Hedrick, 2008). The x, y, z coordinates can then be used to calculate the; velocity, acceleration, thrust and angle of elevation of the flight, within a specific flight volume, through time. By determining the wing position temporally and spatially then the wing beat kinematics can also be resolved. The animal's morphological and wing beat kinematics can then be used to calculate the different components of, and total, aerodynamic power used during the flight.

The sections below outline the methodology and calculations required to assess the take-off performance, in terms of power, of different individuals and species of bird, so as to determine the effects of body mass (M_b), wing morphology and wing beat kinematics on take-off ability both intra- (chapter 3) and inter-specifically (chapters 4).

2.1 Filming and video analysis

Two Troubleshooter high speed cameras (Fastec Imaging, San Diego, CA, USA) were set-up at approximate right angles to each other. Cameras were calibrated via modified DLT (Hatze, 1988), so as to reduce errors due to linear and non-linear lens distortions such as parallax (Hedrick et al., 2004). This meant that cameras did not need to be at exact right angles to each other. A calibration object (Figure 2-1) that contained a minimum of nine non co-planar control points with known x, y, z coordinates, was filmed before each trial to define the flight volume. The control points were identified using custom built Matlab software (Matlab R2009b, The MathWorks Inc, Natick, MA, USA) DLTcal5 (Hedrick, 2008) and the calibration mean squares residual was always less than 0.3 to minimise reconstruction errors.

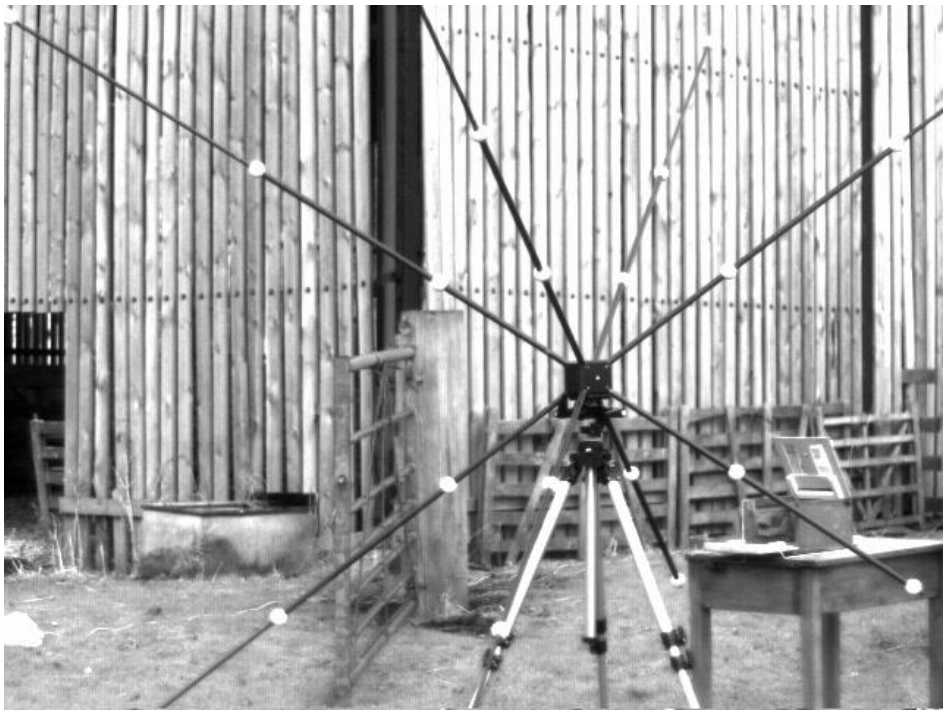

Figure 2-1 *Photograph of the calibration object and custom built release box. The calibration object used to calibrate the flight volume. The* $\boldsymbol{x, y, z}$ *coordinates of the reflective balls are known as the relative distances between them are known.*

Birds were released from a custom built release box (Figure 2-1) and were filmed taking off from within the calibrated flight volume by the two high speed cameras (Figure 2-2), operating at 250 frames s^{-1}, with a shutter speed between 0.4 and 0.8 ms^{-1}, depending on the light intensity. The release box had a height of 13.5 cm, a length of 19.5 cm and a width of 20 cm, approximately. The cameras were synchronised so that when the master camera was externally triggered the slave camera was also triggered. A 25% trigger was used so as to capture 25% of the recorded frames prior to triggering to make sure the take-off flight was captured when filming as the triggering was done manually. The front and lid of the release box sprang open when triggered to allow the bird to escape and also to startle the bird to encourage maximal take-off. The DLT coefficients file that was generated from the calibration object allowed the reconstruction of the birds' position in three dimensional space to be resolved by tracking the birds' body's centre of mass (CoM) in each camera view, frame by frame, using DLTdv5 in Matlab (Hedrick, 2008). The CoM was estimated to lie at the intersection between two axes: one axis lying equidistance between the dorsal and ventral surfaces of the body and a second axis lying equidistance between the base of the beak and the base of the tail. The bird was tracked from the point when its' feet left the box so as to remove the initial acceleration resulting from the legs (for explanation see Chapters 3 and 4). The wing root and wing tip positions at the extreme downstroke and upstroke positions for each wing beat were also digitised and used to calculate wing beat kinematics (section 2.2). The DLT root mean squares residual for each point was always below 5mm, which is an error of 1% or less for the x, y, z points.

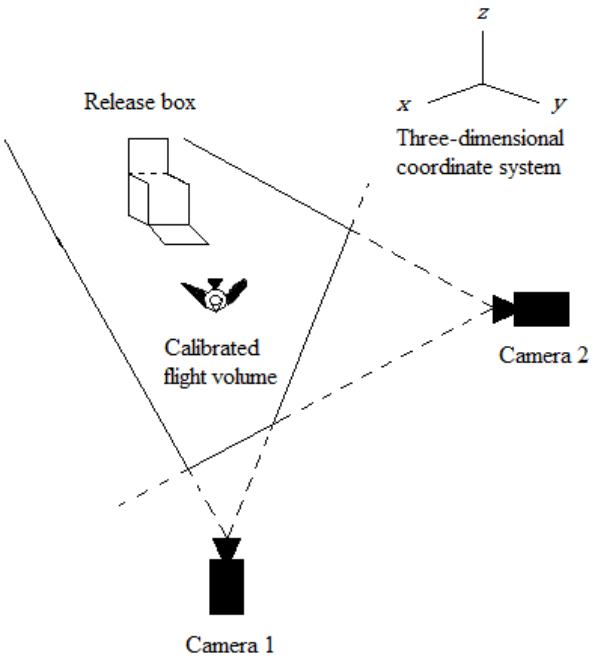

Figure 2-2 *Two-dimensional schematic to show the set-up of the take-off area. The calibrated flight volume (within the solid lines) combines the areas visible in both camera views and is defined by the calibration object.*

2.2 Wing stroke kinematics

To determine the wing beat amplitude (Φ), stroke plane angle (β), wing beat frequency (f) and downstroke ratio (D%), the position marking the extreme up- and downstroke needs to be known for each wing beat by digitising these points as described above. The wing beat kinematic variables were an average of the wing beats that formed the take-off flight.

Wing beat amplitude was calculated as:

$$\Phi = \left(\cos^{-1}\left(\frac{c'-c}{CD} \times \frac{h'-h}{HI}\right) + \left(\frac{d'-d}{CD}\right) \times \left(\frac{i'-i}{HI}\right) + \left(\frac{e'-e}{CD}\right) \times \left(\frac{j'-j}{HI}\right)\right) \quad [2.1]$$

where

$$CD = \sqrt{(c' - c)^2 + (d' - d)^2 + (e' - e)^2} \quad [2.2]$$

and

$$HI = \sqrt{(h' - h)^2 + (i' - i)^2 + (j' - j)^2} \quad [2.3]$$

CD vector represents the coordinate positions of the wing root and wing tip in the extreme upstroke positions while HI vector is the position in the extreme downstroke position. Lower case letters represent x, y and z coordinates of the wing root and wing tip (prime).

The β was calculated relative to the horizontal and was the angle between the wing tip coordinates at the extreme upstroke, and the wing tip coordinates at the extreme downstroke. The start of a wing beat was taken as the beginning of the downstroke and ended at the end of the upstroke (for definitions see Pennycuick, 1990; Pennycuick, 2008). From this, f in Hertz was determined as the number of wing beats relative to flapping phase (Pennycuick, 1990; 2008) for the analysed flight period. $D\%$ is defined as the proportion of a wingstroke spent in downstroke.

2.3 Take-off velocity, angle and power calculations

The body's CoM positional data was inputted into Mathcad 15 (PTC, Needham, MA, USA) to calculate flight velocity, take-off angle and power, following the equations of Askew et al. (2001) unless otherwise stated.

2.3.1 *Take-off velocity and angle*

To determine take-off velocity, it is assumed that flight acceleration was constant (Askew et al., 2001). The x, y, z coordinates of the birds' body's CoM were regressed against relative time and both cubic and quadratic equations were fitted to the data. Flights where the r^2 values for the cubic and quadratic regressions were similar indicated that flight acceleration was constant (Askew et al., 2001; Wakeling and Ellington, 1997b). Only the section of flight between the

time when the feet had left the ground and the bird had flown 0.5 m was analysed to standardise the analysis. The velocity was determined in the x, y and z directions ($\dot{x}, \dot{y}$ and $\dot{z}$) and the quadratic equations were differentiated for each axis, to remove fluctuations in energy that occurred during the wing stroke, to calculate overall velocity (v), as shown in equation 2.1 below.

$$v = \sqrt{\dot{x}^2 + \dot{y}^2 + \dot{z}^2} \quad [2.4]$$

The take-off angle (θ) was determined using equation 2.2 using the velocities in the x, y and z dimensions.

$$\theta = tan^{-1}\left(\frac{\dot{z}}{\sqrt{\dot{x}^2+\dot{y}^2}}\right) \quad [2.5]$$

2.3.2 *Power calculations*

The take-off power (P_{CoM}) is the power a bird uses to increase the rate of change of the potential (E_P) and kinetic ($E_{K,ext}$) energy of the body's CoM, so as to climb and accelerate. Measuring take-off power is this way incorporates acceleration, velocity and take-off angle into a single measure of take-off performance (Hedenstrom, 2003; Swaddle et al., 1999; Williams and Swaddle, 2003). This is an independent measure of take-off performance as by using speed and angle of take-off as separate measures of performance doesn't exclude behavioural influences as velocity and angle can be traded off against each other (Swaddle et al., 1999). The take-off power is given by summing;

$$\frac{dE_P}{dt} = M_b g \dot{z} \quad [2.6]$$

and

$$\frac{dE_{K,ext}}{dt} = \frac{M_b}{2}\frac{(v_{max}^2 - v_{min}^2)}{\Delta t} \quad [2.7]$$

where M_b is body mass, g is gravitational acceleration, Δt is flight duration and v_{max} and v_{min} are the maximum and minimum velocities respectively. P_{CoM} is one of the constituents of the induced power (P_{ind}) required to create a downwash or induced velocity (w), as by imparting a downward momentum onto the air, lift is created to support the body weight (Askew et al 01). The w is calculated from classical actuator disc theory and follows the equations of Wakeling and Ellington (1997a). The total P_{ind} is calculated as;

$$P_{ind} = M_b\,(g + \ddot{z}\,)(kw + \dot{z}) = M_b kw(g + \ddot{z}\,) + M_b g\dot{z} + M_b \ddot{z}\dot{z} \qquad [2.8]$$

where $M_b g\dot{z}$ and $M_b \ddot{z}\dot{z}$ are the rate of increase of the potential and kinetic energy respectively, and determine the kinetic energy of the wake (Askew et al 01).

The power necessary to create the w is termed $P_{ind'}$ and is calculated as;

$$P_{ind'} = M_b kw(g + \ddot{z}\,) \qquad [2.9]$$

where k is a correction factor, as classical actuator disc theory assumes w to be constant and steady over the disc area (Askew et al., 2001), and $\ddot{z}$ is the vertical acceleration. The value of k used was 1.2, and was based on experiments on aeroplane wings and helicopter blades (Pennycuick, 2008), as well as having been used in previous studies of flight in insects and birds (Askew and Ellerby, 2007; Askew et al., 2001; Ellington, 1984b; Pennycuick, 2008).

The parasite power (P_{par}) is required to overcome the drag of the body and is given by

$$P_{par} = \frac{1}{2}\rho S_b C_{D,par} v^3 \qquad [2.10]$$

The value used for air density ρ was 1.2 kg m^{-3}, S_b is the bodies frontal area (equation follows (Pennycuick et al., 1989), $C_{D,par}$ is the body's drag coefficient (0.13), and v is the speed of the birds' CoM (Askew et al., 2001). The $C_{D,par}$ is related to the Reynolds number and values have been revised in the literature based on observed disparities between the minimum flight speed and the speed used at minimum n (Askew et al., 2001; Pennycuick et al., 1996). The 0.13 used here follows Askew et al (Askew et al., 01) based on corrections to $C_{D,par}$, suggested by Rayner (1999). Differences in the value used for $C_{D,par}$ are unlikely to have a large effect on the total

aerodynamic power as parasite drag is minimal compared to induced and profile drag (Askew et al., 2001).

The power required to overcome wing drag (Pennycuick, 2008), termed the profile power (P_{pro}), is calculated as:

$$P_{pro} = 2(\tfrac{1}{2}\rho {V_R}^3 S_w C_{D,pro}) \quad [2.11]$$

where S_w is the area of one wing, $C_{D,pro}$ is the profile drag coefficient and was given as 0.02 (Pennycuick et al., 1992; Rayner, 1979). It has been suggested that the value for $C_{D,pro}$ used here is low when looking at the results of a fixed rotating wing (Usherwood, 2009a). Bird wings during flapping flight are readily deformable and can vary in span and shape affecting the boundary layer and the lift coefficient (Pennycuick et al., 1992; Tucker and Heine, 1990). They are also able to separate and deflect their flight feathers (Carruthers et al., 2008; Carruthers et al., 2007; Rayner, 1979) affecting the air flow around the wings and maintaining the near zero optimal lift-drag coefficient (Rayner, 1979). V_R is the resultant velocity of the air that passes over the wings and is determined from the induced, flapping and forward velocity of the bird:

$$V_R = \sqrt{(w + \dot{z}\sin(\theta) - (\phi 0.67 \mathrm{l_w} \tfrac{\mathrm{f}}{\mathrm{D\%}})\sin(\beta))^2 + (\dot{z}\cos(\theta) - (\phi 0.67 \mathrm{l_w} \tfrac{\mathrm{f}}{\mathrm{D\%}})\cos(\beta))^2} \quad [2.12]$$

The total aerodynamic power (P_{aero}) required for take-off is therefore the sum of the induced, profile and parasite power.

2.4 Summary

In the following two chapters (3 and 4) the filming procedure and determination of the wing beat kinematics and power components follow the methodologies described above. Birds were filmed taking off through a calibrated flight volume (section 2.1) and their body's CoM, wing root and tip positions were determined spatially and temporally. Intra-specifically (chapter 3), this meant that the effects of wing morphology on take-off power and total aerodynamic power

(section 2.2) could be investigated within blue tits to see if variation in wing morphology due seasonal moult and changes in body mass impacted on take-off performance. Variation in wing morphology could also potentially affect take-off performance inter-specifically (chapter 4). The methods described above were therefore also used to investigate these effects by filming (section 2.1) a range of passerine species that represented a number of avian families and ecologies. The above methods were used to quantify the different power requirements for take-off (section 2.2) to determine how any inter-specific differences in wing morphology were reflected in take-off performance (chapter 4).

3 Intra-specific variation in wing morphology and wing beat kinematics and their impact on take-off performance within blue tits (*Cyanistes caeruleus*)

Take-off is the most energetically demanding mode of flight and is important for understanding the biomechanical limits that operate to shape morphology and flight performance. Take-off ability is important to ethology and ecology in terms of flight initiation and predator evasion. Wing planform (wing loading; WL, and aspect ratio; AR) is under selective pressure to meet varying ecological demands. Intra-specifically, variation in wing morphology results from changes in feather condition, moult and body mass (M_b), impacting on take-off ability and survival. Individuals may also be able to compensate for sub-optimal morphology by altering their wing beat kinematics.

The effects of intra-specific variation in wing morphology and wing beat kinematics on take-off performance were investigated by biomechanical and aerodynamic analysis. Take-off flight of blue tits (*Cyanistes caeruleus*, Linnaeus 1758) was filmed and the birds' position was tracked three-dimensionally to determine the energy imparted to their body's centre of mass (CoM), quantifying take-off power. This was related to the total aerodynamic power requirements using wing morphological and positional measurements.

Low WL improved take-off performance as larger wing areas (S) favoured lift production, increased acceleration and wing beat frequency. Reduced AR increased take-off ability due to the relationship to; low WL, high wing beat frequency and downstroke ratio. Greater wing beat frequency and downstroke ratio may indicate higher muscle cycle frequency and that a higher proportion of the cycle is spent shortening, respectively. This may increase the mechanical power available for take-off, improving take-off performance as more power is available to increase the rate of change of the potential and kinetic energies of the body's centre of mass.

3.1 Introduction

Take-off is the means by which animals initiate flight and become airborne (Earls, 2000; Pennycuick, 2008). In some instances take-off is also an important component of predator avoidance, and performing rapid take-off flights can increase an individual's chances of survival (Fernandez and Lank, 2007; Kullberg et al., 1998; Williams and Swaddle, 2003; Witter et al., 1994). Wing morphology impacts different aspects of flight performance and is under selective pressure to meet differing ecological demands. How well a particular morphology satisfies these varying requirements will inform the ecological and behavioural decisions a bird makes, which is why it is important to view the biomechanics of flight in an ecological context (Tobalske, 2007). Take-off performance is limited by the mechanical power available from the flight musculature, but how much power can be diverted to elevating and accelerating the body's centre of mass (CoM) depends on the power required to generate the induced velocity and overcome the drag on the wings and body. Lift is needed to support body weight ($M_b g$) and any force to accelerate the body's centre of mass, and is proportional to wing area (S) and velocity^2 (Askew et al., 2001; Norberg, 1990). Forward velocity and therefore airflow over the wings are likely to be low during take-off as a bird begins from a stationary position. Wing morphology relative to body mass is therefore crucial for lift generation and will impact greatly on the power required to fly and therefore flight performance. Low wing loading (WL; body weight/wing area) should improve take-off performance by reducing the power required to generate the induced velocity so that more of the available power can be used to accelerate and elevate the body's CoM. During low speed or hovering flight, the major component of the aerodynamic power is the induced power required, and is proportional to body mass and inversely proportional to wingspan (Norberg, 1990; Warrick, 1998). A larger wingspan of high aspect ratio (AR; wingspan/mean wing chord) may therefore facilitate improved take-off by reducing the induced power requirement that dominates at low speed. However, long wings could also hamper ground take-off by hitting the ground during the flapping motion, making them more prone to damage. Longer wings may also have increased wing inertia reducing wing accelerations and lift generation (Warrick, 1998).

Intra-specifically, wing morphology varies seasonally due to changes in wing area during moult (Chai, 1997; Hedenstrom, 2003; Lind, 2001; Rayner and Swaddle, 2000; Williams and Swaddle, 2003) and to changes in body mass (M_b) (Chai, 1997; Hedenstrom, 2003; Kullberg et al., 2002; Kullberg et al., 1998; Lind, 2001; Swaddle and Witter, 1997), both seasonally and diurnally, affecting a birds' wing loading (Chai et al., 1999; Hedenstrom, 2003; Lind, 2001; Rayner and Swaddle, 2000; Senar et al., 2002a) and aspect ratio. In blackcaps WL increased by 60% prior to migration due to higher body mass (Kullberg et al., 1996) and by 10 – 25% in starlings and hummingbirds due to reduced wing area (Chai et al., 1999; Rayner and Swaddle, 2000). Birds may have to trade-off the risk of starvation with depleted fuel reserves with the benefit of maintaining a low body mass to improve escape ability from predators. In support of this hypothesis, Gosler et al. (1995) found that body mass increased in the absence of predators, whereas if the perceived risk of predation was higher then body mass decreased (Zimmer et al., 2010; Zimmer et al., 2011). However, empirical data supporting a link between flight performance and *WL* is equivocal. Several studies report that flight performance is reduced in birds with a higher wing loading resulting from diurnal changes in body mass or wing area (simulated moult), consistent with the expected changes in performance (Kullberg et al., 1996; Lind et al., 1999; MacLeod 2006; Swaddle et al., 1999). However, other studies report no significant change in flight performance in relation to diurnal changes in body mass and wing loading (van der Veen and Lindstrom, 2000; Macleod, 2005, 2006; Williams and Swaddle, 2003). Not all studies have performed a complete biomechanical analysis of performance, but instead have focused on behavioural aspects, considering single, possibly correlated components of performance such as flight velocity or take-off angle, and in some cases positional data have low time resolution. Studies that have quantified take-off performance in terms of the rate of change of the potential and/or kinetic energies of the centre of mass, have not always related this to total aerodynamic power requirements of flight. These factors may have obscured the hypothesised relationship between *WL* and take-off performance. To our knowledge there has been no consideration of intra-specific variation in *AR* in relation to take-off performance.

The aim of this study was to use a detailed kinematic and aerodynamic analysis to determine the effects of intra-specific variation in wing morphology on take-off performance in wild caught

blue tits. Birds were filmed taking off by two high speed video cameras and the position of their bodies centre of mass, wing root and wing tip were reconstructed three-dimensionally both spatially and temporally to allow the aerodynamic analysis of take-off to be determined. Take-off performance was quantified as the rate of change of the kinetic and potential energies of the centre of mass of the bird during escape take-off flights. It was hypothesised that individuals with low WL and high AR will be able to use a greater proportion of the power available from the flight muscles to accelerate and gain height due to the relatively higher lift production by their wings. A full aerodynamic analysis was also performed in order to assess the total flight power requirements to help understand differences in take-off performance.

3.2 Materials and Methods

3.2.1 *Birds and wing measurements*

Blue tits were caught using mist nets, under license (British Trust of Ornithology license A to Chris Wright) at two sites in North Yorkshire, UK (Malham and Thorganby) between June 2011 and June 2013. Individuals were sexed and aged when possible before being weighed (Svensson, 1992). A digital photograph (Canon EOS 30D digital, Uxbridge, Middlesex, UK) was taken of the outstretched wing and body to calculate wing area (S) and span (b), following Pennycuick (2008), using ImageJ software (Rasband, W.S., ImageJ, U.S. National Institutes of Health, Bethesda, Maryland, USA). WL ($\frac{body\ weight}{wing\ area}$) and AR ($\frac{wing\ span^2}{wing\ area}$) were calculated (Norberg, 1990; Pennycuick, 2008) from the M_b, S and b measurements for each bird.

3.2.2 *Filming analysis*

Individuals were released from a custom-built release box that sprung open to act as a startle stimulus and invoke maximal response (section 2.1, Figure 2-2). Only flights where birds took-

off instantly on release were analysed as it was assumed these individuals were taking off maximally. A total of twenty-nine blue tits took flight immediately. Take-off flights were filmed using two high speed video cameras (Troubleshooter, Fastec Imaging, San Diego, CA, USA) operating at 250 frames second^{-1}, shuttered at 0.4 to 0.8ms^{-1} depending on light levels (chapter 2, Figure 2-1). Calibration of the flight volume follows section 2.1 in chapter 2. A calibration object (Figure 2-1, section 2.1) with points of known distance respective to each other, was digitised using DLTcal5 (Hedrick, 2008) in custom built Matlab software (Matlab R2009b, The MathWorks Inc, Natick, MA, USA). The DLT x, y, z coordinates file generated was used to determine the position of the bird as it flew within the calibrated flight volume.

3.2.3 *Velocity and power calculations*

The x, y, z coordinates of the CoM outputted by the DLTdv5 (Hedrick, 2008) custom built software in Matlab (Matlab R2009b, The MathWorks Inc, Natick, MA, USA) were used to calculate the overall velocity (v), velocities in the x, y, z dimensions ($\dot{x}$, $\dot{y}$ *and* $\dot{z}$) of the body's CoM and take-off angle (θ), as described in section 2.3.1. Individuals were compared by determining the velocities at an absolute distance of 0.5m from the point of take-off. The take-off power (P_{CoM}) is the sum of the change in rate of the potential (E_P) and kinetic energy ($E_{K,ext}$) of the *CoM*. Calculations of E_P and $E_{K,ext}$ follow the equations 2.6 and 2.7 (chapter 2; section 2.3.2).

3.2.4 *Wing beat kinematics*

The wing beat kinematic variables were an average of the wing beats that formed the take-off flight. Wing beat amplitude (Φ) in radians, is the maximum angle between the three-dimensional wingtip position in extreme upstroke and extreme downstroke, and was calculated as:

$$\Phi = \cos^{-1}\left(\frac{c'-c}{CD}\right) \times \left(\frac{h'-h}{HI}\right) + \left(\frac{d'-d}{CD}\right) \times \left(\frac{i'-i}{HI}\right) + \left(\frac{e'-e}{CD}\right) \times \left(\frac{j'-j}{HI}\right) \quad [3.1]$$

where

$$CD = \sqrt{(c'-c)^2 + (d'-d)^2 + (e'-e)^2} \quad [3.2]$$

and

$$HI = \sqrt{(h'-h)^2 + (i'-i)^2 + (j'-j)^2} \quad [3.3]$$

CD represents the coordinate positions of the wing root and wing tip in the extreme upstroke positions while HI is the position in the extreme downstroke position. Lower case letters represent x, y and z coordinates of the wing root and wing tip (prime). The stroke plane angle (β) was calculated relative to the wing root and was the angle between the wing tip coordinates at the extreme upstroke, and the wing tip coordinates at the extreme downstroke. Wing beat frequency (f) in Hz, is the number of times the wings are beaten within the total flight time taken to fly 0.5m. Downstroke ratio ($D\%$) is the proportion of the wing stroke that is downstroke (Riskin et al., 2012). The downstroke was the part of the wing stroke where the wings move forward and downwards (Riskin et al., 2012) and began when the wings were fully extended and pronated above the plane of the body of the bird, and ended after the wings had completed their forward, downward motion, below the plane of the body.

All calculated powers were normalised to M_b and expressed in W kg^{-1}, and were calculated in Mathcad 15 (PTC, Needham, MA, USA).

3.2.5 *Aerodynamic power*

The total aerodynamic power (P_{aero}) needed to take-off is the sum of the; induced power (P_{ind}) which constitutes P_{CoM} and the power required to create the downwash, or induced velocity (w) to balance body weight ($P_{ind'}$), profile power (P_{pro}) to overcome wing drag, and the parasite

power (P_{par}) to overcome body drag. Calculations of the different power components follow the equations that are described in chapter 2 (section 2.3.2).

3.2.6 *Statistical analysis*

Statistical tests were conducted in Minitab 16 (Minitab Inc, State College, Pennsylvania, USA). Data was tested for normality prior to statistical analyses. Parametric tests were used on the data if it was normally distributed and when it was not, the data was transformed so as to normalise. In some instances, logarithmic, arcsine or square-rooting the data still did not normalise it and therefore non-parametric tests were used. One-way ANOVA or Mann-Whitney U tests were used to determine if there were differences in the response and explanatory variables due to age or sex. There were no significant differences between adults and juveniles but there were some differences between males and females (see section 3.3). A one-way ANOVA followed by a Tukey *post-hoc* test was conducted to determine the differences in the power components. The least-squares regression slopes showing the relationships between; P_{aero}, P_{CoM} and the explanatory variables for males and females were also determined, as was whether the slopes differed from each other significantly. The test statistic was calculated as described by C. Zaiontz (http://www.real-statistics.com/regression/hypothesis-testing-significance-regression-line-slope/comparing-slopes-two-independent-samples/). As the slopes did not differ significantly (see section 3.3) the relationships between; P_{aero}, P_{CoM} and WL, AR and the different wing beat kinematic variables were determined by general linear model (GLM) with both season and site where the birds were collected included in the analysis, on the pooled data. This meant that individuals that had been excluded due to sex being indeterminate could be included as sex can be difficult to determine outside the breeding season.

3.3 Results

The total aerodynamic power requirement of escape take-off flights in blue tits was 51.28 ± 1.51 W kg^{-1} body mass. Of the total P_{aero}, approximately 55 % (range 51-60%) was used to accelerate and increase the height of the *CoM* during take-off. The bulk of the remaining power was required to generate the induced velocity ($P_{ind'}$, representing 39% of P_{aero}), with a much smaller amount being required to overcome the drag on the wings and body (approximately 5% and 0.2% of P_{aero}, respectively; Figure 3-1). The majority of the blue tits' P_{CoM} was used to accelerate their body's CoM, with less power dedicated to elevating the body's CoM (87% and 13% respectively, Figure 3-1B). As the profile and parasite power requirements are so small (Figure 3-1) they will not be analysed further.

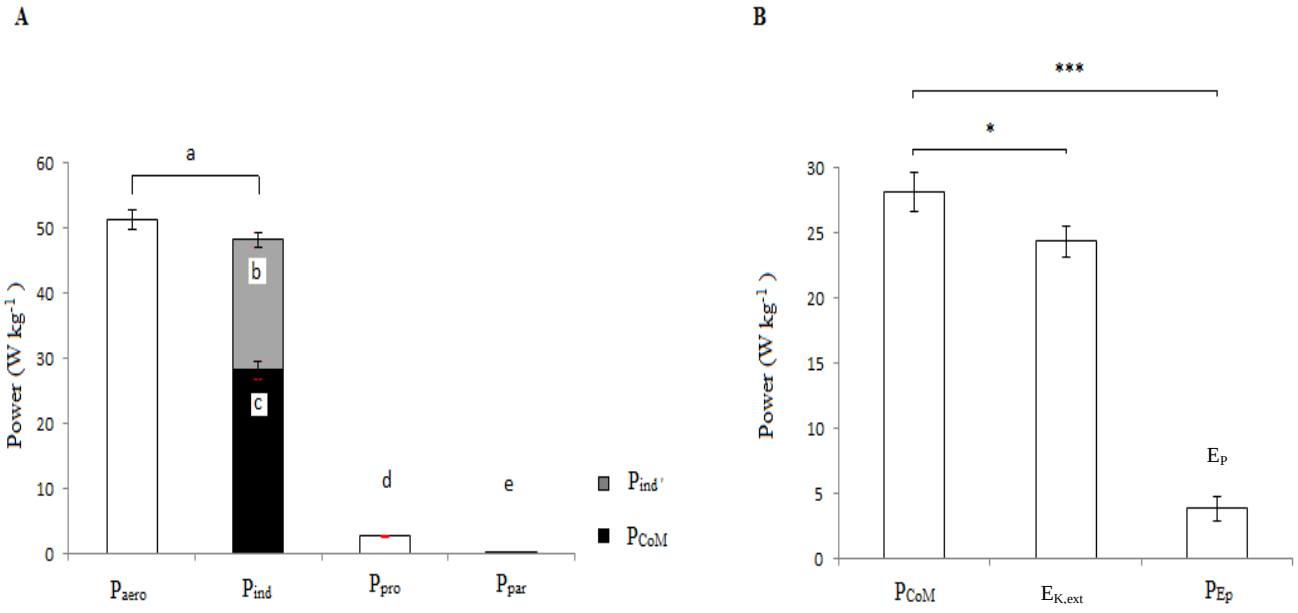

Figure 3-1 *How the aerodynamic power required for take-off is apportioned within the blue tits. How the (A)* $\boldsymbol{P_{aero}}$ *is allocated to the power requirements of take-off. Bars are shown with standard errors and different letters indicate significant differences (Tukey post-hoc test, P < 0.05). (B) The allocation of* $\boldsymbol{P_{CoM}}$ *into* $\boldsymbol{\dot{E}_P}$ *and* $\boldsymbol{\dot{E}_{K,ext}}$ *(*** P < 0.001, * P < 0.05).*

Males were heavier (W = 158.5, n_1 = 11, n_2 = 11, P < 0.05), had greater *D*% ($F_{1,21}$ = 5.79, P < 0.05) and higher P_{aero} (W = 163.0, n_1 = 11, n_2 = 11, P < 0.05) and P_{CoM} ($F_{1,21}$ = 6.11, P < 0.05) than females. However, when analysing the relationships between P_{aero} and P_{CoM}, and M_b, wing morphology and wing beat kinematic traits, the slope for the males and females did not differ significantly (Table 3.1). Further analyses were therefore carried out on the pooled blue tit data. The inclusion of season, site and the interaction between these two factors did not improve the model when determining the effect of mass on log P_{aero} ($F_{2,26}$ = 1.60, P = 0.22) and P_{CoM} ($F_{2,26}$ = 0.55, P = 0.58), and therefore were removed from the model.

Table 3.1 *Analysis of the differences between male and female blue tits in take-off performance (aerodynamic,* $\boldsymbol{P_{aero}}$ *and take-off,* $\boldsymbol{P_{CoM}}$ *power) relative to morphological and kinematic traits. Least-squares regression results for males and females including whether the slopes differed significantly from each other. If the least-squares regression slope for male and female blue tits for any of the relationships between the response and explanatory variables had a P-value of <0.05, the sexes were considered to be significantly different from each other.*

Variables	Slope difference

Explanatory	Response	t_{18}	P
Body mass	P_{aero}	0.80	0.43
	P_{CoM}	0.20	0.84
Wing loading	P_{aero}	0.11	0.92
	P_{CoM}	-0.46	0.65
Aspect ratio	P_{aero}	-0.49	0.63
	P_{CoM}	0.43	0.67
Wing beat frequency	P_{aero}	1.00	0.33
	P_{CoM}	1.09	0.29
Stroke plane angle	P_{aero}	0.24	0.81
	P_{CoM}	-0.13	0.89
Wing beat amplitude	P_{aero}	0.62	0.54
	P_{CoM}	0.31	0.76
Downstroke ratio	P_{aero}	-0.32	0.75
	P_{CoM}	-0.01	0.99

3.3.1 *Wing morphology and take-off performance*

Blue tits with lower AR also had significantly lower WL ($F_{1,27}$ = 37.33, r^2 = 0.58, P < 0.001 ; Figure 3-2). Intra-specific variation in wing morphology affected take-off performance in terms of the aerodynamic power available (P_{aero}) and the P_{CoM} (Figure 3-3). *WL* varied 1.7 fold across the individuals studied, ranging from 14.6 to 24.5 N m^{-2}. Individuals with larger wing areas had lower WL ($F_{1,27}$ = 137.39, r^2 = 0.84, P < 0.001), whereas M_b did not significantly affect WL ($F_{1,27}$ = 0.13, r^2 = 0.004, P = 0.72). AR varied by approximately 16% across the individuals studied, ranging from 4.3 to 6.4.

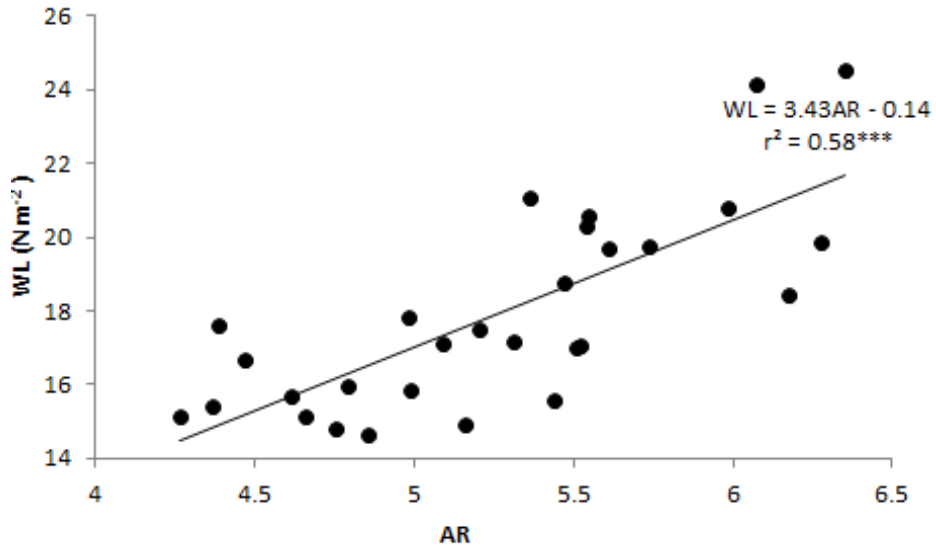

Figure 3-2 *The relationship between wing loading (**WL**) and aspect ratio (**AR**) within blue tits. A least-squares regression showing the relationship between **WL** and **AR**. *** P < 0.001.*

Models testing for the relationship between P_{aero} ($F_{2,26}$ = 0.28, P = 0.76), P_{CoM} ($F_{2,26}$ = 1.80, P = 0.19) and WL, and between P_{aero} ($F_{2,26}$ = 0.72, P = 0.50), P_{CoM} ($F_{2,26}$ = 0.62, P = 0.55) and AR, that included season and site did not improve the models fit to the data and therefore were removed. There was a significant relationship between WL and P_{CoM} ($F_{1,27}$ = 6.91, r^2 = 0.20, P < 0.05), with P_{CoM} increasing with decreasing WL (Figure 3-3A). Individuals with a lower WL were able to divert more power to moving the CoM (Figure 3-3A) and had a higher take-off performance, with most of the power being associated with increasing the kinetic energy of the CoM (Figure 3-3B). Intra-specific variation in WL affected the total aerodynamic power required during take-off (P_{aero}), with P_{CoM} increasing with decreasing WL ($F_{1,7}$ = 18.17, r^2 = 0.40, P < 0.001; Figure 3-3A). There was a relationship between WL and acceleration of the *CoM*, with birds with the highest WL exhibiting the lowest acceleration (and consequently the lowest rate of change of KE; $F_{1,27}$ = 6.92, r^2 = 0.20, P < 0.05; Figure 3-3B). There is a slight trend for blue tits with lower AR to have a higher take-off performance, however the relationship was not significant ($F_{1,27}$ = 2.76, r^2 = 0.09, P = 0.11; Figure 3-3C). Individuals with lower AR do have higher P_{aero} ($F_{1,27}$ = 9.14, r^2 = 0.25, P < 0.01; Figure 3-3C).

Table 3.2 *The relationship between take-off performance and body mass, wing beat amplitude and stroke plane angle. Least-squares regression results showing the non-significant relationships between the different power components: aerodynamic ($\boldsymbol{P_{aero}}$) and take-off ($\boldsymbol{P_{CoM}}$), and body mass ($\boldsymbol{M_b}$), wing beat amplitude ($\boldsymbol{\Phi}$) and stroke plane angle (β).*

x variable	P_{aero}			P_{CoM}		
	$F_{1, 27}$	r^2	P	$F_{1, 27}$	r^2	P
M_b	0.09	0.00	0.77	0.14	0.01	0.72
Φ	0.08	0.00	0.78	0.74	0.03	0.40
β	0.05	0.00	0.82	0.15	0.01	0.70

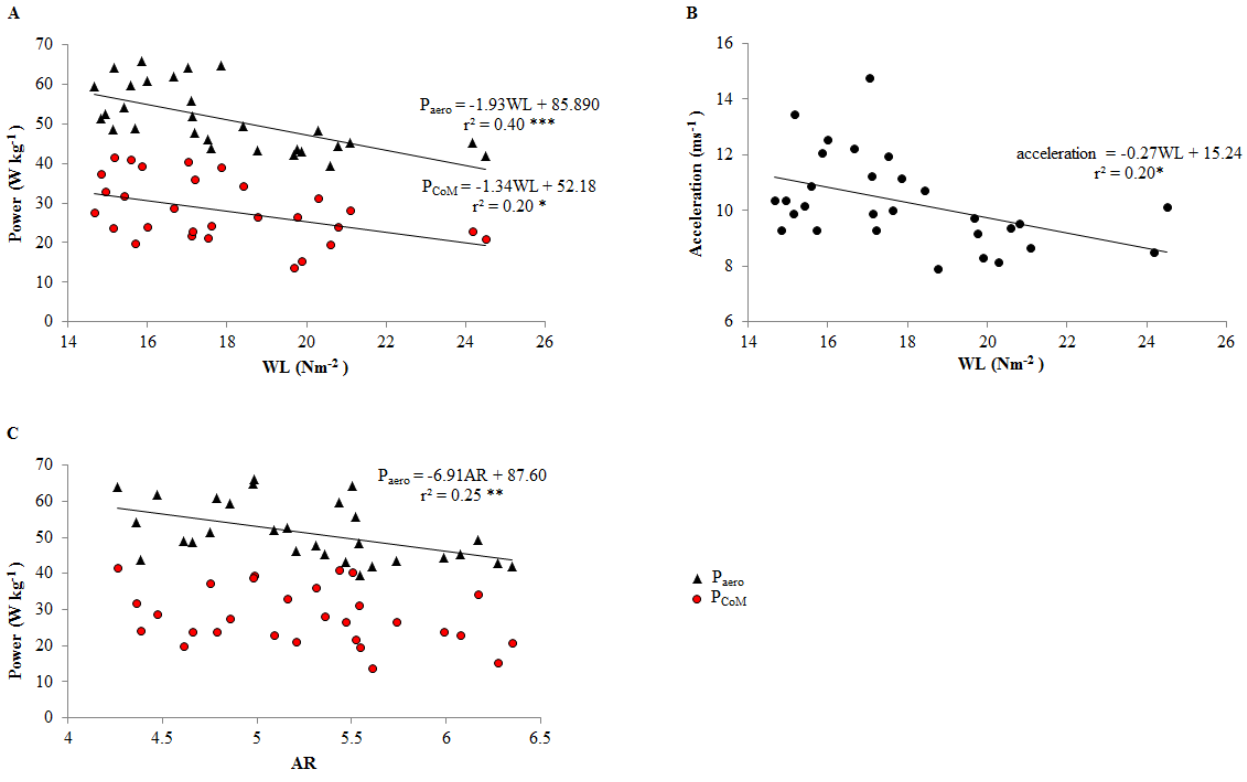

Figure 3-3 *The effect of wing morphology on aerodynamic and take-off power, and acceleration. The relationship between: the aerodynamic ($\boldsymbol{P_{aero}}$) and take-off ($\boldsymbol{P_{CoM}}$) power and (A) WL, (B) acceleration and WL; (C) AR. * P < 0.05, ** P < 0.01 and *** P < 0.001.*

3.3.2 *Wing beat kinematics and take-off performance*

Birds with a high *WL* ($F_{1,27}$ = 18.10, r^2 = 0.40, P < 0.001) and a high AR ($F_{1,27}$ = 14.35, r^2 = 0.35, P < 0.001) had a lower wing beat frequency (Figure 3-4), after removing season and site from the model as neither improved the fit of the model to the data. Blue tits with higher f had higher P_{aero} ($F_{1,27}$ = 10.89, r^2 = 0.29, P < 0.01) and P_{CoM} ($F_{1,27}$ = 6.76, r^2 = 0.20, P < 0.05; Figure 3-5), improving their take-off performance. Higher *D*% was related to higher P_{aero} ($F_{1,27}$ = 6.78, r^2 = 0.20, P < 0.05) and P_{CoM} ($F_{1,27}$ = 12.61, r^2 = 0.32, P < 0.001; Figure 3-6A). There was a relationship between *AR* and the proportion of the wingstroke represented by the downstroke ($F_{1,27}$ = 4.51, r^2 = 0.14, P < 0.05), with the relative downstroke duration increasing with decreasing *AR* (Figure 3-6B). Models testing for the relationship between P_{aero} ($F_{2,26}$ = 1.45, P = 0.25), P_{CoM} ($F_{2,26}$ = 0.45, P = 0.64) and wing beat amplitude, and between P_{aero} ($F_{2,26}$ = 1.92, P = 0.17), P_{CoM} ($F_{2,26}$ = 0.40, P = 0.68) and stroke plane angle, that included season and site did not improve the models fit to the data. Wing beat amplitude and stroke plane angle are not related to either P_{aero} or P_{CoM} (Table 3-2).

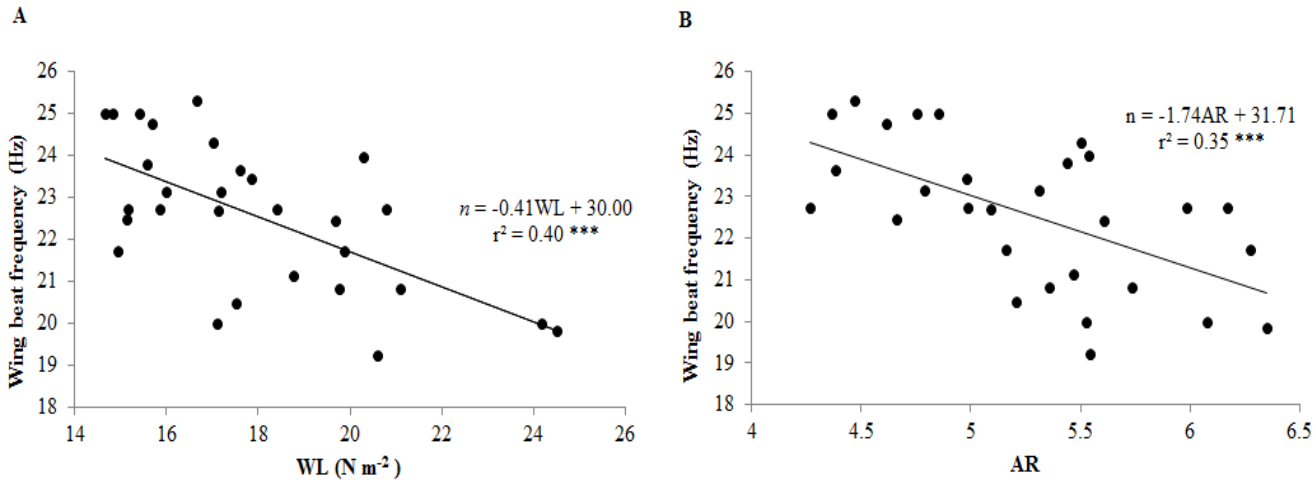

Figure 3-4 *The relationship between the wing beat frequency and wing morphology. Least-squares regression of wing beat frequency (**n**) in Hz against, (A) wing loading (**WL**) and (B) aspect ratio (**AR**). * P < 0.05, ** P < 0.01 and *** P < 0.001.*

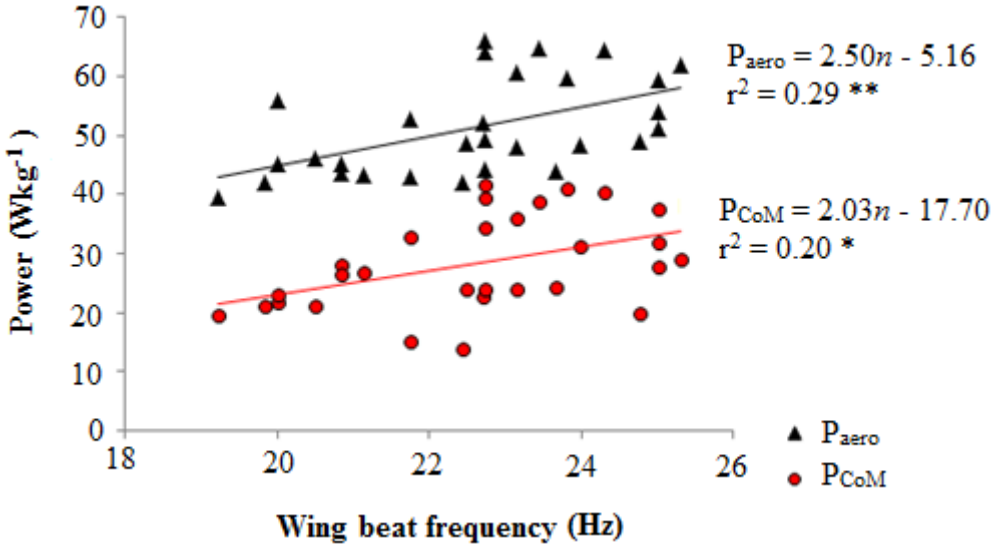

Figure 3-5 *The relationship between take-off performance and wing beat frequency. Least-squares regression of aerodynamic (**P_{aero}**) and take-off (**P_{CoM}**) power, against wing beat frequency (**n**) in Hz. *** P < 0.001.*

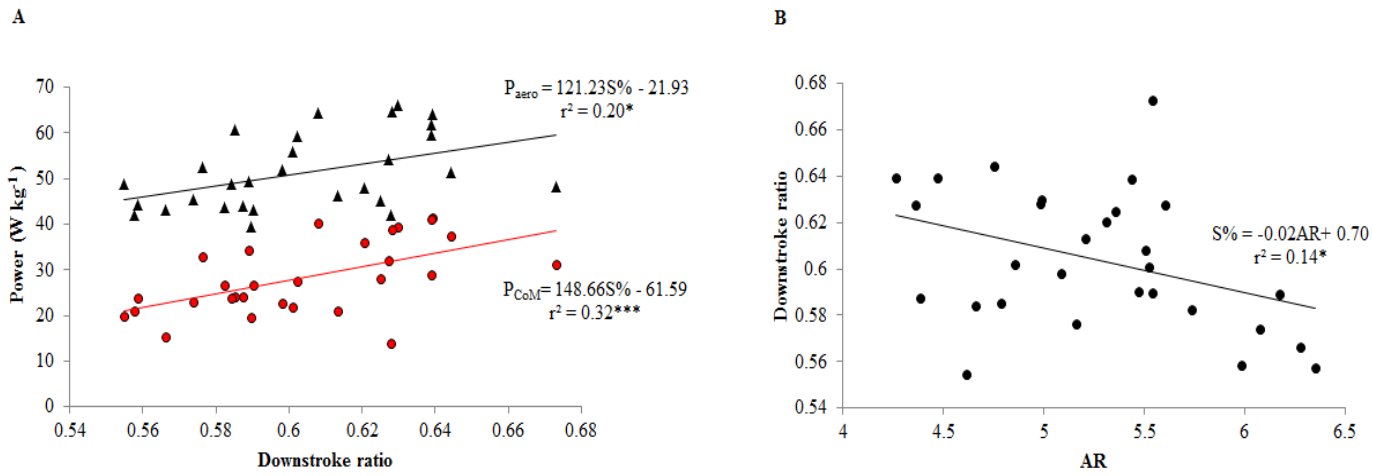

Figure 3-6 *The relationship between take-off performance and downstroke ratio (**S**%) and how there is an inverse relationship between **S**% and aspect ratio (**AR**). The least-squares regression of; (A) the aerodynamic ($\boldsymbol{P_{aero}}$) and take-off ($\boldsymbol{P_{CoM}}$) power against downstroke ratio (**S**%), and (B) **S**% and **AR**. * P < 0.05, ** P < 0.01 and *** P < 0.001.*

3.4 Discussion

Individuals with low WL and low AR had improved take-off performance compared to their conspecifics as their larger, broader wings increased lift and acceleration. Low AR improved take-off due to the inverse relationship between AR and WL. Wing morphology also affected the wing beat kinematics with high f related to low WL and AR, and high D% to low AR. Greater f and D% may indicate higher muscle cycle frequency and that a higher proportion of the cycle is spent shortening, respectively, suggesting more muscle power is available. The main constraint on take-off performance within blue tits was the P_{ind} required as, at the slow flight velocities that characterise take-off, lift creation to support body weight (Chai et al., 1999) is the main constraint on performance so approximately 95% of the total aerodynamic power is dedicated to meeting the P_{ind} requirements (Figure 3-1). The power required to overcome the profile and parasite drag of the wings and body respectively, are negligible in comparison (Figure 3-1), as it is at high flight velocities where these power components increase in importance relative to flight

performance. The majority of the P_{ind} needed was used to meet the P_{CoM}, approximately 60%, with significantly less power required to create w (Figure 3-1). In terms of take-off performance, as blue tits have lower $P_{ind'}$ demands, possibly due their low body weight and WL, more power can be dedicated to accelerating and elevating the CoM.

Intra-specific variation in wing morphology had a significant effect on take-off performance. Individuals with a lower WL were able to use a higher proportion of the P_{aero} to increase the rate of change of the potential and kinetic energy of the body's centre of mass (Figure 3-3A). As low WL is significantly related to having larger S, and therefore take-off performance is improved due to lift being proportional to S (Norberg, 1990). Induced power dominates at slow speeds (including take-off) because most of the circulation needed to produce lift must be produced by flapping the wings since the forward motion of the bird produces a relatively small amount of circulation around the wings. A wing morphology that is able to produce more lift reduces the amount of power that must be used to create lift and therefore the power margin between that available from the flight muscles and required for flight is greater. Individuals with a low WL are able to use more power to accelerate their CoM (Figure 3-3B) due to this larger power margin, increasing burst take-off performance. Seasonal moult may adversely affect take-off performance as some passerine species can reduce in S by 10 % or more (Hedenström, 1998; Swaddle and Witter, 1997), and WL can increase by 20 % (Hedenström, 1998). The effect of this will be to increase WL which in blue tits could result in lower lift generation and more power being required to create w to balance weight. If more P_{aero} is needed to balance weight then to maintain performance an individual would either need to reduce M_b (Chai, 1997; Swaddle and Witter, 1997; Zimmer et al., 2010), increase flight muscle mass but without significantly increasing body weight (Lind, 2001; Lind and Jakobsson, 2001), or alter wing beat kinematics (Crandell and Tobalske, 2011; Hedenström et al., 2007; Tobalske, 2000; Tobalske and Dial, 2000; Usherwood et al., 2003; Williams and Swaddle, 2003). Variation in flight muscle mass is outside the scope of this study but could potentially be a mechanism for maintaining take-off performance, as has been seen in tree sparrows, *Passer montanus* (Lind, 2001; Lind et al., 1999).

In addition to calculating take-off performance (P_{CoM}), the total flight power requirements (P_{aero}) was also determined. It was hypothesised that P_{aero} would be constant between individuals, reflecting a constant muscle power output as there is no mechanical reason why the flight muscle power output should vary. However, contrary to this expectation, it was found that P_{aero} decreased with increasing WL. There are several potential reasons for this. First, it could indicate that birds with a higher WL have relatively smaller flight muscles, thereby producing less power per unit body mass. As all birds were released unharmed, it was not possible to obtain flight muscle mass in these experiments to establish whether there were differences in relative flight muscle mass, but differences in relative flight muscle mass could be a potential determinant of take-off performance (Chai, 1997; Lind, 2001; Lind and Jakobsson, 2001). Second, it could result from birds with a higher WL operating with sub-maximal effort. We were unable to assess the level of motivation of individual birds. Take-off initiation was identical in all birds and so it seems unlikely that motivation was dissimilar in the birds and as a further precaution individuals that did not take-off instantly were removed from the analysis. However, it cannot be ruled out that differences in WL could affect flight behaviour. Third, it could be due to birds with a higher WL having less powerful flight muscles, either by having weaker muscles *per se* or as a result of the muscles operating under suboptimal muscle length trajectories compared to birds with a lower WL. In gray catbirds, although there was hypertrophy of the pectoralis muscles in response to pre-migartory fat loading, there was no difference in muscle fibre type composition or the muscle's oxidative or glycolytic capacity (Marsh, 1984).

Changes in muscle physiological properties are not the only mechanical factor that can cause variation in the flight muscle power output. The mechanical power output of the flight muscles also determined by; the pattern of motor unit recruitment, the muscle length trajectory, which depends on the reciprocal interaction between the muscle properties and the load acting upon the wing as it moves through the air (Marsh, 1999; Askew and Marsh, 2002). Flapping wings of varying WL and AR experience different aerodynamic forces, impacting on the muscle's length trajectory and mechanical power output. Wing stroke kinematics were significantly related to wing morphology, with birds possessing a lower WL and a lower AR having a higher wingbeat frequency and a relatively longer downstroke (Figure 3-4 & 3-5). Increasing wing beat frequency

and the proportion of the cycle spent shortening are both factors that can lead to an enhanced muscle mechanical power output, varying around an optimum cycle frequency (Askew and Marsh, 1997; Askew and Marsh, 1998), and this could also help to explain the increase in total aerodynamic power with decreasing WL and decreasing AR.

Blue tits have short, broad wings of low WL and AR due to their habitat and foraging niche, as this is a species that lives in woodlands and gardens where manoeuvrability and the ability to initiate short, rapid take-off to move between food and roosting sites (Norberg, 1990; Peterson et al., 2004), is important for survival. The need for manoeuvrability and burst take-off may have provided a selective pressure at the level of the individual to combine low WL and AR, where blue tits with this wing morphology survived and passed on their genes to the next generation, as shown by the highest take-off performance being found in individuals with short, broad wings. Short wings of low b and AR may be favoured due to the blue tits habitat as long wings could get damaged when taking off or manoeuvring through dense vegetation. Low AR indirectly improves performance by allowing for higher wing accelerations and therefore increased n (Warrick, 1998). Higher $D\%$ is also related to lower AR as the shorter relative b and potentially reduced wing inertia (Norberg, 1995; Warrick, 1998). The site or season when the blue tits were flown did not affect the relationship between take-off performance and morphology. The sites where the blue tits were collected were very similar and the effects of season were restricted to autumn and the summer, as this is when birds were caught. It would be interesting to see if the differing foraging requirements of winter and spring and the effects these could have on body mass, could potentially impact upon take-off performance.

3.4.1 *Summary*

Blue tits vary intra-specifically in their ability to take-off due to differences in wing morphology and kinematics. Wings of low WL improve take-off performance due to having larger wing areas, as S is proportional to lift. Decreased take-off ability and higher predation risk may therefore be a cost to moult. Low AR can indirectly benefit take-off ability due to the

relationship with low WL, high n and S%. Increasing f and D% may also increase the power available for take-off, respectively by; increasing muscle cycle frequency and potentially using asymmetrical strain trajectories so more force is generated during muscle shortening. Seasonal variation in wing morphology may be detrimental to take-off performance if S is lower reducing the lift and acceleration the wings can generate, and therefore the ability to survive predation.

4 Inter-specific variation in take-off performance within Passerines (Aves: Passeriformes): impacts of wing morphology on power requirements.

Take-off is one of the most energetically demanding types of flight and is crucial in terms of flight initiation and predator avoidance. Inter-specific variation in wing morphology; relative wing loading (rWL) and aspect ratio (AR) is likely due to selection for different ecological requirements. Differences in wing planform may affect wing beat kinematics as well as impacting on take-off performance. As wing morphology may reflect adaptation and/or shared evolutionary history, it is important to consider phylogeny when examining the effects of wing morphology on take-off performance. The effects of body mass and wing morphology on wing beat kinematics and take-off performance were considered and species compared after correcting for the effects of phylogeny.

The take-off flight of eleven species, representing eight families of passerine bird were filmed. The position of a bird's body's centre of mass was reconstructed three-dimensionally to determine the take-off power required to increase the rate of change of the potential and kinetic energy of the centre of mass. Wing and body kinematics and morphometrics were used to calculate aerodynamic power requirements.

Body mass, wing shape and wing beat kinematics affected take-off performance, after accounting for the effects of phylogeny. Heavier species performed better than expected possibly due to having larger, shorter wings and therefore lower rWL and AR then predicted by geometric similarity, favouring lift generation. Shorter, broader wings also improved take-off ability due to the relationship between take-off power and higher wing beat amplitude and stroke plane angle. Species vary in terms of their take-off performance due to differences in wing morphology and the related wing beat kinematics.

4.1 Introduction

Take-off is crucial to birds as it is how they initiate flight and impacts their survival in terms of predator evasion (Fernandez and Lank, 2007; Kullberg et al., 1998; Williams and Swaddle, 2003; Witter et al., 1994), influencing both ecology and ethology. The ecological and behavioural decisions made, therefore, are likely to be determined by the biomechanical constraints under which a bird has to operate (Askew et al., 2001). It is important to view these limitations within an evolutionary as well as an ecological context by studying a range of species, including taxa that are closely related (Tobalske, 2007).

Take-off is one of the most energetically demanding modes of flight (Askew and Marsh, 2002; Swaddle et al., 1999) and is limited by the mechanical power available from the muscles that can be used to meet the aerodynamic flight requirements needed to generate the induced velocity and overcome induced, wing and body drag (Askew et al., 2001; Norberg, 1990; Pennycuick, 2008). Due to the high power demands required to generate the aerodynamic forces needed for the ground to air transition (Earls, 2000; Jackson and Dial, 2011; Pennycuick, 2008), especially as flight speed is likely to be slow (Jackson and Dial, 2011; Pennycuick, 2008), the induced power requirement will be high (Askew et al., 2001; Rayner, 1994) and is likely to dominate the aerodynamic power requirement. Power is needed by a bird to accelerate and climb after take-off, by increasing the rate of change of the potential and kinetic energies of its body's centre of mass (CoM). The shape of the wings will affect the aerodynamic forces generated as lift is proportional to wing area (S) and velocity^2 (Askew et al., 2001; Norberg, 1990) and as velocity is low during take-off, the wing area that defines the rWL (Mg / S ${M_b}^{0.33}$) will be the main determinate of take-off performance. A large wing span (b) and therefore high AR (b^2 / S) means a larger area of can be swept during the wing stroke, potentially increasing lift production. Wings of high AR also reduce the induced drag as this is inversely proportional to wing span (Norberg, 1990; Pennycuick, 2008) so more of the available power may be used to accelerate and elevate the body's CoM. However, wing morphology is a trade-off dependent on the ecology and phylogeny of a species, so wings of high AR may be beneficial if the need to

minimise flight cost is the main flight constraint, but long wings may hamper ground take-off and may increase wing inertia and decrease wing acceleration (Warrick, 1998), adversely affecting take-off ability. The load acting on a wing as it moves through the air will also be affected by the wing morphology and associated wing beat kinematics, impacting on take-off performance in terms of the reciprocal interaction between load and muscle properties (Askew and Marsh, 2002; Marsh, 1999), and the aerodynamic forces generated. The morphology of some species therefore means that they are more likely to be better adapted to rapid take-off.

Our understanding of the of take-off performance has come from behavioural studies of escape responses (Burns and Ydenberg, 2002; Krams, 2002; Kullberg, 1998; Kullberg et al., 1996; Kullberg et al., 2002; Kullberg et al., 1998; Lind et al., 1999; Lind et al., 2003) that don't provide a measure of mechanical performance in respect of the energy (Hedenstrom, 2003; Swaddle et al., 1999; Williams and Swaddle, 2003) and power required, or have only looked at a small number of individuals (Earls, 2000) from one or two species (Swartz et al., 2008), and not always from within a phylogenetic context (Dudley, 2002; Swartz and Biewener, 1992; Tobalske et al., 2004). As small birds operate at Reynolds numbers of a similar range to micro-air vehicles (MAVs), the mechanical laws associated with performance, strength and stability in nature are highly likely to be applicable to MAVs (Muijres et al., 2011; Norberg, 2002; Trizila et al., 2011). With research into flapping MAVs to improve their performance, a greater understanding of the morphology and kinematics of flapping flight (Shang et al., 2009), and therefore take-off, is required.

This study examined the effects of wing morphology, in terms of wing shape characteristics, on take-off performance, which is defined by the power required to increase the rate of change of the potential and kinetic energies of a body's CoM. Variation in wing morphology may be due to adaptation to optimise flight type (Outomuro et al., 2013; Rayner, 1995), such as to improve take-off performance, but may also relate to geometric scaling (Alexander 2003; Norberg, 1990; Pennycuick, 2008), dynamic similarity (Alexander, 2003) and evolutionary relatedness (Tobalske, 2004; Van Truong et al., 2011). A range of species were therefore examined so as to represent different avian families (Turdidae, Sittidae, Paridae, Hirundinidae, Passeridae,

Prunellidae, Fringillidae and Emberizidae) and habitats (farmland, woodland, open and closed), while maintaining that birds came from the same order, Passeriformes, with the effects of phylogeny being accounted for. Deviation of wing morphological or kinematic traits, such as wing beat frequency and wing shape, from isometry may suggest adaptation (Alexander, 2003; Outomuro et al., 2013; Rayner, 1995) to optimise performance, but may also relate to phylogeny or the need to maintain dynamic similarity (Alexander, 2003). It is important to understand variation in wing shape and movement characteristics that affect flight performance, whether due to adaptation or as a reflection of phylogeny, as this informs our knowledge of the spatial and temporal ecology of a species both currently, and within that species' evolutionary history (Outomuro et al., 2013).

To my knowledge this is the first study of the aerodynamics of take-off performance that; studies a range of wild caught species, taking off from within their natural habitat and not from within a laboratory environment (Jackson, 2009), within a phylogenetic context. It is hypothesised that the best performing species in terms of take-off ability will have the highest rate of change of the potential and kinetic energies of their bodies' centre of mass (P_{CoM}) and these will be species with short, broad wings of low rWL and AR. Low rWL increases the mean coefficient of lift by maximising wing area (Norberg, 1990) and low AR ratios make stall less likely at low flight speeds (van den Hout et al., 2010; Warrick, 1998) and shorter wings reduce the rate at which the wings need kinetic energy (Usherwood, 2009b), decrease wing inertia and increase wing accelerations (Warrick, 1998). Species may also improve take-off performance by varying wing beat kinematics, possibly being able to compensate for non-optimal morphology. It is predicted that species with low AR and rWL will have higher wing beat frequencies and spend a larger proportion of the wing beat in downstroke to maximise take-off performance. Increased wing beat frequency may indicate higher flight muscle contraction frequency so more muscle power will be available (Robertson and Biewener, 2012). Higher downstroke ratio means more time is dedicated to the power generating downstroke and birds can increase wing beat amplitude and decrease stroke plane angle to increase lift (Williams and Swaddle, 2003) and redirect the resultant aerodynamic force to generate thrust (Berg and Biewener, 2010), respectively.

4.2 Materials and Methods

4.2.1 *Animals and filming*

Birds were caught using mist nets, under license (British Trust of Ornithology license A to Chris Wright) at four sites in West and North Yorkshire, UK (Malham, Thorganby, Harewood, Tadcaster), between November 2006 and August 2013. Species were chosen to represent different families within the Passeriformes and to represent a range of different habitats. Some species had to be removed as they were too big for the custom-built release box or the box clearly affected their behaviour on release. Blackbirds (*Turdus merula, Linnaeus 1758*) jumped clear of the box before initiating flight, and were only able to complete a few wing beats in the set distance, compared to the minimum of five wing beats completed by the other species. Individuals were identified, sexed and aged (following Jenni and Winkler, 1994) and weighed. Birds caught in Tadcaster were from a previous study and were weighed, photographed and filmed by Marion Kauffmann. Species represented eight different families (Turdidae, Sittidae, Paridae, Hirundinidae, Passeridae, Prunellidae, Fringillidae and Emberizidae) and included; robins (*Erithacus rubecula, Linnaeus 1758*), nuthatches (*Sitta europaea, Linnaeus 1758*), coal tits (*Periparus ater, Linnaeus 1758*), blue tits (*Cyanistes caeruleus, Linnaeus 1758*), great tits (*Parus major, Linnaeus 1758*), barn swallows (*Hirundo rustica, Linnaeus 1758*), tree sparrows (*Passer montanus, Linnaeus 1758*), dunnocks (*Prunella modularis, Linnaeus 1758*), chaffinches (*Fringilla coelebs, Linnaeus 1758*), greenfinches (*Carduelis chloris, Linnaeus 1758*) and yellowhammers (*Emberiza citrinella, Linnaeus 1758*). For the other birds caught as part of this study, a digital photograph (Canon EOS 30D digital, Uxbridge, Middlesex, UK) was taken of the outstretched wing and body to calculate wing area (S) and span (b), following Pennycuick (Pennycuick, 2008), using ImageJ software (Rasband, W.S., ImageJ, U.S. National Institutes of Health, Bethesda, Maryland, USA). rWL (Mg / S ${M_b}^{0.33}$) and AR (b^2 /S) were calculated (Norberg, 1990; Pennycuick, 2008) from the M_b, S and b measurements for each bird. rWL was used instead of WL as the latter is body mass dependent. Body mass can vary greatly intra-

specifically and can therefore have a large impact on WL, for example in blackcaps WL increases by as much as 60% prior to migration due to increased fat load (Kullberg et al., 1996). The inter-specific effects of wing morphology on take-off performance and therefore the effect of body mass are considered separately from the effect of WL, so as to determine the importance of wing morphology on take-off ability independently from the influence of body mass.

The experimental setup (Figure 2-1) and filming follows methods described previously (chapter 2). The majority of birds were released from the custom built release box and filmed by two high speed cameras flying through a calibrated flight volume (section 2.1). The position of the bird's body's CoM, wing root and tip, were digitised in Matlab (R2009b, The MathWorks Inc, Natick, MA, USA) using DLTdv5 (Hedirck, 2008) to determine their positions three-dimensionally in space and time (section 2.1). The digitised point are converted to x, y, z coordinates so that the wing beat kinematics, velocities and accelerations can be calculated (section 2.2). These are then used to determine; the take-off, the power to generate the induced velocity, the power to overcome wing and body drag, and the total aerodynamic power (section 2.2). The remaining birds were caught by M. Kauffmann in Tadcaster, North Yorkshire. The flight volume was calibrated using two chequered calibration boards, positioned at right-angles to each other, and the birds' body's CoM and wing root and tip were digitised using Videopoint 2.5 (Lenox Software Inc, Lenox, MA, USA) and pixel coordinates were converted to positional coordinates (following Askew et al., 2001) using custom-built software in Mathcad 15 (PTC, Needham, MA, USA).

4.2.2 *Power calculations*

Power calculations followed the equations of chapter 2 (section 2.2). The induced power (P_{ind}, equation 2.9) required constitutes the sum of take-off power (P_{CoM}), which is the sum of E_P and $E_{K,ext}$ (equations 2.6 and 2.7; section 2.3.1), and $P_{ind'}$, which is the power needed to create a downwash, or induced velocity (w), to balance a bird's $M_b g$ and vertical acceleration force (equation 2-8; section 2.3.2). The profile (P_{pro}) and parasite (P_{par}) power were determined as in

chapter 2 (section 2.3.2). The P_{pro} requires the determination of the resultant velocity (V_R; equation 2.12), which in turn needs the wing beat kinematics to be known. These variables were an average taken across the take-off flight. The wing beat amplitude (Φ), frequency (f), stroke plane angle (β) and downstroke ratio ($D\%$) have been described previously (chapter 3, section 3.2.4). The Φ, n and $S\%$ for birds caught in Tadcaster were an average taken over three wing beats and were determined previously (M.Kauffmann, unpublished data). The β was calculated as described in section 2.2, using the x, y, z coordinates of the wing root and tip for three wing beats.

The total aerodynamic power (P_{aero}) of take-off was the sum of P_{ind}, $P_{par}$and P_{pro} and was normalised to M_b, expressed in W kg^{-1}. The power components were calculated using the same equations for all birds studied and all were standardised so they all had flown 0.5m in distance.

4.2.3 *Phylogenetic independent contrasts*

To account for the influence of phylogeny, standardised independent contrasts (Felsenstein, 1985; Garland et al., 1992) were computed for the analysed variables from species means using Felenstein's phylogenetic independent contrast method (Felsenstein, 1985) in the PDAP: PDTREE module [v. 1.15 (Maddison and Maddison, 2007; Midford et al., 2005)] of Mesquite [v. 2.75 (Maddison and Maddison, 2010)] so as to correct for the effect of shared evolutionary origins when examining the geometric scaling relationships and which variables affect take-off performance. The phylogenetic dependence of characters (Felsenstein, 1985; Hedenstrom, 2008) needs to be accounted for as species are not evolutionary independent from one another (Alerstam et al., 2007; Felsenstein, 1985; Garland et al., 1992). The phylogenetic tree (Figure 4-1) used was based on DNA-DNA hybridisation (Sibley and Ahlquist; Slikas et al., 1996) and provided the branch lengths required for generating the standardised independent contrasts (Slikas et al., 1996). The standardised independent contrasts were normalised by exponentially transforming the branch lengths (Felsenstein, 1985). The scaling exponents and relationships between wing morphology and wing beat kinematics were analysed using least-squares

regressions of the standardised independent contrasts of the traits being investigated, with the regression lines plotted through the origin (Garland et al., 1992). Species means were used to compare the phylogenetically corrected and uncorrected models to determine the model slopes and 95% confidence intervals. These model slopes were compared to determine whether the phylogenetically corrected and uncorrected results were statistically significantly different (using the confidence intervals).

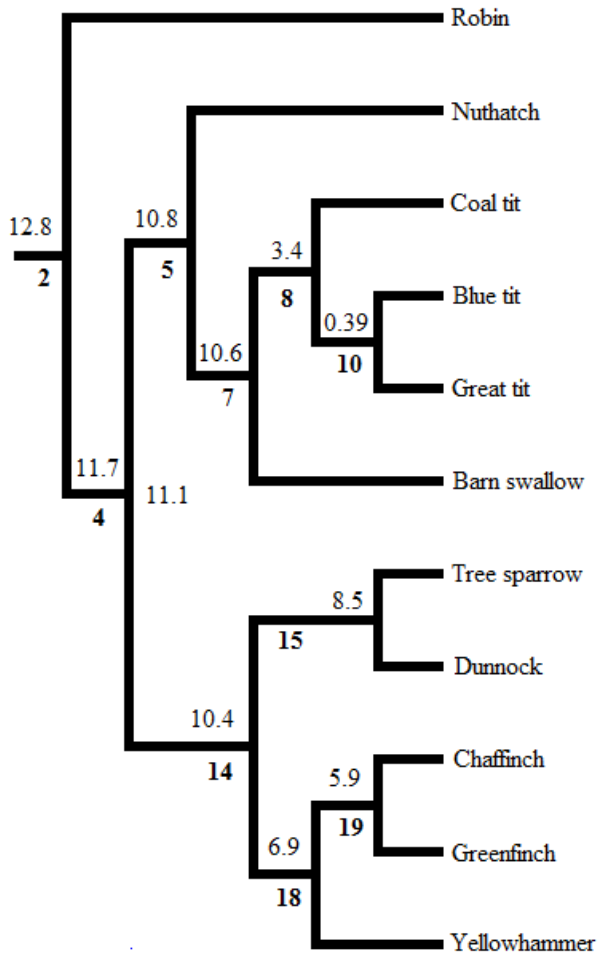

Figure 4-1 *Phylogenetic tree for the passerines studied. The tree nodes separating branches are shown in bold (below branches) and the numbers above branches show the untransformed DNA-DNA hybridisation branch distances. Topology and branch lengths are adapted from Sibley and Ahlquist (1990) and Slikas et al. (1996) for the Paridae nodes (coal tit, blue tit, great tit).*

4.2.4 *Statistical analysis*

The differences between species in terms of the explanatory and response variables were studies by one-way ANOVA followed by Tukey post-hoc tests if the ANOVA was significant so as to determine where differences lay, for the normally distributed data. A non-parametric Kruskal-Wallis with Mann-Whitney U tests were used for variables that were not normal even after transformation. Least-squares regression was used to determine if species conformed to geometric similarity as reduced major axis regression (RMA) can over exaggerate the slope values (Gardiner and Nudds, 2011). The inter-specific differences in body masses were small and therefore to determine if geometric similarity could have a significant impact on take-off performance, the total power required as predicted by geometric similarity was calculated as shown (following Rayner, 1995)

$$Power\ required = 23.0{M_b}^{1.594}b^{-1.772}S^{0.246} \qquad [4.1]$$

ANOVA was used to test whether difference in the power required predicted by geometric similarity were significantly different.

Species may also be dynamically similar to each other if the cyclic motions of their wings equate. This was determined by calculating the Strouhal number (St = $f\beta\ /v$) (Taylor et al. 2003) followed by a one-way ANOVA. Least-squares regression was used to examine if there was a relationship between the morphological variables and P_{aero} and P_{CoM}. Prior to this the residuals variation of the response variable were determined to make sure that the variance was the same for any value of the residual variance in the explanatory variable, as this is one of the

assumptions of a regression analysis. Data were logarithmically transformed and the test of the above assumption was re-done before continuing with a least-squares regression analysis. Statistics were conducted within R Studio (R Studio, R, version 3.0.0, R Foundation for Statistical Computing, Vienna, Austria), Minitab 16 (Minitab Inc, State College, Pennsylvania, USA) and Microsoft Excel 2010 (Microsoft UK, Reading, Berkshire, UK).

4.3 Results

4.3.1 *Power requirements for take-off*

The majority of the total power was used to meet the induced power required to support body weight (P_{ind}) and to accelerate and climb (P_{CoM}) (Figure 4-2). Species dedicated over 90% of their aerodynamic power to overcoming the induced drag and to generating the induced velocity with the exception of the barn swallows that dedicated 86% (Figure 4-2). On average, 63% of the induced power requirement is devoted to accelerating and climbing and therefore P_{CoM}. The $P_{ind'}$ is less than 40% for most species (Figure 4-2). The exceptions to this are the blue tits (41%), greenfinches (43%) and dunnocks (52%) that have higher $P_{ind'}$ demands. As the contribution of P_{pro} and P_{par} are negligible, and P_{CoM} constitutes over 60% of P_{aero}, take-off performance is determined by using P_{aero} and P_{CoM} as the response variables. Species varied in their take-off performance in terms of both P_{aero} ($H_{10} = 83.25$, $P < 0.001$) and P_{CoM} ($F_{10,187} = 12.35$, $P < 0.001$) (Table 4.1).

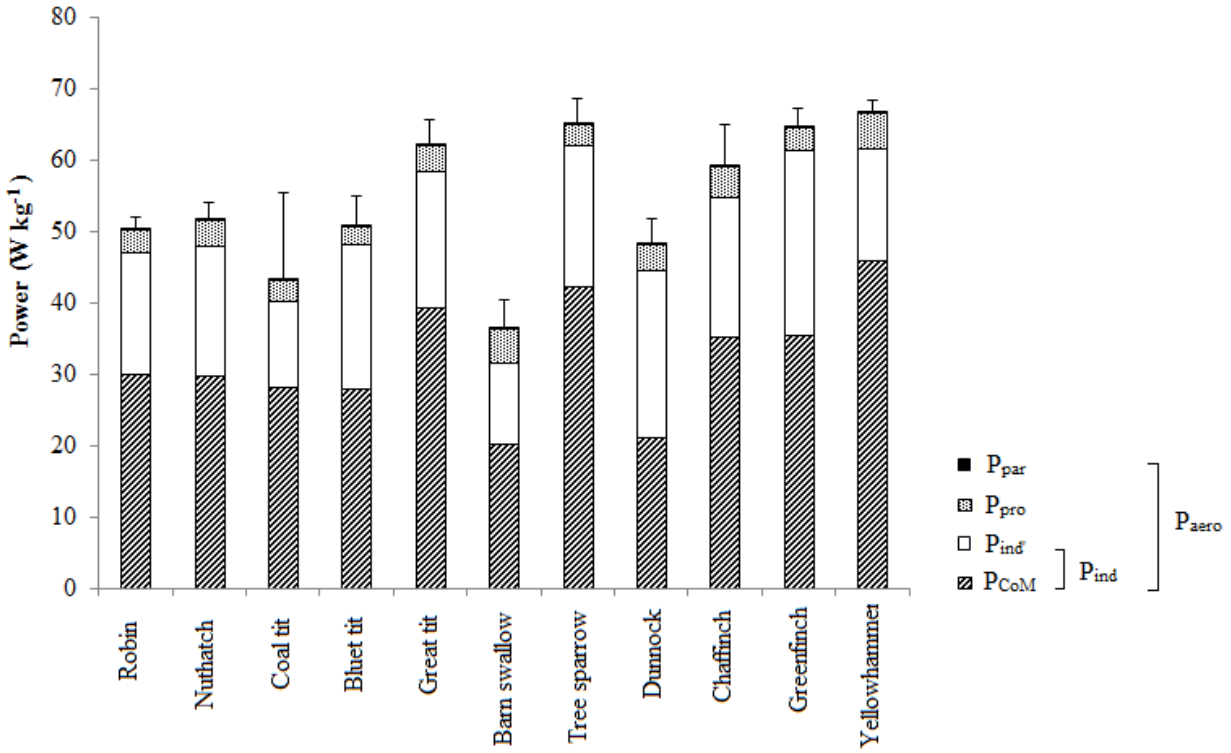

Figure 4-2 *The total body mass-specific power output is used to meet the different power requirements across the species studied. The total power requirements are the sum of* $\boldsymbol{P_{CoM}}$*, the power needed to generate the induced velocity (*$\boldsymbol{P_{ind'}}$*), parasite power (*$\boldsymbol{P_{par}}$*) and profile power (*$\boldsymbol{P_{pro}}$*). The total induced power is the sum of* $\boldsymbol{P_{CoM}}$ *and* $\boldsymbol{P_{ind'}}$*. How much of the mean total power is used to meet the mean induced, profile and parasite power requirements for each species. The positive standard errors are shown for the total aerodynamic power (*$\boldsymbol{P_{aero}}$*).*

4.3.2 *Inter-specific variation in body mass and wing morphology*

Species differed significantly in their M_b ($F_{10,187}$ = 347.05, P < 0.001), rWL (H_{10} = 116.64, P < 0.001) and AR ($F_{10,187}$ = 28.32, P < 0.001) (Table 4.1). To determine what factors affect take-off performance, the relationship between M_b and wing shape, f, v and P_{ind} was examined to see if they scaled geometrically (Pennycuick, 2008; Rayner, 1995; Taylor et al., 2003) as deviations from allometry may indicate adaptation (Alexander, 2003; Alexander, 2005). There was a small

two-fold difference in body mass but species differed significantly in the power required predicted by geometric similarity ($F_{10,187}$ = 220.02, P < 0.001).

The geometric relationships were studied by regressing; the mean values for the species, and the independent contrasts, so as to see if phylogeny affects the scaling relationships (Table 4.2). Only the least-squares regression of log S against log M_b had a slope within the confidence intervals of the slope given by analysis of the independent contrasts (Table 4.2). Analyses therefore focus on relationships using independent contrasts so as to account for the phylogenetic effect running through the data set.

With the exceptions of b and v which both scale isometrically ($b \approx {M_b}^{0.33}$ and $v \approx {M_b}^{0.17}$), the other measured variables scale allometrically. Larger birds have larger S and therefore lower rWL (Table 4.2), than the expected scaling to ${M_b}^{0.67}$ and ${M_b}^{0.0}$, respectively (Alexander, 2002; Norberg, 1990; Norberg and Rayner, 1987; Rayner, 1979). The slope for AR is predicted to be ${M_b}^{0.0\text{-}0.05}$ (Norberg, 1990; Norberg and Rayner, 1987; Rayner, 1979) but is actually negatively related to M_b (Table 4.2), while n should decrease with increasing body size to ${M_b}^{-0.17}$ (Taylor et al., 2003), but actually does not appear to vary much with M_b (Table 4.2). Species differed significantly in Strouhal number (Kruskal Wallis; H_{10} = 27.39, P < 0.01). However, with the exception of the chaffinch and barn swallows, the species studied have Strouhal numbers that are similar to each other (Table 4.3) and are therefore dynamically similar (Alexander, 2003). All of the species have Strouhal numbers that are within the range over which propulsion efficiency is high: > 0.2 to < 0.4 (Taylor et al 03). The induced power required to overcome induced drag and to create w is predicted to be high, scaling with ${M_b}^{1.17}$ if speed scales with ${M_b}^{0.17}$, as it does here ($F_{1,9}$ = 973.60, r^2 = 0.99, P < 0.001), (Norberg and Rayner, 1987). Larger species in this study however, have a lower induced power requirement (Table 4.2).

Table 4.1 *Inter-specific variation in body mass, wing morphology, wing beat kinematics, total aerodynamic and take-off power. Species mean values for the different variables. Means are shown with standard errors. Differing letters indicate significant differences (P<0.05) between species within a variable (one-way ANOVA followed by a Tukey post-hoc test).*

** If data was not normally distributed and wouldn't normalise after transformation, then a Kruskal-Wallis test followed by Mann-Whitney U tests was used.*

Species/ Variable (N)	M_b (kg) (±<0.001)	rWL* ((M_bg/S)/$M_b^{0.33}$))	AR (b^2/S)	n (Hz)	β * (°)	Φ (°)	S%	P_{aero} * (Wkg^{-1})	P_{CoM} (Wkg^{-1})
Robin (9)	0.018^{e}	69.73^{c} ±2.9	5.03^{b} ±0.2	20.70^{d,e} ±0.4	54.52^{a-c} ±6.1	149.36^{a,b} ±3.1	0.615^{a} ±0.01	50.54^{b-e} ±4.1	30.21^{b-d} ±2.7
Nuthatch (9)	0.022^{b}	65.41^{c} ±3.9	5.04^{b} ±0.1	20.06^{e} ±0.5	46.67^{b,c} ±9.0	123.37^{c} ±3.4	0.592^{a} ±0.01	51.74^{b-d} ±1.7	30.00^{b-d} ±1.4
Coal tit (11)	0.009^{g}	74.92^{b} ±2.1	5.29^{b} ±0.2	23.54^{a,b} ±0.6	48.69^{b-d} ±4.7	137.82^{b,c} ±5.2	0.605^{a} ±0.01	43.34^{e} ±3.5	28.35^{c,d} ±2.6
Blue tit (29)	0.011^{f}	79.05^{b} ±2.2	5.26^{b} ±0.1	22.58^{b,c} ±0.3	44.73^{d} ±2.7	135.30^{b,c} ±2.1	0.604^{a} ±0.01	51.28^{d} ±1.5	28.18^{c,d} ±1.5
Great tit (25)	0.019^{d,e}	74.96^{b} ±1.4	4.92^{b} ±0.1	22.78^{b,c} ±0.2	47.66^{c,d} ±3.4	138.58^{b,c} ±2.8	0.595^{a} ±0.01	62.11^{a-c} ±3.5	39.38^{a,b} ±2.0
Barn swallow (30)	0.018^{e}	46.82^{d} ±1.8	7.61^{a} ±0.1	13.10^{f} ±0.2	56.43^{a,b} ±2.0	133.88^{b,c} ±2.3	0.540^{b} ±0.004	36.31^{e} ±1.2	20.33^{d} ±1.0
Tree sparrow (20)	0.020^{c,d}	94.46^{a} ±2.1	4.82^{b} ±0.1	24.30^{a} ±0.3	38.52^{d} ±3.8	134.37^{b,c} ±1.8	0.609^{a} ±0.01	65.25^{a} ±2.7	42.44^{a,b} ±2.8
Dunnock (6)	0.022^{b,c}	80.59^{a,b} ±6.8	5.27^{b} ±0.1	22.84^{a-d} ±0.5	54.04^{a-c} ±8.0	127.80^{b,c} ±17.1	0.586^{a} ±0.01	48.36^{b-e} ±5.7	21.19^{d} ±3.0
Chaffinch (29)	0.022^{b}	68.40^{c} ±1.8	5.12^{b} ±0.1	20.38^{e} ±0.2	43.10^{d} ±2.9	135.81^{b,c} ±2.8	0.587^{a} ±0.004	59.25^{,b} ±3.2	35.28^{a-c} ±2.4
Greenfinch (28)	0.027^{a}	78.86^{a,b} ±1.2	5.34^{b} ±0.1	21.79^{c,d} ±0.2	52.86^{b,c} ±3.1	145.05^{b,c} ±2.2	0.578^{a} ±0.004	63.82^{a} ±2.2	35.61^{a-c} ±1.4
Yellowhammer (7)	0.026^{a}	81.20^{a,b} ±3.3	5.20^{b} ±0.5	21.49^{c,d,e} ±0.2	68.52^{a} ±2.1	161.16^{a} ±2.4	0.505^{b} ±0.01	68.10^{a-d} ±12.2	46.04^{a} ±5.7

Table shows body mass (M_b), relative wing loading (rWL), aspect ratio (AR), wing beat frequency (n), stroke plane angle (β), wing beat amplitude (Φ), downstroke ratio (S%), aerodynamic (P_{aero}) and take-off (P_{CoM}) power for the species studied.

Table 4.2 *Geometric scaling relationships within the passerines. Least square regressions to show the scaling of different variables with body mass. All variables were log-transformed and the results from regression of the phylogenetic independent contrasts and the raw mean values for each species were compared. The 95% confidence intervals around the slopes are also given.*

Variable	Independent contrasts				Raw data			
	Slope	$F_{1, 9}$	r^2	P	Slope	$F_{1, 9}$	r^2	P
S	$0.75^{\pm 0.04}$	2050.0	1.0	<0.001	$0.73^{\pm 0.39}$	18.38	0.67	<0.01
b	$0.31^{\pm 0.02}$	3487	1.0	<0.001	$0.37^{\pm 0.31}$	7.21	0.44	<0.05
rWL	$-0.07^{\pm 0.02}$	28.05	0.76	<0.001	$-0.15^{\pm 0.41}$	0.67	0.07	0.43
AR	$-0.13^{\pm 0.02}$	388.5	0.98	<0.001	$0.02^{\pm 0.29}$	0.02	0.00	0.89
n	$0.03^{\pm 0.02}$	7.37	0.45	<0.05	$-0.12^{\pm 0.37}$	0.53	0.06	0.49
v	$0.17^{\pm 0.01}$	973.6	0.99	<0.001	$0.08^{\pm 0.21}$	0.81	0.08	0.39
P_{ind}	$0.33^{\pm 0.06}$	128.28	0.93	<0.001	$0.15^{\pm 0.52}$	0.46	0.05	0.51

Table shows wing area (S), wing span (b), relative wing loading (rWL), aspect ratio (AR), wing beat frequency (n), take-off velocity (v), wing beat amplitude (Φ) and total induced power (P_{ind}).

Table 4.3 *Strouhal numbers of the different species. Species varied in Strouhal number (Kruskal Wallis). Different letter indicate significant differences (Mann-Whitney U test)*

Species (N)	Strouhal number (± s.e.m)
Robin (9)	$0.35^{a} \pm 0.04$
Nuthatch (9)	$0.29^{a} \pm 0.06$
Coal tit (11)	$0.37^{a} \pm 0.03$
Blue tit (29)	$0.32^{a} \pm 0.02$
Great tit (25)	$0.31^{a} \pm 0.02$
Barn swallow (30)	$0.26^{b} \pm 0.01$
Tree sparrow (20)	$0.27^{a,b} \pm 0.03$
Dunnock (6)	$0.36^{a} \pm 0.06$
Chaffinch (29)	$0.24^{b} \pm 0.02$
Greenfinch (28)	$0.33^{a} \pm 0.02$
Yellowhammer (7)	$0.35^{a} \pm 0.02$

4.3.3 *The relationship between wing morphology and take-off performance*

There was a significantly positive relationship between M_b, P_{aero} (Figure 4-3A) and P_{CoM} (Figure 4-3B), as heavier passerines had higher aerodynamic power requirements ($F_{1,9} = 416.53$, $r^2 = 0.98$, $P < 0.001$) but also had increased P_{CoM} ($F_{1,9} = 327.04$, $r^2 = 0.97$, $P < 0.001$). The

relationships between the mean P_{aero} (Figure 4-3C) and P_{CoM} (Figure 4-3D), and mean body mass for the species studied has also been shown for comparison. The latter showed no relationship between P_{aero} ($F_{1,9}$ = 3.88, r^2 = 0.30, P = 0.08) and P_{CoM} ($F_{1,9}$ = 0.04, r^2 = 0.00, P = 0.84) and body mass (Figure 4-3 C and D, respectively).

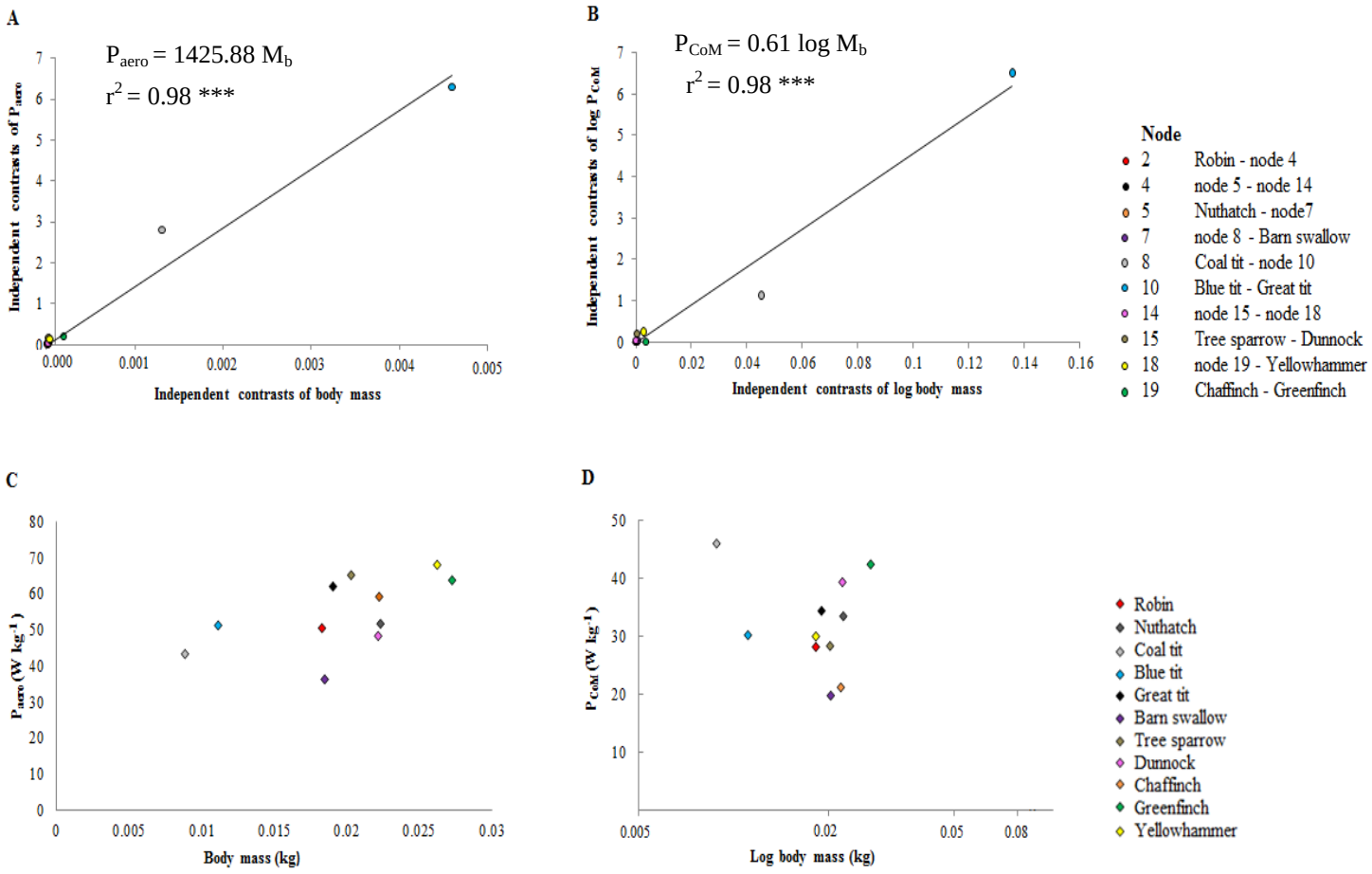

Figure 4-3 *Bivariate scatter plots between independent contrasts and species means of take-off power (log_{10} P_{CoM} and log_{10} P_{aero}) and body mass (log_{10} M_b). The relationship between the independent contrasts for; (A)* $\boldsymbol{P_{aero}}$ *and body mass and (B)* $\boldsymbol{P_{CoM}}$ *and body mass. The relationship between the species means for; (C)* $\boldsymbol{P_{aero}}$ *and body mass and (D)* $\boldsymbol{P_{CoM}}$ *and body mass. ** P < 0.01 and *** P < 0.001.*

Species with significantly lower mean *AR* had lower mean *rWL* ($F_{1,9}$ = 43.01, r^2 = 0.83, P < 0.001), as shown in figure 4-4A. The opposite relationship is shown in figure 4-4B where

phylogeny has not been accounted for ($F_{1,9}$ = 12.24, r^2 = 0.58, P < 0.01). Lower rWL was significantly related to higher P_{aero} ($F_{1,9}$ = 17.75, r^2 = 0.96, P < 0.01) and P_{CoM} ($F_{1,9}$ = 46.83, r^2 = 0.84, P < 0.001) (Figure 4-5A and B). The relationships between the species mean P_{aero} (Figure 4-5C), P_{CoM} (Figure 4-5D) and rWL, suggest that higher P_{aero} ($F_{1,9}$ = 4.86, r^2 = 0.35, P = 0.05) and P_{CoM} ($F_{1,9}$ = 5.54, r^2 = 0.38, P < 0.05) is related to higher rWL. The same positive relationships between P_{aero} ($F_{1,7}$ = 6.80, r^2 = 0.49, P < 0.05) and P_{CoM} ($F_{1,7}$ = 4.52, r^2 = 0.39, P = 0.07) and rWL are seen if the node containing the blue tit and great tit is removed from the phylogenetic analysis.

A

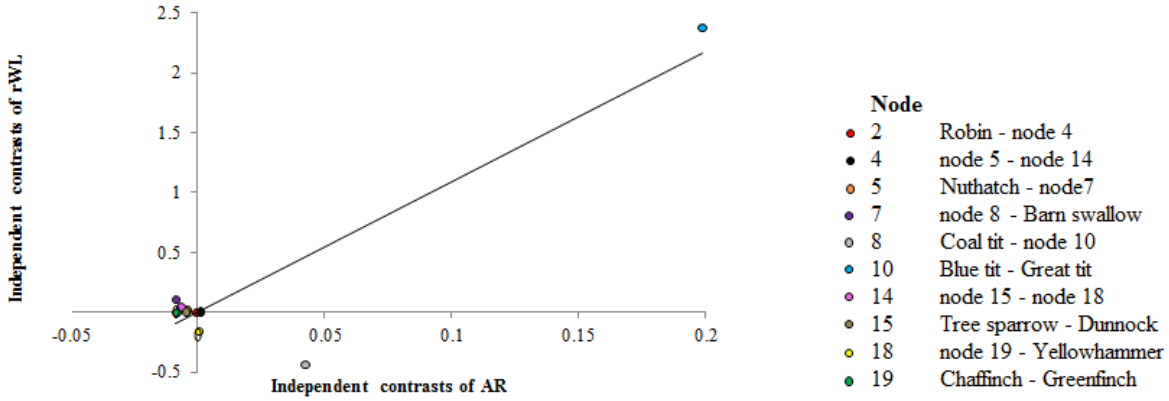

B

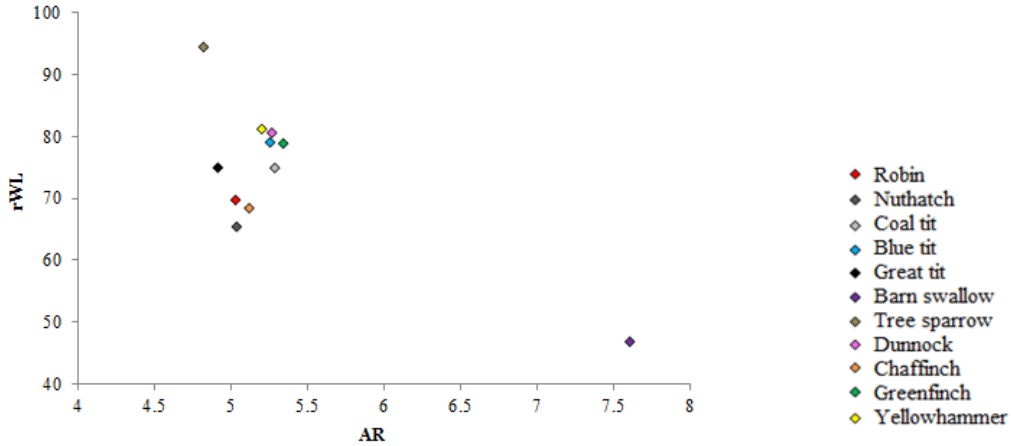

Figure 4-4 *The relationship between relative wing loading (**$\boldsymbol{rWL}$**) and aspect ratio (**$\boldsymbol{AR}$**). (A) Shows the relationship of the independent contrasts for **$\boldsymbol{rWL}$** against **$\boldsymbol{AR}$**. Nodes relate to those shown in the phylogenetic tree (Figure 4-1). (B) The relationship between **$\boldsymbol{rWL}$** and **$\boldsymbol{AR}$** for the species means.*

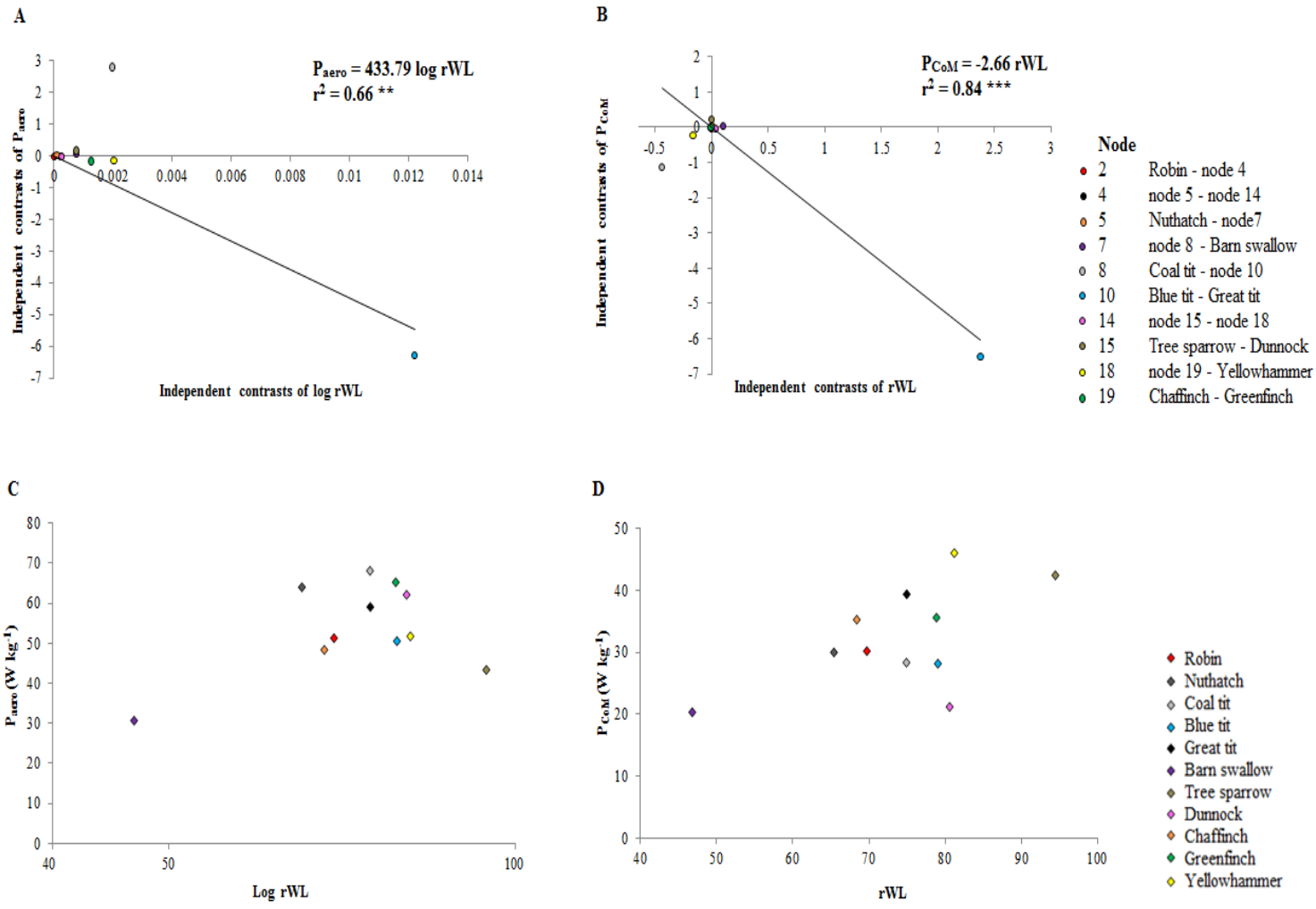

Figure 4-5 *Bivariate scatter plots between independent contrasts and species means of take-off power (**P_{CoM}** and **P_{aero}**) and relative wing loading (**rWL**). The relationship between the independent contrasts for; (A) **P_{aero}** and **rWL** and (B) **P_{CoM}** and **rWL**. The relationship between the species means for; (C) **P_{aero}** and rWL and (D) **P_{CoM}** and **rWL**. ** $P < 0.01$ and *** $P < 0.001$.*

Species with lower *AR*s had significantly higher P_{aero} ($F_{1,9}$ = 90.34, r^2 = 0.91, P < 0.001) and P_{CoM} ($F_{1,9}$ = 1807.80, r^2 = 0.99, P < 0.001) (Figure 4-6A and B). For comparison the raw data showing the relationships between mean P_{aero} (Figure 4-6C), P_{CoM} (Figure 4-6D) and *AR* are also shown and demonstrate the same inverse relationship between P_{aero} ($F_{1,9}$ = 23.16, r^2 = 0.72, P < 0.001), P_{CoM} ($F_{1,9}$ = 11.16, r^2 = 0.55, P < 0.01) and *AR*.

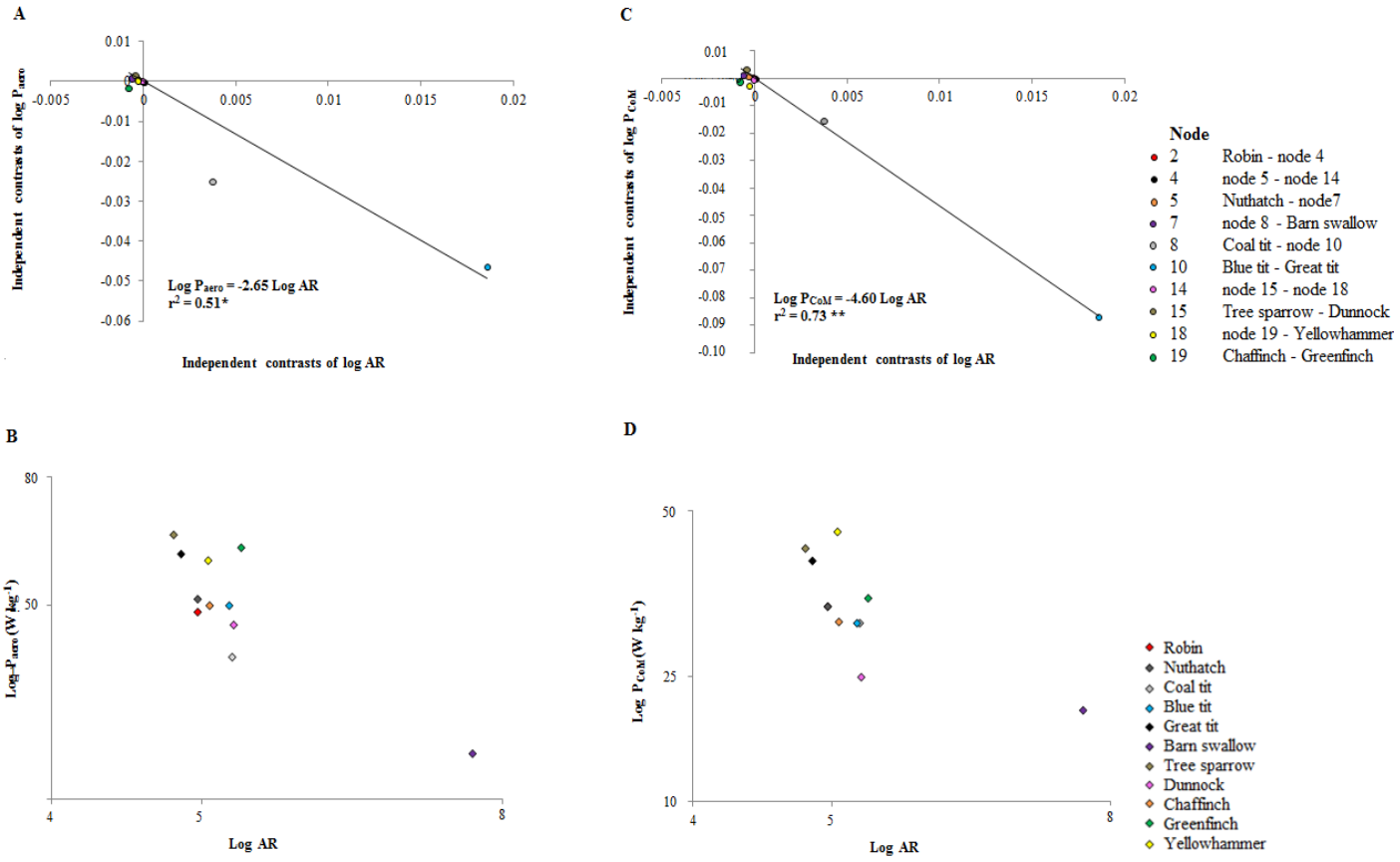

Figure 4-6 *Bivariate scatter plots between independent contrasts and species means of take-off power (**P_{aero}** and **P_{CoM}**) and aspect ratio (**AR**). The relationship between the independent contrasts for; (A) **P_{aero}** and **AR** and (B) **P_{CoM}** and **AR**. The relationship between the species means for; (C) **P_{aero}** and **AR** and (D) **P_{CoM}** and **AR** (the robin is obscured by the nuthatch). ** P < 0.01 and *** P < 0.001.*

4.3.4 *Wing morphology effects on wing beat kinematics.*

Lower wing beat stroke plane angle ($F_{1,9}$ = 32.74, r^2 = 0.78, P < 0.001) and amplitude ($F_{1,9}$ = 36.14, r^2 = 0.80, P < 0.001) were related to lower rWL (Figure 4-7A and B). A greater proportion of the wingstroke was spent on the downstroke when rWL was higher ($F_{1,9}$ = 21.05, r^2 = 0.70, P < 0.001) (Figure 4-7C). There was trend for higher wing beat frequency with lower rWL ($F_{1,9}$ = 4.67, r^2 = 0.34, P = 0.06).

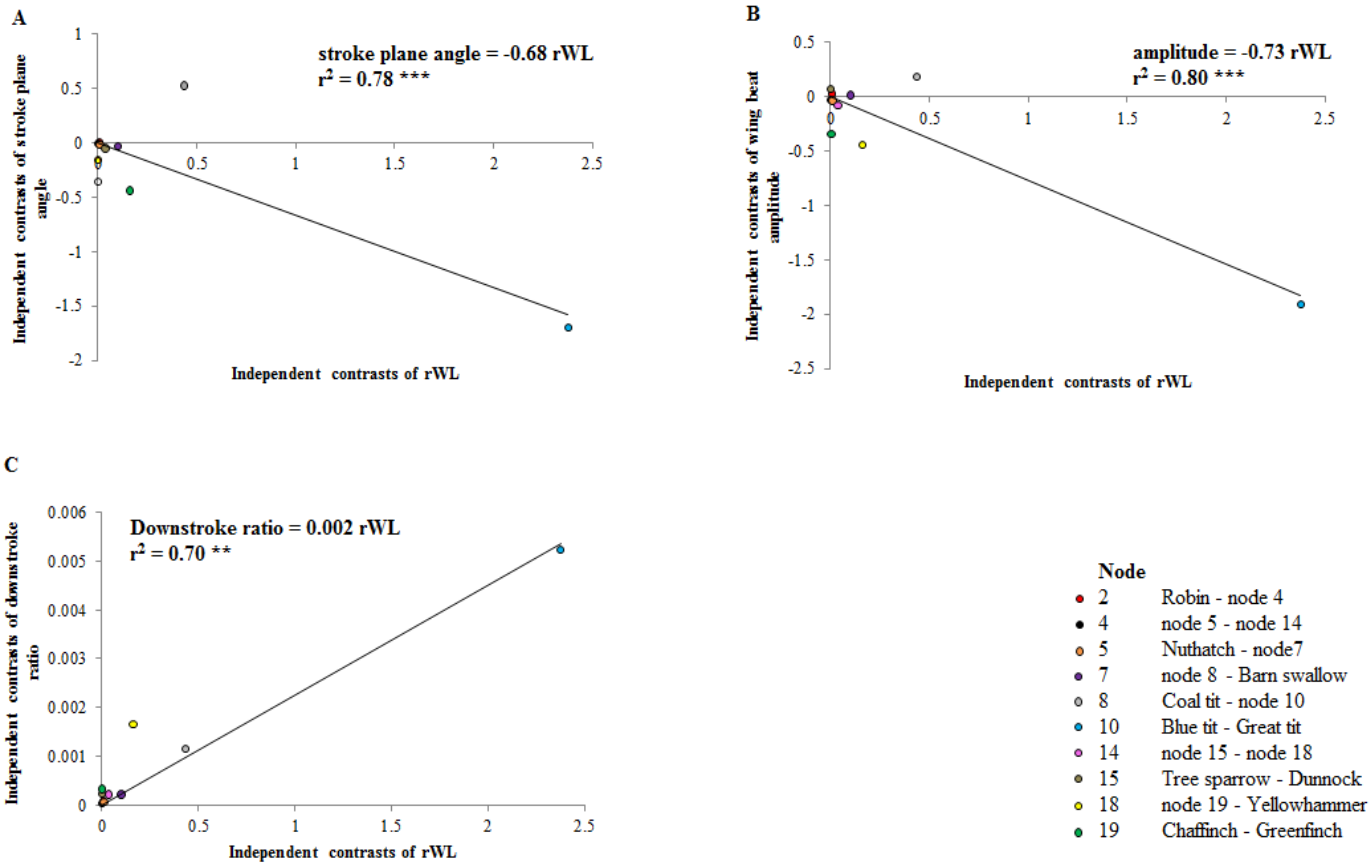

Figure 4-7 *Bivariate scatter plots between independent contrasts and relative wing loading (**rWL**). The effect of the independent contrasts and **rWL** on; (A) stroke plane angle (B) wing beat amplitude and (C) downstroke ratio. ** P < 0.01 and *** P < 0.001.*

The same relationships were observed when determining the effects of *AR* on wing beat kinematics. Stroke plane angle ($F_{1,9}$ = 18.10, r^2 = 0.67, P < 0.01) and wing beat amplitude ($F_{1,9}$ = 41.25, r^2 = 0.82, P < 0.001) were lower with lower *AR* and downstroke ratio was greater with high *AR* ($F_{1,9}$ = 74.37, r^2 = 0.89, P < 0.001) (Figure 4-8). The relationship between wing beat frequency and *AR* was not significant ($F_{1,9}$ = 1.10, r^2 = 0.11, P = 0.32).

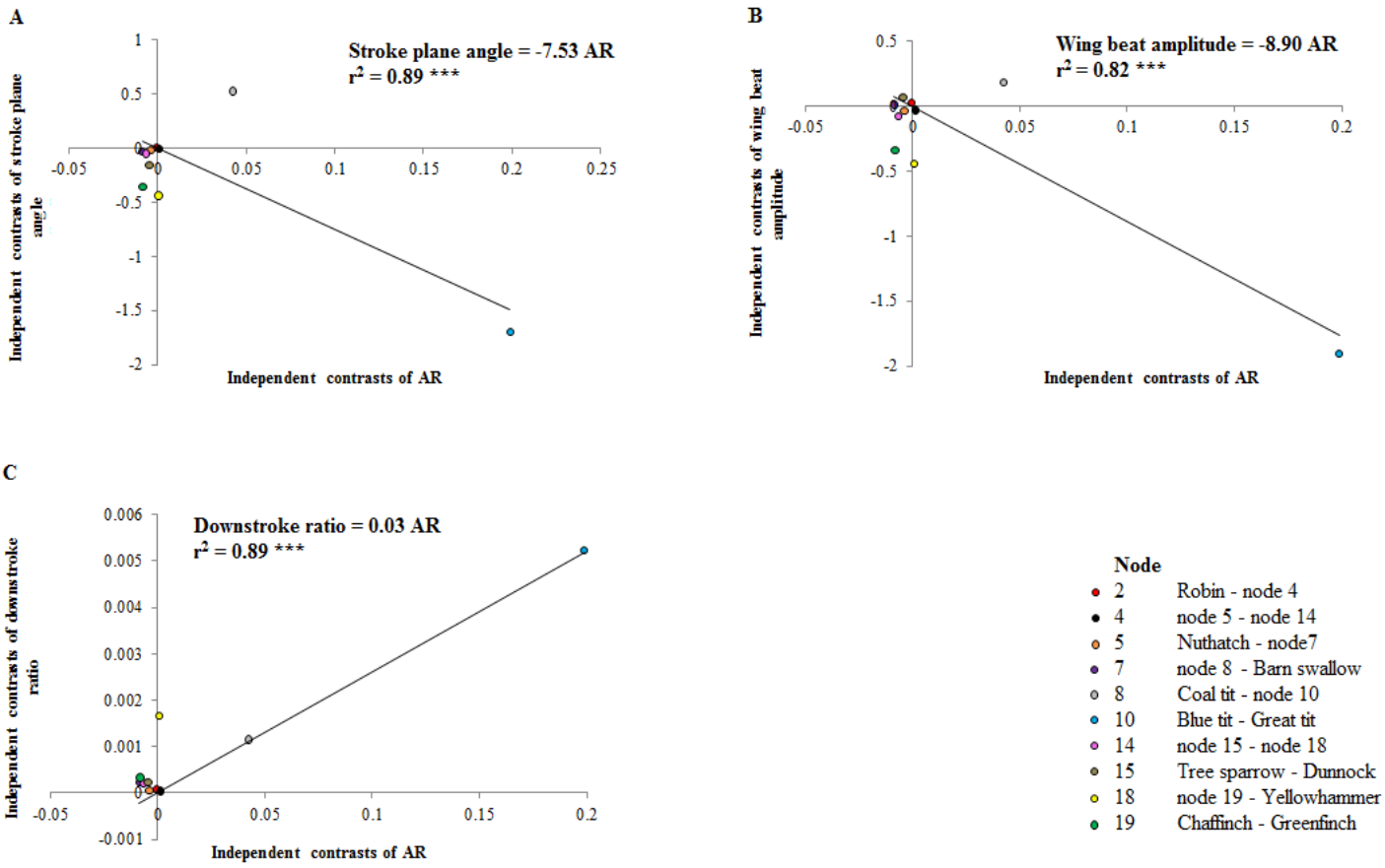

Figure 4-8 *Bivariate scatter plots between independent contrasts and aspect ratio (**AR**). The effect of the independent contrasts and **AR** on; (A) stroke plane angle (B) wing beat amplitude and (C) downstroke ratio. * P < 0.05, ** P < 0.01 and *** P < 0.001.*

High stroke plane angle (P_{aero}, $F_{1,9}$ = 9.51, r^2 = 0.51, P < 0.05; P_{CoM}, $F_{1,9}$ = 24.23, r^2 = 0.73, P < 0.001) and wing beat amplitude (P_{aero}, $F_{1,9}$ = 22.14, r^2 = 0.77, P < 0.001; P_{CoM}, $F_{1,9}$ = 59.32, r^2 =

0.87, P < 0.001) are both related high P_{aero} and high P_{CoM} respectively, when the data was phylogenetically corrected. There was however, no relationship between P_{aero} and stroke plane angle ($F_{1,9}$ = 0.04, r^2 = 0.04, P = 0.85), wing beat amplitude ($F_{1,9}$ = 2.83, r^2 = 0.24, P = 0.13) or downstroke ratio ($F_{1,9}$ = 0.18, r^2 = 0.02, P = 0.69), when phylogeny was not controlled for. There was also no relationship between P_{CoM} and stroke plane angle ($F_{1,9}$ = 0.10, r^2 = 0.01, P = 0.76), wing beat amplitude ($F_{1,9}$ = 4.57, r^2 = 0.34, P = 0.06) or downstroke ratio ($F_{1,9}$ = 0.36, r^2 = 0.04, P = 0.56) when phylogeny was not incorporated into the analysis. High downstroke ratio however, is related to low P_{aero} ($F_{1,9}$ = 65.11, r^2 = 0.88, P < 0.001) and low P_{CoM} ($F_{1,9}$ = 56.78, r^2 = 0.86, P < 0.001) when the species means include the effect of phylogeny.

4.4 Discussion

When accounting for the effect of phylogeny, there was inter-specific variation in both the rWL and AR (due to the high AR of the barn swallows) of the passerines studied and this variation affected their take-off performance. The species investigated had larger wing areas and lower rWL and AR than expected for their body mass, and the combination of having this wing morphology (Figure 4-4B) improved take-off performance. The positive relationship between take-off power and lower rWL (Figure 4-5B) was predicted as wings with large S generate proportionally more lift (Askew et al., 2001; Norberg, 1990) so more power can be expended on increasing the rate of change of the potential and kinetic energies of the centre of mass, improving a bird's ability to climb and accelerate after take-off. The opposite relationship is seen between take-off performance and rWL when the species' means without phylogenetic correction are analysed (Figure 4-5D). The relationship between the standardised independent contrasts of P_{CoM} and rWL is dominated by the three parid species as the nodes containing the blue tit and great tit and the node containing the coal tit are discrete from each other, and the other passerines studied (Figure 4-5B). Compared to the other species studied, the barn swallow and tree sparrow represent extremes in morphology with the former having the highest AR but low rWL, while the tree sparrow has a high rWL but low AR. This may explain the differences between the results for the phylogeny corrected and uncorrected analyses as there is an inverse

relationship between rWL and AR when the barn swallow and tree sparrow are included in the analyses whereas the trend is for a slightly positive relationship when these two species are removed (Figure 4-4B). Alternatively, removing the node containing the great tit and blue tit from the phylogenetic tree resulted in a positive relationship between both rWL and AR and a trend between high P_{CoM} and high rWL. It is therefore difficult to determine the relationship between P_{CoM} and rWL as the direction of the relationship is species dependent and is likely to only be resolved with the addition of more parid species and species reflecting more diverse morphologies (see section 4.4 below). The inverse relationship between P_{CoM} and AR (Figure 4-6B) for the standardised independent contrasts, may be due to functional needs applying selection pressure on this wing morphology as short broad wings improve take-off performance but also may improve manoeuvrability (Norberg, 1990; Norberg and Rayner, 1987). With the exception of the barn swallow most of the species studied forage and nest in woodland, garden or hedge habitats (Peterson et al., 2004) where manoeuvrability is likely to be important to survival. They also forage by flying short distances between patches and therefore take-off ability is likely to be important, unlike for the barn swallows which are migratory and therefore have long, narrow wings to optimise flight efficiency (Pennycuick, 2008). Low AR may also improve take-off performance by reducing the rate at which kinetic energy is required by the wings by reducing wing inertia. Rounder wings may also increase lift distally, as well as thrust (Swaddle and Lockwood, 2003). The same inverse relationship between take-off performance and AR is reflected when phylogeny is not accounted for (Figure 4-6D).

The relationship between the total aerodynamic power requirement and wing morphology was predicted to be constant between individuals as P_{aero} is dependent on the flight muscle power available and there is no mechanical reason why this should vary. However, this is not what was observed here. High P_{aero} was significantly related to low rWL (Figure 4-5AC) and low AR (Figure 4-6AD). This could reflect variation in muscle masses or flight muscle physical properties, but as birds were released unharmed this was outside the scope of this study. Species could vary in flight muscle fibre type (Tobalske, 1996) or muscle mass (Norberg, 1990) affecting the power available from the muscles. Species can vary in power modulation strategies (Morris and Askew, 2010b) and differences in wing morphology will affect the load on the wing due to

the difference in the aerodynamic force acting upon the wing as it moves through the air (Askew and Marsh, 2002; Marsh, 1999). This in turn may affect muscle length trajectory due to the mutual interaction between muscle physiological properties and the load applied to a wing as it moves through the air (Askew and Marsh 2002; Marsh, 1999). Wing morphology is therefore also likely to impact upon the wing beat kinematics which may influence take-off performance.

4.4.1 *Take-off performance: wing morphology effects on wing beat kinematics*

The analysis of the standardised independent contrasts demonstrated that there was an effect on wing beat kinematics due to inter-specific variation in wing morphology. There is a relationship between species with low rWL and low AR having higher β and Φ. By altering the wing beat kinematics, a bird can maintain the angle of its' wings relative to the angle of the airflow and its' body's CoM (Berg and Biewener, 2008). Larger wings are being swept through larger angles, potentially altering the direction of the net aerodynamic force generated, potentially forcing more air backwards and accelerating the bird forward (Berg and Biewener, 2010). Rounder, shorter wings of low AR are also associated with increased β and Φ. This may be a compensation for the cost of low AR wings on efficiency due to higher induced drag (Norberg, 1990; Warrick 1998). High β and Φ was significantly related to high take-off performance. During take-off, species had a stroke plane averaging approximately forty five degrees (Table 4.1), favouring lift and thrust production by forcing air downwards and backwards respectively, such as has been observed in pigeons during take-off (Berg and Biewener, 2008; Berg and Biewener, 2010). It appears that during slow speed take-off when the induced power requirements are high, varying the β and Φ may provide additional weight support (Berg and Biewener, 2008). As birds flap their wings they are rotated relative to the body, altering the air flow. The high Φ is likely to increase to profile drag (Pennycuick, 2008), and therefore the P_{pro} requirement, as seen here ($F_{1,9}$ = 62.36, r^2 = 0.89, P < 0.001). The benefits of increased Φ at low speeds in terms of take-off appear to outweigh the cost as profile power is a minor component of the total aerodynamic

power demand. The strategy of increasing Φ to increase wing velocity and generate more lift has been observed in *Drosophila melanogaster* fruit flies with variation in Φ increasing with reducing aerodynamic force (Lehmann and Dickinson, 2001) as the flies modulate their wing beat kinematics to enhance aerodynamic force production. High Φ may also reflect flight muscle strain trajectories or variation in flight muscle motor recruitment, as seen in the Anna's hummingbird that experienced a 1.7 fold increase in electromyography spike amplitude with increasing Φ (Altshuler et al., 2010b).

Previous studies have found that increased n improves take-off (Berg and Biewener, 2010; Robertson and Berg, 2012), but a significant relationship between n and increased P_{CoM} is not seen here. It was expected that increased n would indicate higher muscle contraction frequency (Robertson and Biewener, 2012), meaning more flight muscle power may be available. Birds can alter their n but within a limited range due to: bone and muscle stress, angular acceleration of the wing and moment of inertia, constraining the maximum, while the need for sufficient airflow over the wings during slow flight to generate the necessary thrust and lift, provides a minimum (Norberg, 1990). For high propulsion efficiency the optimum Strouhal number should be greater than 0.2 and less than 0.4 (Taylor et al., 2003). Species that are dynamically similar to each other should have Strouhal numbers that do not differ significantly (Alexander, 2003; Taylor et al., 2003). This may explain the relationship between n and M_b as the larger species beat their wings faster than predicted by geometric similarity (Table 5.2) to conform to dynamic similarity, as their Strouhal numbers are very similar with the exceptions of the chaffinch and barn swallow (Table 5.3). The average Strouhal number for the species is 0.31, which is very close to expected value of 0.3 where propulsion efficiency is predicted to peak (Taylor et al., 2003). It is important to note, however, that the Strouhal numbers calculated may be an under estimate as velocity was taken to be flight velocity and not the velocity of the wake. Future studies of birds flying at different speeds are therefore required with calculations of the velocity of the wake determined using particle image velocimetry techniques. Higher n could therefore benefit take-off by reducing the power required to generate lift for weight support.

The significantly inverse relationship between S% and take-off performance was unexpected as the opposite has been seen in other studies (Askew et al., 2001). However, it is important to note that all of the species studied dedicated more of the wingstroke to downstroke than upstroke, ranging from 51% (yellowhammer) to 62% (robin). A higher S% may suggest asymmetrical strain trajectories with the pectoralis spending more of the cycle shortening, allowing higher strain amplitudes, increasing muscle work and power output (Askew and Marsh, 1997; Askew and Marsh, 1998; Askew and Marsh, 2002; Askew et al., 2001). If muscle shortening durations are longer then more work and therefore power will be generated due to the more complete muscle activation (Askew et al., 2001; Askew and Marsh, 1998; Askew and Marsh, 2001), without a cost to initial mechanical efficiency (Holt and Askew, 2012). Over time, increasing S% further may reduce efficiency by increasing the rate at which metabolic substrates are needed to support the higher mechanical power output (Askew and Marsh, 2002).

The relationship between P_{aero}, P_{CoM} and wing beat kinematic traits is not reflected when the data is analysed without including the effect of phylogeny. The importance of wing beat kinematics on take-off performance has been observed in other studied, as discussed above, so the lack of a relationship may indicate the importance of including the effect of phylogeny in analyses, or could suggest that the effects of wing beat kinematics are species dependent. These hypotheses are not mutually exclusive but do demonstrate the importance of studying a diverse range of species.

4.4.2 *Take-off performance: effects of body mass*

There should be a cost to increased M_b as less muscle power is expected to be available due to the inverse scaling of n, and therefore muscle contraction frequency (to $M_b^{-0.33 \text{ to } -0.17}$, Rayner, 1995) to M_b, and also because of the positive relationship between P_{ind} and M_b (to $M_b^{1.10}$). The aerodynamic power requirement did increase significantly with M_b (Figure 4-3A) but this was due to the positive relationship between P_{CoM} and M_b (Figure 4-3B) which is only present when the phylogeny is incorporated in the analysis. It was predicted that heavier species would have

to expend more power to supporting body weight and therefore would have less power to accelerate and climb. There are several, not mutually exclusive, reasons why this may be the case. Larger species may have higher flight muscle masses relative to body fat, and may be able to produce more mechanical power. The total induced power is actually scaling with $M_b^{0.33}$ (Table 4.2), showing that the induced power required to create the downwash for weight support and to overcome the induced drag is less than expected for geometric similarity.

4.4.3 *Power requirements*

The high energetic demands of take-off are clearly apparent as all of the species studied had the majority of their P_{aero} requirement used to meet the P_{ind} (Figure 4-2) required to overcome the induced drag and weight support demands. This is not surprising considering the inverse relationship between flight velocity and w as P_{ind} is proportional to w (Pennycuick, 2008). Take-off is initiated from a stationary position and therefore the wings need to impart a downward momentum onto the air to generate the lift and thrust required to take-off and accelerate (Askew et al., 2001; Norberg, 1990; Pennycuick, 2008), increasing the work the flight muscles must do (Pennycuick, 2008). Both parasite and profile drag are expected to be relatively low at slow flight speeds (Pennycuick, 2008). The drag of the wings is more complicated as bird wings are not fixed like that of an aircraft, but flap and therefore the flapping speed and zero-lift profile drag coefficient are required (Norberg, 1990). Zero lift would be the optimum condition and a value of 0.02 was proposed by Rayner (Rayner, 1979) as bird wings are efficient aerofoils. This is the value that is used here but there is some uncertainty surrounding this value (Askew and Ellerby, 2007; Morris and Askew, 2010) and Usherwood (2009a) found that the $C_{D,\,pro}$ of a rotating pigeon wing was higher. The value used will affect the total aerodynamic power so the 0.02 $C_{D,\,pro}$ value used here may be a slight underestimate, but birds wings are deformable with feathers that can be separated (Rayner, 1979) and deflected (Carruthers et al., 2008; Carruthers et al., 2007) so as to maintain a near zero-lift drag coefficient.

4.4.4 *Implications*

Inter-specific variation in take-off performance is likely to influence a species ecological and behavioural responses due to the importance of take-off to flight initiation and predator evasion (Witter, Cuthill et al. 1994; Kullberg, Jakobsson et al. 1998; Williams and Swaddle 2003; Fernandez and Lank 2007). Trade-offs are likely to exist between the optimal morphologies that favour different types of habitat. Species that are non-migratory and occupy cluttered woodland habitats are likely to have evolved a wing morphology that differs from a species that forages in open habitat and migrates for long distances. The effect of phylogeny is therefore an important factor to consider when investigating the effects of morphological variation on performance. Even after controlling for the effects of evolutionary relatedness, inter-specific variation in wing morphology affected wing beat kinematics and take-off performance significantly.

The barn swallows (Figure 4-2), dedicated the least amount, 86%, of their aerodynamic power to overcoming the induced drag and to generating the induced velocity. This is possibly due to their lower induced drag as they have significantly higher AR than the other species whose AR do not differ from each other significantly (Table 4.1). The importance of increasing the potential and kinetic energy of the body's CoM is clear as all except the dunnock have higher P_{CoM} than $P_{ind'}$ (Figure 4-2). Blue tits and greenfinches also have relatively high $P_{ind'}$, demands compared to the other species (Figure 4-2). The higher mean rWL and therefore smaller wing areas of blue tits, as well as lower average n may explain this (Tables 4.1). Greenfinches are the heaviest species (Table 4.1) and therefore require more power to support their weight, $P_{ind'}$ constituting 43% of their P_{ind} requirement, whereas $P_{ind'}$ is less than 40% of the P_{Ind} in most of the other species (Figure 4-2). Dunnocks have the highest $P_{ind'}$ requirement as 52% of the P_{ind} is required for weight support (Figure 4-2). There relatively small wings and low Φ may mean they can't generate the extra lift needed to improve their take-off performance. The top performers are the yellowhammer, coal tit and tree sparrow that devote 68 and 65% of their P_{ind}, and 73, 70 and 68% of their P_{aero} respectively to P_{CoM} (Table 4.1). Yellowhammers have the highest Φ and β, coal tits are the lightest species and have high n and S%, and tree

sparrows have the highest n as well as high $S\%$ and low AR (Table 4.1). Short wings can be beat faster, at higher acceleration (Alexander, 2002; Warrick, 1998), increasing the amount of thrust and lift produced by the wings, and therefore P_{CoM}.

With the exception of the barn swallow, the species studied here are resident or partial migrants that forage and nest in woodlands, gardens and field edges and therefore have similar habitat and potentially flight requirements. There are however differences in wing morphology and take off performance. Yellowhammers and tree sparrows appear to be able to compensate for non-optimal rWL for take-off, due to their low AR and wing beat kinematics that favour enhanced take-off, such as high Φ and β. The node containing both the tree sparrow and the dunnock have slightly higher, and the yellowhammer node has a much higher n than predicted for geometric scaling as should n should scale to $M_b^{-0.17}$. This may be to maintain high propulsion efficiency, conforming to dynamic similarity in that these species have Strouhal numbers within the optimum range for high propulsion efficiency (Table 4.3). As these three species spend much of their time in cover or on the ground, selection for large S for improved manoeuvrability and take-off may not be that strong, especially as they have the plasticity to alter their wing beat kinematics to enhance rapid take-off if required. Small differences in wing morphology that relate to variation in performance may reflect niche separation within a habitat. Blue tits and great tits are close relatives that forage in the same habitat both temporally and spatially. Great tits, however have better take-off performance potentially due to their relatively larger, broader wings and high n (Table 4.1). It has previously been observed that great tits will feed lower down and on the ground more often than blue tits (Diaz et al., 1998), possibly due to their reduced perceived predation risk, allowing vertical niche separation.

The species studied here represent a range of families but a limited number of habitats. Future studies will hopefully add not just to the number of taxa represented, but also include species that occupy more habitat types. The barn swallow was the only species that forages in open habitat, on the wing, and migrates, and therefore it is not surprising that this species take-off performance differs with low aerodynamic requirements but also low P_{CoM} (Figure 4-5A and B, Figure 4-6A and B). This species is specialised for endurance flight, spending most of its time on the wing

and this is reflected by wing morphology and movements to optimise efficiency such as high AR and b, and related low n and Strouhal number as flow separation from the edge of their high AR wings is weak (Taylor et al., 2003). Studying birds performing energetically demanding flight directly, using particle image velocimetry, would enable comparison with the indirect methods used here to see how models compare with direct measurements. Flight muscle power output has not been looked at here which would allow power requirements to be examined relative to the power available. This has been studied in quail (Askew et al., 2001) but for a greater understanding of the importance of take-off ecologically and how this may be reflected morphologically, further studies on more species are needed.

4.4.5 *Summary*

The variation in take-off ability that is observed across the species studied likely reflects differences in size, wing morphology and phylogeny. Once the effects of phylogeny were considered, larger species had shorter, broader wings than predicted by isometry, favouring improved take-off ability both directly and indirectly by affecting wing beat amplitude and stroke plane angle, which related to higher take-off power. Selection favours shorter, broader wings of low rWL and AR due to the interaction between ecology and take-off performance. Species that live in cluttered habitat that make many, short foraging trips may have evolved a wing morphology that improves their flight initiation. Improved take-off ability is also likely to improve an individual's ability to escape predation, improving survivorship. Species n were also positively allometric due to the need to maintain high propulsion efficiency, conforming to dynamic similarity. The ecological and behavioural decisions of a species are therefore likely to be influenced by differences in take-off performance due to variation in wing planform and movements. The interpretation of the effects of wing morphology and wing beat kinematics on performance is likely to be species dependent, as shown by the differences in the relationships observed when phylogeny is not incorporated in the analyses.

5 The mechanical function of the proximal wing musculature of the pigeon (*Columba livia*): during different modes of flight

Modulation of bird flight performance requires complex changes in the wing stroke kinematics. How the mechanical function of the wing muscles is co-ordinated to produce the complex changes during different modes of flight is unknown. In this study we determined the mechanical function of the pigeon biceps and scapulotriceps muscles during take-off, slow flight and landing. In order to determine the muscle's mechanical function, the muscle length change and activity patterns *in vivo* were simulated *in vitro* using the work loop technique for each of the three modes of flight.

The biceps muscle actively lengthened generating force from mid-upstroke to mid-downstroke. The muscle absorbed energy, doing negative work while actively lengthening. Force was high at the start of muscle shortening but net work was near zero. The scapulotriceps muscle was active from mid-downstroke to mid-upstroke when lengthening. Force generation started during muscle lengthening and the muscle absorbed energy. Force generation continued into shortening and the muscle generated net positive work.

The pattern of muscle force generation is consistent with the biceps muscle doing positive work to flex the elbow from mid downstroke to early upstroke, and then absorbs energy and increases force output to resist elbow and stabilise the elbow as the wing decelerates at the end of the upstroke and into the downstroke. The scapulotriceps muscle generated positive work to re-extend the elbow at the end of the upstroke through the upstroke-downstroke transition, stabilising the elbow by producing force during lengthening to stabilise the elbow during the downstroke. The function of both muscles was generally consistent between the three modes of flight studied, but variation in the biceps muscle activation between slow flight and landing, may modulate muscle work and power output, maintaining stereotypy of wing beat kinematics.

5.1 Introduction

To understand the biomechanical constraints acting on flight requires knowledge of the function of the skeletal muscles involved in moving the limbs and imparting forces to the environment. Flight is a demanding mode of locomotion (Robertson and Biewener, 2012) as power is required to generate forces by doing muscular work, so as to support body weight, accelerate, overcome drag on the wings and the body (Pennycuick, 2008), and to move the limbs of the bird. The mechanical function of the flight muscles may be modulated to meet varying power requirements due to the hypothesised U-shaped relationship between total flight power required and flight velocity (Askew and Ellerby, 2007; Morris and Askew, 2010a; Pennycuick, 2008; Rayner, 1979; Tobalske et al., 2010). At different flight velocities, the importance of induced, profile and parasite drag will change (Norberg, 1990) and therefore a bird may change their wing beat kinematics in response. This is made possible by intrinsic wing muscles that are crucial for controlling the shape and position of the wings. Natural selection acts on skeletal muscles to optimise function (Ellerby and Askew, 2007; Hoppeler and Flück, 2002). The work done by the pectoral muscles: the pectoralis muscle that is the main wing depressor and pronator (Proctor and Lunch, 1993), and the supracoracoideus muscle that is the main elevator and supinator of the wings (Sokoloff et al., 2001), but the control of wing shape and posture relies on the mechanical function of the muscles within the wings. An understanding of the mechanical function of these muscles is therefore important in understanding how birds control the shape and position of their wings during the wing stoke, and therefore wing beat kinematics. The energetic requirements of skeletal muscles are also linked to their mechanical function so an understanding of the energetic requirements of a mode of flight can only be obtained by knowing mechanically how the flight muscles are functioning.

Previous studies of wing muscle activity patterns (Dial, 1992) and strain trajectories (Robertson and Biewener, 2012) relative to the wingstroke, as well as the attachments of the biceps and scapulotriceps within the proximal wing, suggest that they function as an elbow flexor and extensor, respectively. Robertson and Biewener (2012) from their measurements of muscle: strain trajectory, activity, intensity and duration, hypothesised muscle function, predicting when

force was likely to be high, and when work was being done by or on the muscle studied. However, predicting force from muscle activation does not account for the force that is generated after muscle deactivation (Biewener, 2011), and net work, and therefore muscle-mass specific power, was not measured. The scapulotriceps muscles are active as the muscles are stretched and also at the start of muscle shortening (Robertson and Biewener, 2012), so it is predicted that force will rise during lengthening, stabilising the elbow by resisting elbow flexion, and remain high at the beginning of shortening as the elbow extends. Net work will therefore be positive. The biceps muscles are active primarily during the lengthening of these muscles (Robertson and Biewener, 2012), suggesting force will peak at around maximal muscle length as work is done onto the muscle to lengthen it. It is however difficult to predict the pattern of force generation as the latency between activation and force production and the rates of rise and relaxation of force are unknown for these muscles. Net work and power output is expected to be low as the energy required to shorten and do positive work to flex the elbow, is likely to be partially offset by the kinetic energy absorbed during muscle lengthening. As the duration of muscle activity in the biceps and scapulotriceps was found not to vary across flight types (Robertson and Biewener, 2012), it is also hypothesised that muscle function will be stereotypical, regardless of flight mode. Muscle function could potentially vary with flight velocity but as the flight velocities that the pigeons flew at are similar and relatively slow, it is unlikely that muscle function will differ with flight mode. By maintaining a constant function may also simplify the neuromuscular control of the position and shape of a wing, with the differing aerodynamic requirements of different modes of flight met by varying body pitch changing the effective angle relative to the body that the wings beat (Robertson and Biewener, 2012).

Our knowledge of the mechanics of the wing musculature is limited to the activity patterns (Dial et al., 2001; Robertson and Biewener, 2012) and strain trajectories relative to the wing stroke (Robertson and Biewener, 2012), and the fibre type found in the triceps brachii, which show interspecific variation and may relate to differences in flight behaviour (Welsh and Altshuler, 2009). The relationship between the wing positions during the wing stroke and the activity of different wing muscles was recorded using electromyography (EMG), further to this Robertson and Biewener (2012) have studied the activity and strain trajectory, additionally using

sonomicrometry to determine muscle length changes, of three proximal wing muscles in the pigeon during three different modes of flight. To elucidate how the wing muscles function to control the shape and posture of the wings during the wing stroke, knowledge of the force generated during a muscle length change cycle is still required.

The aim of this study was to determine the mechanical function of two wing muscles: the biceps brachii (biceps) muscle and scapulotriceps muscle, in controlling wing shape and wing beat kinematics during take-off, slow and landing flight. The function of these muscles and whether this changes with flight mode was investigated in pigeons using the work-loop technique (Josephson, 1985) to ascertain when force was generated in the muscle length cycle~~,~~. The *in vivo* measures of strain and activation during take-off, mid-flight and landing, measured during an earlier study (Robertson and Biewener, 2012), were used to stimulate the biceps muscle and scapulotriceps muscle *in vitro* and aligned to the wing beat kinematics to elucidate muscle function.

5.2 Materials and methods

5.2.1 *Animals*

Eighteen pigeons (*Columba livia*, Gmelin 1789) were sourced from local suppliers from Bradford (West Yorkshire, UK) and Sunderland (Tyne and Wear, UK). They were housed within the University of Leeds animal unit (Leeds, West Yorkshire, UK) and were provided with food and water *ad libitum*.

5.2.2 *Muscle strain and activity patterns*

In a previous study conducted by Robertson and Biewener (2012), the muscle length trajectories and activity patterns were determined using sonomicrometry and electromyography in pigeons performing three different modes of flight: taking-off from a perch (take-off), flying between two perches (mid-flight) and landing on the second perch (landing)

The raw sonomicrometry and EMG data collected for each individual bird was analysed (see Section 5.2.3 and 5.2.4) in Igor Pro (version 6.22a, WaveMetrics Inc., Lake Oswego, Oregon, USA) to determine representative length trajectories and activity patterns for each mode of flight. The values shown in table 5-1 came from one individual that had activity patterns and cycle frequencies representative of what was seen for the different flight types. This was done to make sure that the stimulation the muscle was subject to *in vitro* truly reflected the patterns that can be seen in nature which may not have been the case if the readings for each pigeon were averaged. The strain trajectories used were selected from the pigeon with a typical sonomicrometry trace for the flight mode examined.

Table 5.1 *Muscle strain and activity patterns measured in vivo for each mode of flight (Robertson and Biewener 2012) that were used to stimulate the biceps and scapulotriceps in vitro (± S.E.M).*

Muscle	Flight type	Cycle frequency (Hz)	EMG duration (ms)	Phase (ms)	Strain amplitude
Biceps	Take-off	9.6 ± 0.03	34 ± 0.001	1.0	0.129
	Mid-flight	8.6 ± 0.17	42 ± 0.004	1.3	0.100
	Landing	8.8 ± 0.20	22 ± 0.007	1.0	0.100
Scapulotriceps	Take-off	8.6 ± 0.02	37 ± 0.002	112	0.058
	Mid-flight	8.0 ± 0.21	44 ± 0.002	121	0.055
	Landing	8.2 ± 0.24	41 ± 0.002	118	0.058

5.2.3 *Muscle length trajectory*

For each mode of flight and for each muscle three wingstrokes were analysed. For each analysed wing stroke, the average strain (relative to the muscle's resting length) and cycle frequency were recorded and the timing of peak length noted. An average muscle length trajectory was calculated from the raw sonomicrometry data by fitting a Fourier series of the form:

$$L = \frac{a_0}{2} + \sum(a_n \cos qp + b_n \sin qp) \qquad [5.1]$$

where L is muscle length, a and b are Fourier coefficients, q is the harmonic number and p is the relative time (-π to π). Three, four and five harmonics were fit to the data and the series. Where the standard errors were small and increasing the number of harmonics did not improve the Fourier fit to the raw data, the Fourier series with the fewest harmonics was selected (Figure 5-1). The difference between the raw length change cycle and the Fourier fits of varying harmonics were calculated by subtracting the raw sonomicrometry data from the harmonic fit to the data series.

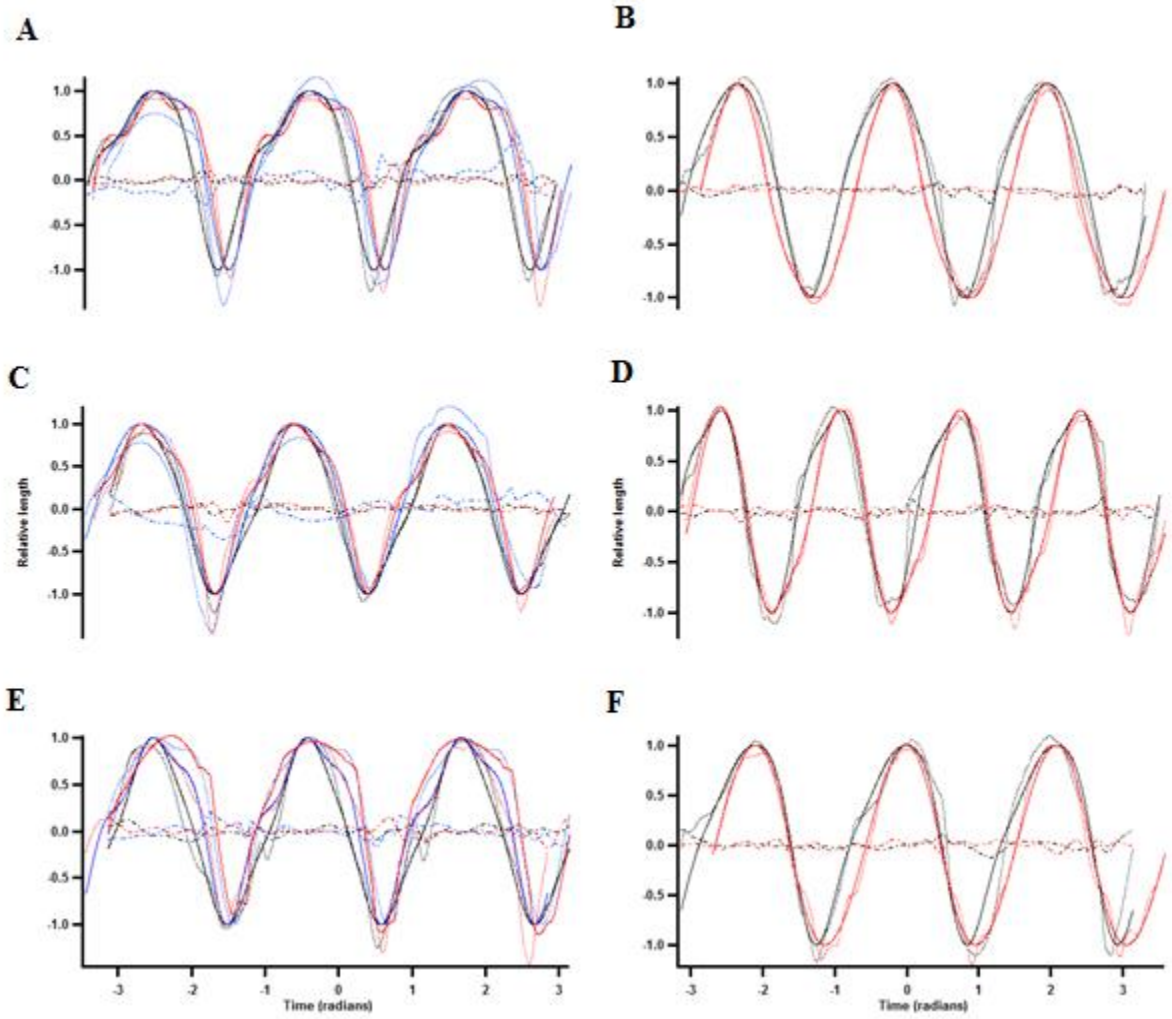

Figure 5-1 *The raw and Fourier smoothed length change traces for the biceps and scapulotriceps across flight mode, for each bird analysed. The raw (dotted lines), Fourier smoothed (solid lines), and standard errors for Fourier smoothing (dashed lines) traces for the three modes of flight; take-off (A and B), mid-flight (C and D), and landing (E and F), are shown. Different birds are represented by different colours with the black indicating the in vivo traces that the biceps (A, C and E) and scapulotriceps (B, D and F) were subjected to in vitro.*

5.2.4 *Analysis of electromyography recordings*

For the same wing strokes for which muscle length trajectory was analysed (Section 5.2.2.1), the electromyography recordings (Robertson and Biewener, 2012) were analysed in order to determine the relative timing and duration of muscle activity in relation to the strain trajectory. The onset, offset and EMG duration were determined for the rectified and filtered EMG signals (100 Hz to 1000 Hz band-pass Butterworth filter; see Robertson and Biewener, 2012). The EMG signals were inspected and the onset and offset of an EMG burst as well as the burst duration were recorded. The phase was also calculated as time of peak muscle length minus the time of EMG onset.

5.2.5 *In vitro muscle work and power output*

Animals were killed using an overdose of isoflurane completed with dislocation of the neck and either one of the scapulotriceps or biceps muscles was removed from the wing. The skin of the wing was removed from the top of the proximal humerus to the proximal ulna and radius, so as to reveal the scapulotriceps muscle and biceps muscle (Figure 5-2). Chilled (temperature of approximately 5 ^{o}C), oxygenated (95% O_2, 5% CO_2) Krebs-Henseleit Ringer's solution (composition in mmol l^{-1}: NaCl, 117; KCl, 4.7; $CaCl_2$, 2.5; $MgSO_4$, 1.2; $NaHCO_3$, 24.8; KH_2PO_4, 1.2; glucose 11.1) with a pH of 7.4 at 40°C, was used to irrigate the muscle during the dissection. The scapulotriceps was removed from its origin at the posterior scapula, at the edge of the glenoid cavity, to where it inserted, *via* a tendon, onto the dorsal olecranon of the ulna (Figure 5-1; Proctor and Lynch, 1993). The biceps (Figure 5-2A) was removed from the proximal humerus to the posterior part of the proximal radius (Figure 5-2) as this is the region of the muscle from which sonomicrometry and electromyography recordings were made (Robertson and Biewener, 2012). To facilitate attachment to the base of the muscle physiology chamber, the muscles were removed with small pieces of bone attached. Once removed, the muscle was put in a Petri dish containing chilled, oxygenated Ringer's solution and examined under a microscope

so any damaged muscle fibres and any additional tissue that was not part of the muscle could be removed.

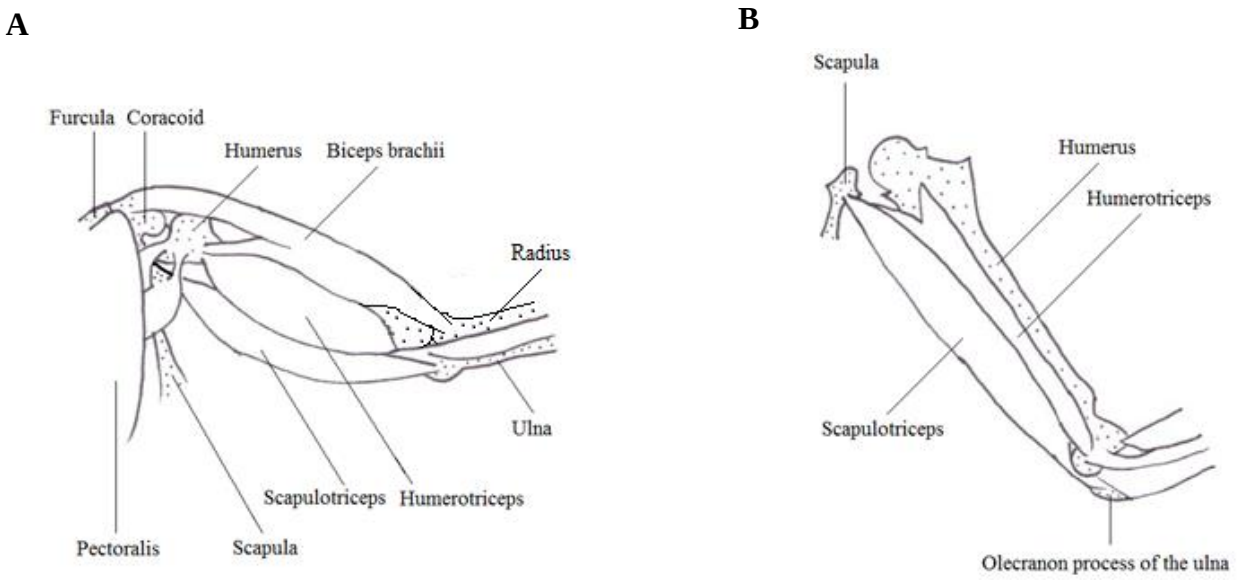

Figure 5-2 *Ventral view of the wing musculature showing the locations and attachments of; (A) the biceps brachii and (B) the triceps brachii (humerotriceps and scapulotriceps).*

The muscle was transferred to a muscle physiology chamber. One end of the muscle was secured, by the attached bone and tendon, to the base of a Perspex flow-through muscle chamber using stainless steel clips (Figure 5-3). The other end of the muscle was attached to a lightweight silver chain (0.41 g) *via* a silk suture (5-0; Sharpoint, Reading, PA, USA) that was tied onto the scapulotriceps tendon, or as near to the end of the biceps muscle fibres as possible without causing damage to the muscle fibres. The silver chain was attached to an ergometer (series 305B-LR; Aurora Scientific Inc., Ontario, Canada) that controlled the muscle strain trajectory (Figure 5-3). The stage the ergometer was mounted on was movable so that the muscle length (L) could be controlled. The muscle operating length(L_0) was set as the muscle length (L) at which maximum isometric force was produced, and the mean muscle length (L_m) was set as the mean muscle length measured *in vivo*, relative to the resting length (see Robertson and Biewener, 2012, figure 7). The muscle was stimulated by two platinum electrodes that were placed both

sides of the muscle, opposite each other, running the length of the muscle. Oxygenated Henseleit-Ringer's solution was circulated through the Perspex chamber. Immediately following the dissection, the Ringer's solution in the muscle chamber was approximately 5 ^{o}C and this was increased to 40^{o}C (the temperature of the flight muscles during flight; Ellerby and Askew, 2007) over a period of approximately 15 mins before starting the muscle physiology experiments.

Prior to starting the *in vivo* muscle length trajectory/ activity pattern simulations, an isometric twitch was performed. The muscle was supramaximally stimulated (0.2 ms pulse width), so as to activate all muscle fibres concurrently (Askew and Marsh, 2001), *via* two platinum electrodes placed adjacent to and running the full length of the muscle. A direct current power amplifier (LPF-202, Warner Instruments Corporation, USA) was used to amplify the stimulus power and ensure supramaximal stimulation. An isometric twitch was run prior to stimulating the muscle as measured *in vivo*. The work-loop technique (Josephson, 1985) was used to measure the force, work and power output of both the scapulotriceps and biceps *in vitro* under simulated *in vivo* conditions for each of the three modes of flight.

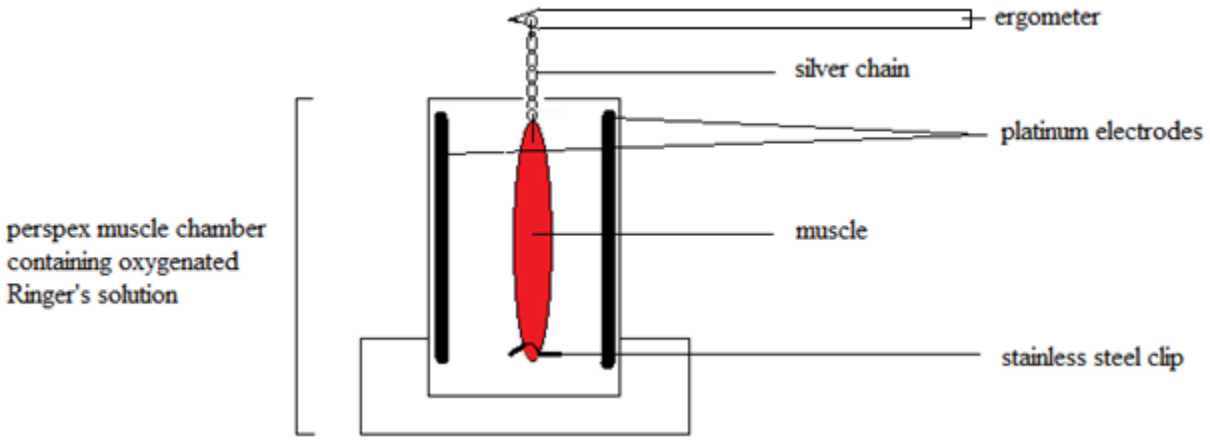

Figure 5-3 *Experimental set-up for the work-loop experiments. Flow-through Perspex muscle chamber containing the muscle irrigated by oxygenated (95% O_2, 5% CO_2) Ringer's solution.*

The biceps and scapulotriceps were subjected to the average strain trajectories and activity patterns (Figure 5-1) that were derived from the *in vivo* sonomicrometry and electromyography recordings (see Section 5.2.2; Table 5-1), for each mode of flight. The muscle was subjected to five cyclical contractions in which the length change of the muscle and pattern of stimulation simulated the *in vivo* conditions, which were preceded by five passive cycles simulating the *in vivo* length trajectory but without stimulation. The order in which the muscle was stimulated to match the flight mode measured *in vivo*, was randomised so that any differences in muscle work and power during different modes of flight reflected variation due to flight type stimulation pattern and not order in which the work-loop experiments were done. A computer-generated wave created by Testpoint (version 5, Capital Equipment Corporation, MA, USA) was converted to an analog signal by a 16-bit A/D converter and this was used to control the ergometer (series 305B-LR, Aurora Scientific Inc., Ontario, Canada). The relevant cycle frequency, activity duration and phase relative to peak length, for the muscle and flight mode were entered into Testpoint (table 5.1). A 12-bit D/A converter (DAS-1801AO; Keithley Metrabyte, Keithley Instruments Inc., Ohio, USA) was used to record the force and length outputs. These outputs were amplified (LPF-202, Warner Instruments Corporation, Connecticut, USA). Cycle's two to four or five were analysed, as quantified in vivo for each mode of flight. Both active (stimulated) and passive (unstimulated) cycles were run for each flight mode. Force, work and power were averaged across the cycles analysed.

Between each set of work-loop experiments, the muscle was left to recover for 5 mins before performing an isometric twitch. Changes in twitch force were used to assess any decline in the muscle's performance. Decline was corrected for (in the simulated cycles) by assuming a linear decline between isometric twitches and if isometric twitch force dropped below 80% of the initial (or highest) twitch recorded, then the muscle performance was deemed to have reduced too much to give a reliable measure of muscle power and subsequent measurements were discarded. The muscle was finally stimulated for 250 ms at a frequency 150Hz to perform an isometric tetanus. The frequency was selected as this is when muscle produced a fully fused tetanus. Peak tetanic force was determined by multiplying the maximum isometric twitch force by the twitch:tetanus ratio determined at the end of the experiment, thereby correcting for any

decline in the preparation. The muscle fibre bundle was then pared down, so that only undamaged fibres remained, and the mass of the remaining muscle fibres was determined. The length cycle was differentiated in respect to time to determine the shortening velocity. The instantaneous mechanical power of the muscle was calculated as force multiplied by shortening velocity relative to muscle-mass. The power output by a muscle *in vitro* were corrected for muscle decline (as previously described) and was given relative to the intensity of muscle activation. To allow comparison between muscles and birds the relative intensity of muscle activation was used which was calculated by normalising the largest muscle intensity for each mode of flight (see Robertson and Biewener, 2012, figure 4C).

5.2.6 *Wing beat kinematics and muscle function*

To determine muscle mechanical function, the strain (ratio of muscle length change relative to initial muscle length) and force during a wing beat were compared to the shoulder and elbow joint positions that had been previously reported (see Robertson and Biewener, 2012). The wing beat kinematics shown graphically in Figure 3 in Robertson and Biewener's article (2012) showed the position of the wrist and shoulder, with the elbow position approximated relative to these, during the wing beat for several wing strokes. The wing beat kinematics for the five wing beats of take-off were digitised using Plot digitiser (SourceForge, Dice Holdings Inc, CA, USA). A Fourier series in the form shown in equation 5.1 was used to fit three, four or five harmonics to the digitised coordinate points. Where there was no improvement in the fit to the raw data, the Fourier series with the fewest harmonics was selected. The position of the elbow and humerus during a wing beat were re-plotted in relation to the muscle strain and force that was measured *in vitro* for both the scapulotriceps and biceps.

5.2.7 *Statistical analysis*

The differences between the tetanic forces and isometric stresses produced by the scapulotriceps and biceps were analysed using a t-test. General linear models (GLM) were used to determine

the effects of muscle type, flight mode and the interaction between these two factors, on the P_{mech} and the muscle-mass specific work which were followed by a Tukey post-hoc test if significant. These tests were carried out in Minitab 16 (Minitab Inc, State College, Pennsylvania, USA) and Microsoft Excel 2010 (Microsoft UK, Reading, Berkshire, UK). The muscle-mass specific lengthening work would not normalise and therefore a Scheirer-Ray-Hare test was used as the non-parametric equivalent of a GLM. The mean sums of squares total (MS_{total}) divided by the sums of squares (SS), degrees of freedom and P statistic are given for this test. The latter test was conducted in SPSS 20.0 (IBM CorpIBM SPSS Statistics for Windows, Version 20.0. Armonk, NY, USA).

5.3 Results

The results of the Fourier smoothing of the raw sonomicrometry data for representative scapulotriceps and biceps, is shown below (Figure 5-4). The trace fitted with three harmonics was used as increasing the number of harmonics did not improve the fit further.

A

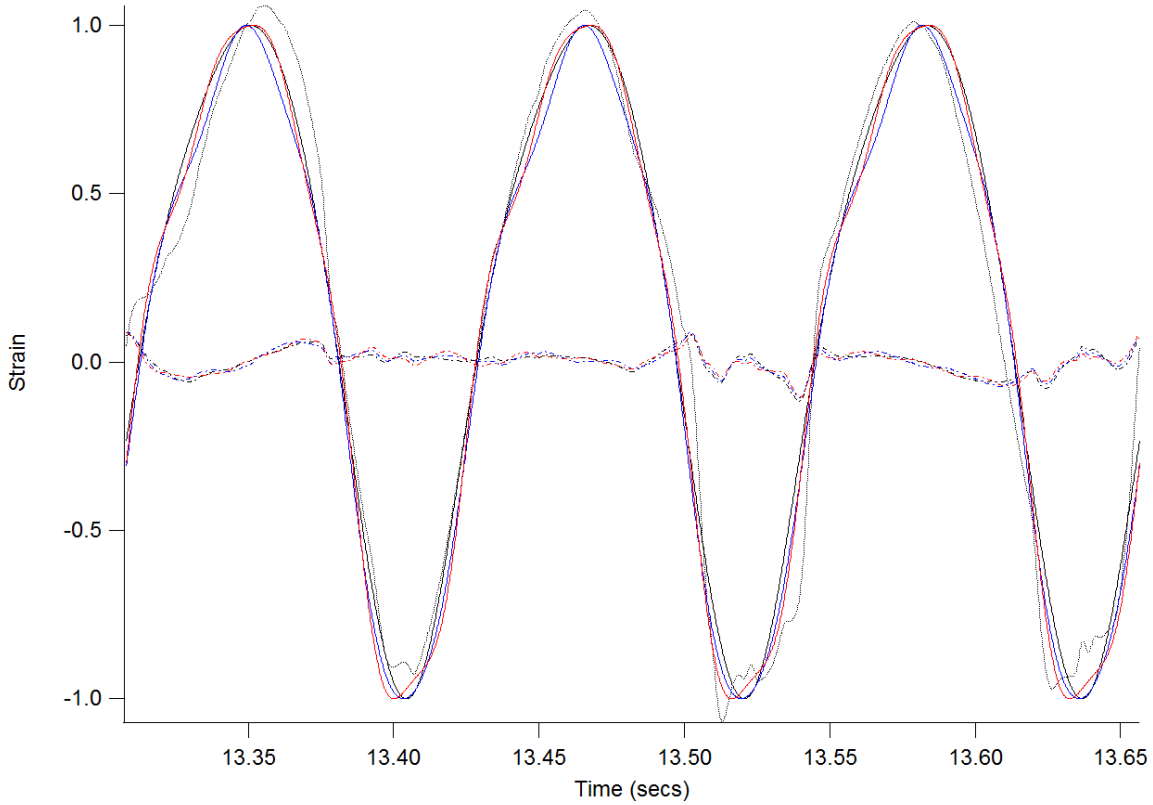
1.0
0.5
0.0
-0.5
-1.0
Strain
13.35
13.40
13.45
13.50
13.55
13.60
13.65
Time (secs)

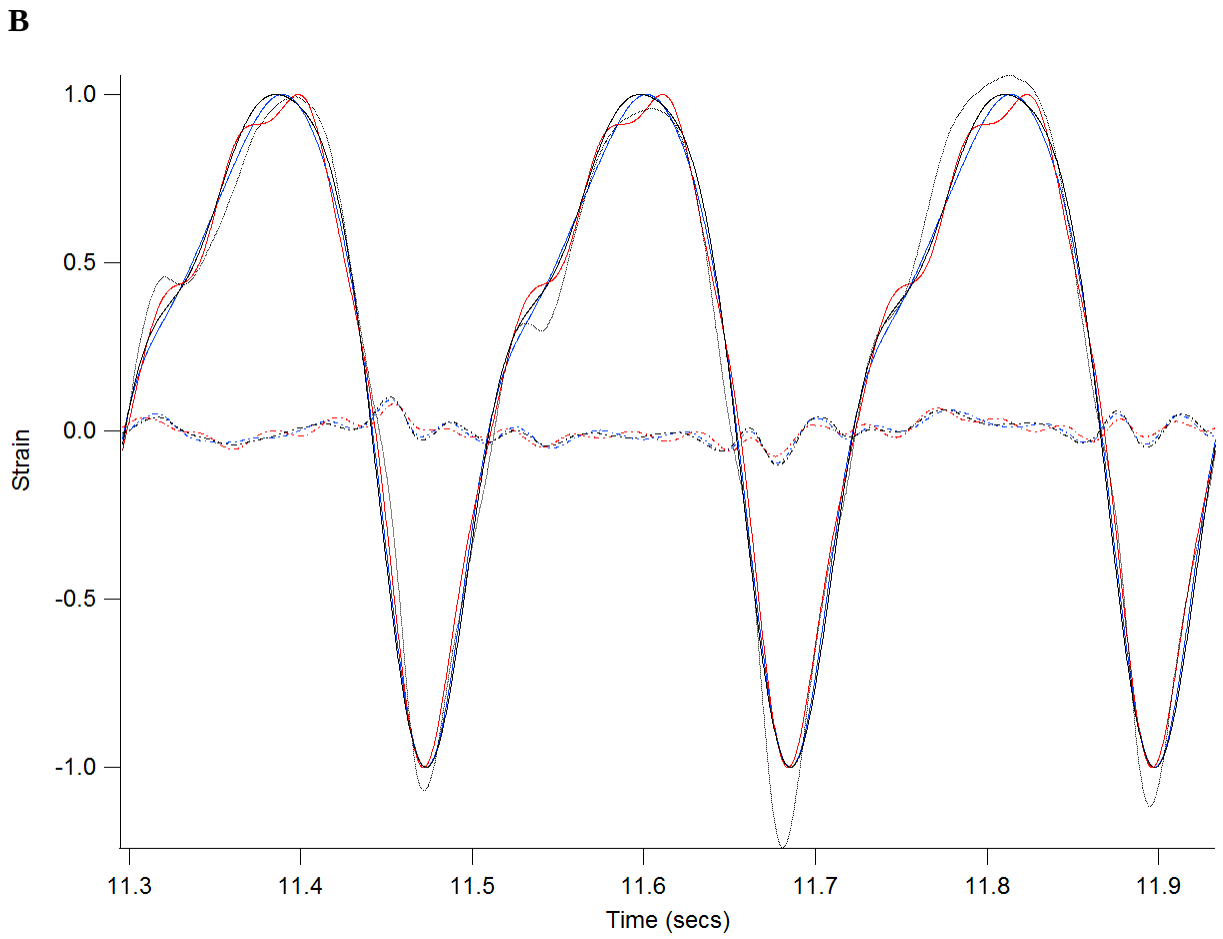

Figure 5-4 *Representative plots of the strain trajectories for the scapulotriceps and biceps after Fourier smoothing. Fourier smoothing using three (solid black), four (solid blue) and five (solid red) harmonics plus their standard errors (dashed lines, colours as above), are shown. The raw sonomicrometry trace is also shown (black dots). These are representative plots for each muscle; (A) scapulotriceps and (B) biceps, taken from one bird recorded during take-off flight.*

Data was obtained from six birds for the scapulotriceps and seven birds for the biceps. The mean body mass (M_b), muscle mass (M_m) and L_O are shown in table 5.2. The mean relaxation time for during take-off, midflight and landing were; 0.046 ± 0.002, 0.050 ± 0.005, and 0.050 ± 0.006 secs respectively for the scapulotriceps, and 0.071 ±0.02, 0.052 ±0.03 and 0.065 ±0.02 secs respectively for the biceps. The time taken from peak twitch force to 90% relaxation ($t_{90\%R}$) during take-off, midflight and landing were; 0.041 ± 0.002, 0.048 ± 0.007, and 0.045 ± 0.005

secs respectively for the scapulotriceps, and 0.064 ± 0.02, 0.047 ± 0.01 and 0.058 ± 0.01 secs respectively for the biceps.

Table 5.2 *The average body mass, muscle mass and operating length for the scapulotriceps (N = 6) and biceps (N = 7). Standard errors are shown.*

Muscle	Body mass (g)	Muscle mass (g)	Muscle operating length (L_m) (mm)
Scapulotriceps	296.63±14.68	0.964±0.05	40.88±0.49
Biceps	286±10.02	0.457±0.06	30.86±0.00

The scapulotriceps produced significantly higher isometric tetanic force than the biceps (t-test: $t_{11} = 5.07$, $P < 0.001$), but the muscles did not vary significantly in isometric stress (t-test: $t_5 = 1.69$, $P = 0.15$). The isometric twitch to tetanic ratio and stresses for the scapulotriceps (Table 5.3) and the biceps (Table 5.4) are summarised below. The isometric tetanus was done at the end of the work-loop experiments so as not to damage the muscle. The stresses shown have been corrected to account for muscle deterioration in the muscle, but stresses vary considerably and are likely to represent the range of stresses possible for the muscles analysed, rather than the definitive mean value for stress obtained for either muscle.

Table 5.3 *The twitch to tetanus ratio and tetanic stress for the scapulotriceps.*

	Bird						Average
	2	3	9	10	11	12	
Twitch: tetanus	0.27	0.24	0.15	0.07	0.33	0.22	0.21
Stress (kNm^{-2})	91.94	174.75	279.47	1064.14	172.95	412.08	365.89

Table 5.4 *The twitch to tetanus ratio and tetanic stress for the biceps*.

	Bird							Average
	6	7	8	14	15	17	18	
Twitch: tetanus	0.34	0.42	0.36	0.21	0.28	0.20	0.24	0.29
Stress (kNm^{-2})	368.30	67.99	25.41	70.86	94.43	77.01	42.91	106.70

5.3.1 *Mechanical power and flight mode*

The P_{mech} reported in the following section have been corrected for muscle decline (as explained in section 5.2.3) and was also calculated to be relative to the intensity of muscle activation (see Roberson and Biewener, 2012, Figure 4C). The scapulotriceps output significantly more muscle-mass specific power (P_{mech}) than the biceps (two-way ANOVA: $F_{1,20} = 63.57$, $P < 0.001$) but the P_{mech} output was not related to flight mode (two-way ANOVA: $F_{2,20} = 0.30$, $P = 0.74$). The differences in P_{mech} for the two muscles across the different flight modes are shown below (Figure 5-5), both before correcting for relative activation of the muscle (Figure 5-5A) and after correction (Figure 5-5B).

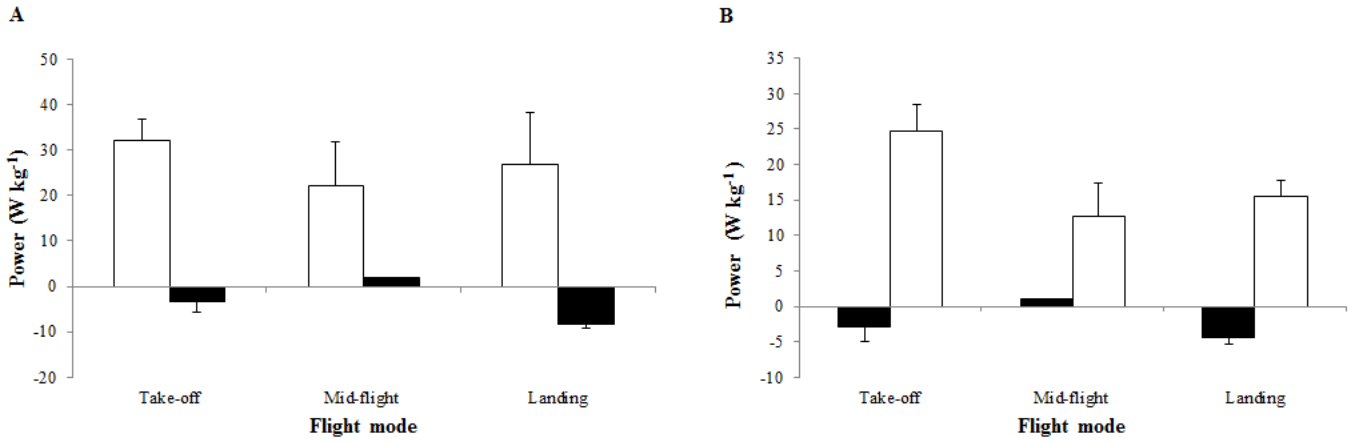

Figure 5-5 *Muscle-mass specific net power output, pre- and post-correction for recruitment, during different modes of flight for the scapulotriceps (open bars) and biceps (solid bars). Powers are corrected for muscle decline and (A) is pre-correction for relative intensity for recruitment and (B) is relative to the intensity of muscle activation.*

5.3.2 *Muscle length change and force production*

The muscle force generated by the scapulotriceps muscle peaked just after peak muscle length, approximately at mid upstroke, as the muscles started to shorten (Figure 5-6A). The scapulotriceps continued to shorten, doing positive work (Figure 5-6B) until the upstoke-downstroke transition, while force dropped (Figure 5-6). The muscle force is low and relatively constant at mid downstroke as the scapulotriceps re-lengthens back to L_o. The muscle is actively lengthened between mid downstroke and mid upstroke (Figure 5-6A) and force rises as work is done onto the muscle (Figure 5-6B).

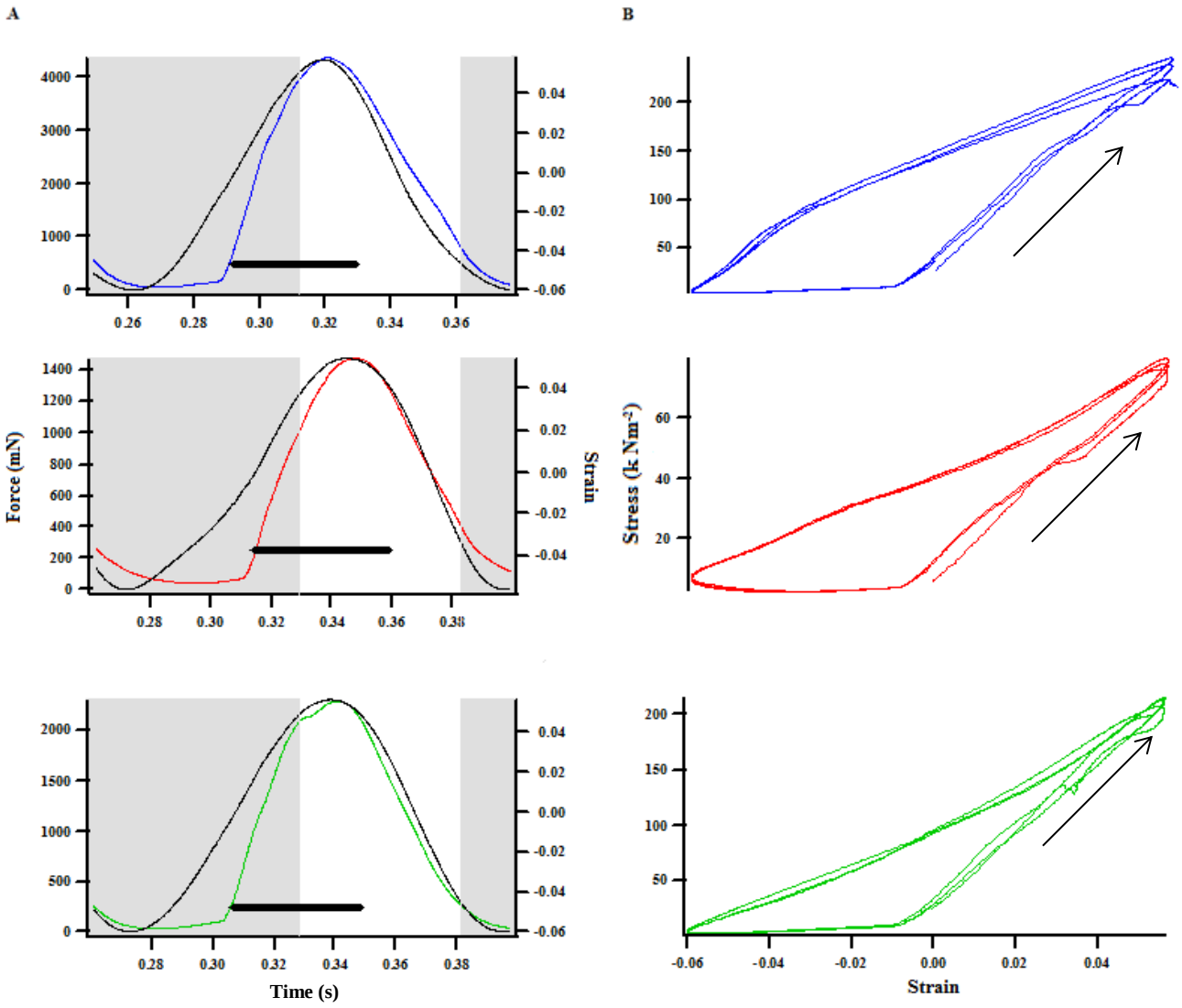

Figure 5-6 *Scapulotriceps muscle force and work relative to muscle strain during the wing beat cycle for each flight mode. Scapulotriceps during; take-off (blue), mid-flight (red) and landing (green). (A) Changes in muscle force and strain, through time. The shaded area represents the downstroke. The black bar shows when the muscle was stimulated (with SEM). (B) work-loops showing stress against strain. Representative plots for the birds analysed.*

The biceps produce most force around mid downstroke when the muscle is at peak length (Figure 5-7A). The muscle shortens, doing minimal positive work (Figure 5-7B), from mid to late downstroke (Figure 5-4A). Force drops to near zero from approximately late downstroke to the downstroke – upstroke transition (Figure 5-7A). Similarly to the scapulotriceps, the biceps are actively lengthened, with force rising to a peak when muscle length is maximal (Figure 5-7A). The muscle is active from the upstroke – downstroke transition to approximately mid downstroke (Figure 5-7A). The biceps do negative work when they are being actively lengthened and positive work during shortening, resulting is near zero net work (Figure 5-7B).

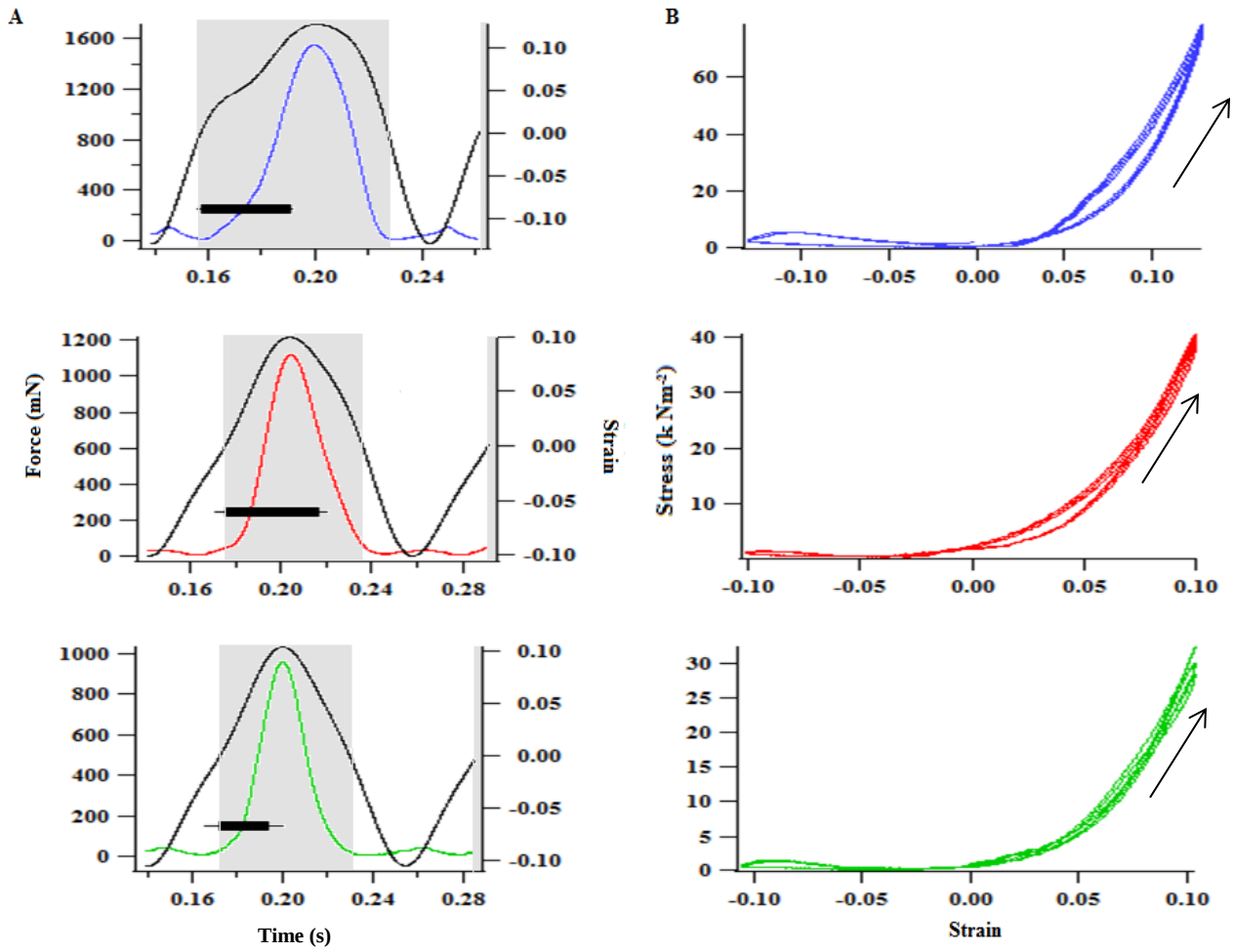

Figure 5-7 *Biceps muscle force and work relative to muscle strain during the wing beat cycle for each flight mode. Biceps during; take-off (blue), mid-flight (red) and landing (green). (A) Changes in muscle force and strain, through time. The shaded area represents the downstroke. The black bar shows when the muscle was stimulated (with SEM). (B) work-loops presented as a plot of stress against Representative plots for the birds analysed.*

The cycle work during different modes of flight for the scapulotriceps and biceps is shown in table 5.5 below. The muscle-mass specific shortening work is not dependent on the muscle type (GLM: $F_{1,20} = 0.59$, $P = 0.45$, log-transformed data) but is dependent on the mode of flight (GLM: $F_{2,20} = 5.51$, $P < 0.05$) as the shortening work done during take-off is greater than that during mid-flight and landing (Tukey post-hoc test: $P < 0.05$). There is a significant interaction between the shortening work and the mode of flight (GLM: $F_{2,20} = 3.90$, $P < 0.05$). There was no difference between the muscles ($MS_{total}/SS = 0.06$, d.f. = 1, $P = 0.81$) or mode of flight ($MS_{total}/SS = 0.22$, d.f. = 2, $P = 0.22$) and the two factors did not interact ($MS_{total}/SS = 0.96$, d.f. = 2, $P = 0.62$) when analysing the muscle-mass specific lengthening work. The variation in the net muscle-mass specific work was due to the type of muscle (GLM: $F_{2,20} = 5.20$, $P < 0.05$) with the scapulotriceps doing more net work than the biceps (Tukey post-hoc test: $P < 0.05$). There was no relationship between the mode of flight and the net work output (GLM: $F_{2,20} = 0.03$, $P = 0.98$). There was also an interaction between the net work and the mode of flight (GLM: $F_{2,20} = 5.20$, $P < 0.05$).

Table 5.5 *Cycle work during different modes of flight in the scapulotriceps and the biceps. Shows the amount of work done by a muscle to shorten and the work done onto a muscle to lengthen it. The muscle-mass specific work is also shown. Work is corrected for muscle activation intensity and is measured in Joules. Means are given with S.E.M.*

Work		Scapulotriceps			Biceps		
		Take-off	Midflight	Landing	Take-off	Midflight	Landing
Shortening (mJ)	absolute	6.64 ± 1.41	2.29 ± 1.11	5.57 ± 1.00	3.86 ± 0.97	1.14 ± 0.30	0.92 ± 0.30
	Muscle-mass specific	7.82 ± 2.07	2.44 ± 1.22	5.77 ± 0.97	10.48± 4.75	2.73 ± 0.34	1.41 ± 0.49
Lengthening (mJ)	absolute	-3.91 ± 0.68	-1.31 ± 1.07	-3.55 ± 1.22	-4.62 ± 1.26	-0.89 ± 0.42	-1.20 ± 0.27
	Muscle-mass specific	-4.54± 1.11	-1.38 ± 1.15	-3.73 ± 1.21	-11.91 ± 5.73	-2.12 ± 0.41	-1.48 ± 0.48
Net (mJ)	absolute	2.73 ± 0.89	0.98 ± 0.90	2.02 ± 0.50	-0.76 ± 0.36	0.25 ± 0.08	-0.11 ± 0.14
	Muscle-mass specific	3.28 ± 1.00	1.06 ± 0.59	2.05 ± 0.28	-1.43 ± 0.60	0.61 ± 0.06	-0.07 ± 0.15

5.3.3 *Mechanical function*

The scapulotriceps actively lengthens, generating force, as the biceps shortens (Figure 5-8). Peak force is reached in the scapulotriceps at the start of muscle shortening, when strain is maximal (Figure 5-8A), as the elbow extends and the humerus is dorso-ventrally elevated and antero-posteriorly retracted (Figure 5-8). This occurs during the upstroke (Figure 5-6A), between when the biceps are at minimum strain to when they re-lengthen back to L_O and zero strain (Figure 5-8). Peak force and strain in the biceps, occurs at mid downstroke as the muscle begins to shorten (Figure 5-7A) and the elbow flexes (Figure 5-8). Biceps shortening also coincides with humeral dorso-ventral depression and the humerus begins to retract antero-posteriorly (Figure 5-8).

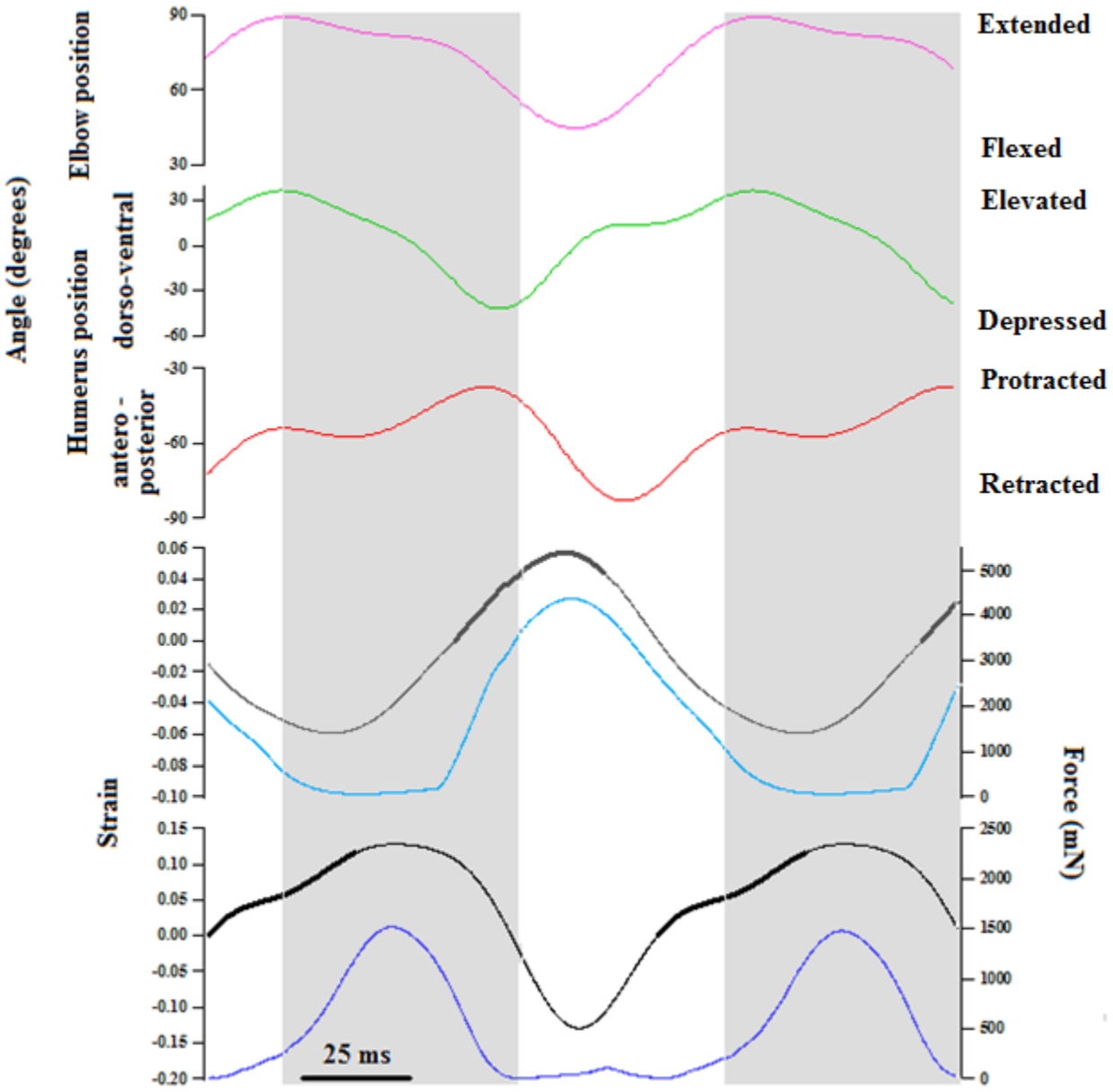
Angle (degrees)
Elbow position
Humerus position
dorso-ventral
antero - posterior
Strain
Force (mN)
Extended
Flexed
Elevated
Depressed
Protracted
Retracted
25 ms

Figure 5-8 *The position of the elbow and humerus during take-off flight relative to muscle strain, activation and force for the scapulotriceps and biceps. Scapulotriceps and biceps: force (light blue, navy) and strain (grey, black) respectively (bold lines indicate when the muscle was stimulated). Elbow (pink) and humerus position (dorso-ventral: green, antero-posterior; red), from the wing beat kinematics, adapted from Robertson and Biewener, (2012), relative to the wingstroke (USDS: upstroke – downstroke transition, DSUS: downstroke – upstroke transition). Shaded area represents the downstroke and muscle strain and force traces reflect when a muscle was stimulated in vitro with the strain and activity patterns measured in vivo during mid-flight.*

5.4 Discussion

Analysis of the strain trajectories and activity patterns of the biceps and scapulotriceps measured *in vivo*, during flight of the pigeon, by Robertson and Biewener (2012), made clear predictions on muscle function. This is the first study to determine the mechanical work and power of intrinsic wing muscles, allowing the hypotheses of mechanical muscle function of intrinsic wing muscles that were made from examining activity patterns and strain trajectories, to be tested. We also determined whether muscle function was stereotypical across flight modes as suggested by Robertson and Biewener (2012).

5.4.1 *Mechanical work and muscle function*

At the end of the downstroke the scapulotriceps is actively stretched, generating force and absorbing energy. This occurs as the elbow is being flexed (Figure 5-8) and may suggest a role for the scapulotriceps in stabilising the elbow as work is absorbed during late downstroke, through the downstroke-upstroke transition, as predicted by Robertson and Biewener (2012). At the start of muscle shortening, the muscle is still active and this coincides with elbow extension (Figure 5-8), indicating a role in this action. Force drops during shortening, possibly as the muscle is relaxing and also in part because of the force-velocity relationship of the muscle. Net work is positive, as is power and the work and power generated by the scapulotriceps does not

vary with flight mode. As the scapulotriceps is biarticular, crossing both the shoulder and elbow joint, the muscle could potentially be involved in humeral elevation. As the scapulotriceps shorten, the humerus is elevated, supporting the potential role in humerus elevation. Robertson and Biewener (2012) also noted that the humerus was elevated as the scapulotriceps shortened but as they had not measured muscle force or work, whether this was coincidental as the supracoracoideus is thought to be the primary wing elevator (Proctor and Lynch, 1993), could not be determined. It has been shown in starlings that the wing can be elevated when the supracoracoideus has been removed, suggesting the role of other muscles in wing elevation (Sokoloff et al., 2001). This research provides some support to the scapulotriceps being one of the muscles potentially involved in wing elevation.

The biceps muscle is activated in late upstroke, when the muscle is being stretched, and remains active until mid-downstroke, prior to muscle shortening (Figure 5-7A). When strain is high and the muscle lengthens, there is a slight protraction of the humerus (Figure 5-8) but humeral retraction and elevation occur during shortening, from late upstroke through the early part of the upstroke. This coincides with elbow flexion, suggesting a role for the biceps in this action, supporting earlier work (Dial 1992). The net power and work generated by this muscle is near zero as similar amounts of work are done onto the muscle as it lengthens as is done by the muscle to shorten. Work generated does vary with flight mode and is discussed below (section 5.4.3), and as force is high during active lengthening, this suggests the biceps may absorb kinetic energy from the distal wing as work is done onto the muscle. Force increases as the elbow is being extended, and may therefore indicate a role for the biceps in elbow stabilisation as the biceps absorb work. Robertson and Biewener (2012) predicted that force would be generated during both lengthening and shortening, and that the biceps may act to stabilise the elbow.

5.4.2 *Antagonistic functioning of the scapulotriceps and biceps*

The anatomical position and muscle attachment of the scapulotriceps and biceps suggests they may act antagonistically to each other. As the biceps and scapulotriceps co-contract, the biceps muscle shortens and the scapulotriceps re-lengthens from below its initial length to

approximately half peak scapulotriceps length. The work performed by the biceps during this co-contraction period is 6.21 mJ in the case shown in figure 5-8 above, whereas 7.98 mJ of work is done to lengthen the scapulotriceps during the same time period. The negative work needed to lengthen the scapulotriceps muscle is greater than the work done by the biceps and therefore another muscle and/or the inertial movement of the wings is likely providing the energy to lengthen the scapulotriceps. The stabilisation of the elbow during flexion by the scapulotriceps may be performed by the absorption of inertial energy during wing motion or due to work done by muscles other than the biceps as the scapulotriceps lengthen.

5.4.3 *Differing roles of muscles*

During flapping flight the pectoralis needs to do a large amount of mechanical work by shortening over a large part of its fibre length (Biewener, 2011). Due to the long fibre lengths within the pectoralis, the muscle can generate large strains (Biewener, 2011). Force enhancement can also occur during active lengthening (Askew and Marsh, 2002) maximising the work that can be done during shortening (Biewener, 2011). The pectoralis modulates the mechanical power output by increasing the amount of a cycle that is spent shortening, increasing the mechanical work done by the muscle (Askew et al., 2001; Ellerby and Askew 2007; Holt and Askew, 2012a; Josephson, 1985), therefore maximising the mechanical power that is available (Askew et al., 2001; Ellerby and Askew, 2007). This has been seen during take-off in a number of bird species (Askew and Marsh, 1997; Askew and Marsh, 1998; Askew and Marsh, 2002; Askew et al., 2001) as more power is required to take-off due to the high induced power requirements at slow flight velocities (Askew et al., 2001; Norberg, 1990; Pennycuick, 2008).

Flight muscles are also required to control wing shape and stroke kinematics, such as the role of the scapulotriceps and the biceps. These muscles need to do positive work when shortening to move joints, but also are involved in elbow stabilisation and therefore absorb work during lengthening (Table 5-5). The muscle-mass specific net work and power generated by the scapulotriceps is positive and is greater than the P_{mech} and net work of the biceps. The

scapulotriceps muscle shortening cycle is near symmetrical, unlike what has been seen in muscles function to produce large amounts of mechanical power to meet the high power requirements of particular tasks such as take-off and low speed flight in some birds (Askew et al 2001, Ellerby and Askew 2007, Holt and Askew 2012), scallops swimming (Holt and Askew 2012, Marsh et al 1992), and frog calls (Gigenrath and Marsh 1997, Holt and Askew 2012). The mechanical power output of the pectoralis in pigeons has been recorded as high as 105 W kg^{-1}, net work of 614 mJ and a strain of 42 in ascending flight. This compares to a maximum power of 25 W kg^{-1}, net work of 3.28 mJ and a strain of 0.12 generated by the scapulotriceps during take-off. The biceps have near symmetrical cycles but spend a slightly larger proportion of the cycle lengthening and absorbing work with near zero net work generated (Table 5-5). The highest mechanical power produced by the biceps is 1 W kg^{-1}, with a net work of 0.61 mJ, and strain of 0.26 during mid-flight. These values are far lower than seen in the pectoralis and demonstrate the important role the biceps play in stabilising the elbow from late downstroke to early upstroke.

5.4.4 *Flight mode*

Previous studies of the scapulotriceps and biceps muscle activity and strain trajectories have shown that intensity of activation (Dial, 1992; Robertson and Biewener, 2012) varies with flight type but muscle length trajectory does not (Robertson and Biewener, 2012). It was found here that the mechanical power output and therefore the power available to meet the power requirements for take-off, mid-flight and landing, did not vary significantly with flight type in either the scapulotriceps or the biceps (see section 5.3.1, Figure 5-5) probably due to the relatively slow flight speed the pigeons experienced.

The muscle-mass specific shortening work did vary significantly with flight mode, with both muscles doing more work to shorten during take-off compared to mid-flight and the biceps also did more shortening work during take-off compared to landing. Robertson and Biewener (2012) noted that during mid-flight the biceps were activated earlier, at the beginning of muscle

shortening, and for longer and predicted that any differences in work generation may be due to differences in duration of muscle activity as may need to alter activity pattern during take-off and landing so as to keep wing motions relative to gravity stereotypical (Robertson and Biewener, 2012), considering the likely difference in the direction and strength of aerodynamic forces acting on the wings as the body angle is likely to be highly pitched during take-off and landing (Robertson and Biewener, 2012). During take-off significantly more work was done by the biceps and scapulotriceps suggesting the importance of elbow flexion at the end of the downstroke through the downstroke-upstroke transition by the biceps to minimise the negative lift generated during the upstroke by reducing the wing area. Whereas the scapulotriceps increase wing area by shortening to extend the elbow at the end of the upstroke into the early downstroke to generate the high lift force required during take-off due to the high induced drag at slow speeds. The differences in muscle shortening work and net work with mode of flight are not reflected in the mechanical power output. This suggests that neuromuscular functioning in terms of power output of these two muscles is stereotypical across the slow flight speeds studied here.

5.4.5 *Summary*

The scapulotriceps and biceps are important wing muscles that are involved in controlling the shape and position of the wing. The scapulotriceps muscle stabilises the flexion of the elbow towards the end of the downstroke and then actively extends the elbow at the end of the upstroke and may also contribute to humeral elevation during the upstroke. The scapulotriceps muscle produces net positive work across all three modes of flight analysed. The biceps muscle serves to stabilise the extension of the elbow at the start of the downstroke and flexes the elbow at the end of the downstroke. Over the wingstroke during take-off, mid-flight and landing, the biceps muscle generates very little muscle-mass specific net work (-1.43, 0.61 and -0.07 mJ respectively). Through part of the wingstroke, the scapulotriceps and biceps muscles act antagonistically, with the time that the scapulotriceps muscle is shortening and producing positive work to extend the elbow during the downstroke, coinciding with the period when the

biceps muscle is being actively lengthened, presumably stabilising the movements of the elbow joint. The scapulotriceps and biceps produce little net mechanical power and work compared to muscles such as the pectoralis which is designed for high power output as these intrinsic wing muscles generate enough work during shortening to move joints but also play a key role in stabilising the elbow and therefore work is also done on the muscles. The function of these muscles in joint stabilisation may explain the differences in work done while shortening and the work done on to the biceps during lengthening with changes in flight mode.

6 General Discussion

The aim of this thesis was to examine the intra- and inter-specific effects of variation in wing morphology on the control of wing shape and wing dynamics on take-off performance and on the mechanical performance of intrinsic wing muscles during a wing stroke. Wing morphology was found to be important predictor of take-off performance, both intra- and inter-specifically, by affecting the lift and acceleration that could be generated directly, and due to the related changes in wing beat kinematics. The mechanical performance and function of the biceps and scapulotriceps during a wing stroke were also determined to increase our understanding on how wing shape and position is controlled as this will affect the forces generated by, and acting upon, the wing during the wing beat. This in turn will influence a bird's ability to meet the varying flight requirements during different modes of flight, demonstrating the importance of understanding the link between the mechanical work and power performed by a muscle, and the aerodynamic requirements that need to be met during flight. Knowledge of the effects of wing morphology and muscle function on wing shape, control and dynamic movement during take-off and other modes of flight may also further the development and performance of flapping unmanned, micro-air vehicles.

6.1 Impacts of variation in wing morphology on take-off performance

The aerodynamics of take-off has been explored in a few species mainly exploring strategies to evade predation using maximal take-off (Gosler et al., 1995; Kullberg et al., 1996; Kullberg et al., 1998; Lee et al., 1996; Lilliendahl, 1997; Lind, 2001; Lind et al., 1999; Lind et al., 2003). Most have compared take-off velocity and angle to see if they traded-off (Witter and Cuthill, 1993), often in a single or small range of species (Swartz et al., 2008). The aim of this study was to examine take-off performance in a way that included a single measure that accounts for changes in acceleration, velocity and angle, as suggested previously (see Hedenstrom, 2003; Swaddle et al., 1999; Williams and Swaddle, 2003), so as to provide an independent measure of

performance (Swaddle et al., 1999). The P_{CoM} does this as it incorporates the power required to increase the rate of change of the potential (angle of elevation) and kinetic (acceleration) energies of the body's CoM. This allows the effect of wing morphology on take-off to be examined in an evolutionary, ecological as well as a behavioural context. The gross morphology in terms of body mass and wing morphology, as well as the associated variation in wing beat kinematics, was also studied intra- (chapter 3) and inter-specifically (chapter 4). This thesis therefore aims to provide a better understand of the aerodynamics of take-off, while also accounting for differences in species that are due to; geometric (Alexander, 2003; Alexander, 2005; Altshuler et al., 2010a; Tobalske, 2007) and dynamic similarity (Alexander, 2003; Alexander, 2005; Taylor et al., 2003), as well as phylogeny (Dudley, 2002; Kaboli et al., 2007; Swartz and Biewener, 1992). All experiments were conducted in the field, using wild birds in their natural environment so species were not habituated (Jackson and Dial, 2011) and responses did not reflect potentially unnatural behaviour or boundary effects that can occur in wind tunnels (Rayner, 1994).

6.1.1 *Intra-specific*

Previously, the variation in the aerodynamics of take-off within a species has focused on variation in body mass (Krams, 2002; Lind and Jakobsson, 2001; Tobalske et al., 2004; Tobalske and Dial, 2000; van den Hout et al., 2010; Zimmer et al., 2010) and moult (Chai et al., 1999; Hedenstrom, 2003; Hedenström, 1998; Hedenstrom and Sunada, 1999; Lind, 2001; Senar et al., 2002a; van den Hout et al., 2010; Williams and Swaddle, 2003; Zimmer et al., 2010) and how this effects wing beat kinematics and take-off strategy (Williams and Swaddle, 2003) in terms of velocity and angle (Kullberg et al., 1996; Kullberg et al., 1998; Lind et al., 1999; Lind et al., 2003; Lind and Jakobsson, 2001; Witter and Cuthill, 1993; Witter et al., 1994; Zimmer et al., 2011).

Chapter 3 offers support to studies that found that natural variation in body mass is not sufficient to result in deficiencies in take-off performance (Kullberg, 1998; Kullberg et al., 1996; Kullberg

et al., 1998). Individuals with small wing area and therefore high wing loading had poorer take-off ability, which may reflect moult as seen previously (Chai et al., 1999; Hedenstrom, 1998; Hedenstrom, 2003; Hedenstrom and Sunada, 1999; Lind, 2001, Senar et al., 2002; van den Hout et al., 2010; Williams and Swaddle, 2003; Zimmer et al., 2010). The blue tits studied also showed that individuals with wings of lower wing loading and aspect ratio varied their wing beat kinematics, increasing their wing beat frequency and downstroke ratio, improving their take-off performance. Higher wing beat frequency may suggest the flight muscles have a higher contraction frequency (Askew and Marsh 1998; Morris and Askew, 2010b) whereas greater downstroke ratio could indicate that more of a muscle contraction cycle is spent shortening and doing mechanical work (Morris and Askew, 2010b; Pennycuick, 2001), both increasing the mechanical power output. If more power is available from the muscles then there may be surplus power the aerodynamic power requirements have been met which can be used to accelerate and climb during take-off. This study included a large number of individuals and an independent measure of take-off ability, demonstrating that even small intra-specific variation in wing morphology and wing beat kinematics can have important impacts on the aerodynamic performance of birds during take-off.

6.1.2 *Inter-specific*

Inter-specific variation in take-off performance was examined phylogenetically within the order, Passeriformes (chapter 4). Evolutionary relatedness did affect the species morphological traits demonstrating the importance of examining performance within a phylogenetic context. After controlling for the effects of phylogeny, inter-specific variation in wing morphology affected take-off ability. Larger species unexpectedly had the greater take-off performance, possibly due to their lower P_{ind} requirements than expected for their body size. This meant they could devote more of their available power to accelerating and elevating their body's CoM. The species studied may have varied in their muscle masses that could have affected their take-off performance but was outside the scope of this study. Having larger, shorter wings improved take-off performance as more energy could be imparted to the air to increase a birds' climbing

and acceleration performance. Larger species of greater body mass also had larger wing areas and therefore lower relative wing loading than expected by geometric similarity, relative wing loading scaling with body mass$^{-0.07 \pm 0.02}$, instead of being independent of body mass (Norberg, 1990). Species such as the coal tit and great tit that combined a low relative wing loading with a low aspect ratio were able to use more of their available power to increase the rate of change of the potential and kinetic energy of their body's centre of mass.

Variation in wing beat kinematics reflected differences in wing morphology, showing the importance of examining both wing shape and dynamics when trying to elucidate what factors are important for take-off. Higher wing beat amplitude and stroke plane angle were related to lower wing loading and aspect ratio, as well as improved take-off performance. High wing beat amplitude may reflect higher motor recruitment within the flight muscles increasing the mechanical power available (Altshuler et al., 2010b) and increase wing velocity increasing lift production (Lehmann and Dickinson, 2001). Species averaged a stroke plane angle near 45^{o} may increase lift and thrust by forcing air downwards and backwards respectively (Berg and Biewener, 2008; Berg and Biewener, 2010). Wing beat frequency was positively allometric so larger species conformed to dynamic rather than geometric similarity therefore maintaining propulsion efficiency. This is shown by the average Strouhal number for the species studied, 0.31, being greater than 0.2 but lower than 0.4 and therefore within the optimal range for propulsion efficiency (Taylor et al., 2003). Inter-specific variation in take-off performance is reflected by differences in wing morphology and associated changes in wing beat kinematics.

Species with larger, broader wings had improved take-off performance. This study demonstrates the importance of considering geometric similarity as the relationship between relative wing loading, aspect ratio and body size was negatively allometric with the higher take-off performance of larger species potentially due to the greater lift and acceleration generated by their wings that were larger and broader than predicted by geometric similarity. This study also demonstrates the importance of including evolutionary relationships when trying to determine the effects of wing morphology and wing dynamics on flight performance as there is a positive relationship between take-off power and relative wing loading when phylogeny is not

accounted for, whereas the inverse relationship is observed when phylogenetic relationships are included.

6.2 Mechanical function of wing muscles and mode of flight

This is the first study to combine information from *in vivo* studies of intrinsic wing muscle strain and activity patterns, to determine muscle mechanical function by calculating mechanical work and power *in vitro* (chapter 5). The biceps and scapulotriceps work to control the shape and position of the wing by; controlling elbow flexion and extension when doing positive work and shortening, and by stabilising the elbow by absorbing energy during active muscle lengthening, therefore doing negative work, respectively. It is also demonstrated that the function and mechanical performance of the biceps and scapulotriceps are stereotypical across flight mode in terms of the mechanical power output, but the work done onto the biceps muscle varied with flight mode, possibly suggesting that the muscles role in elbow stabilisation may vary with flight mode.

An understanding of these two skeletal muscles improves are knowledge of their mechanical function during different locomotive tasks and suggest that homologous muscles in other vertebrates may function similarly in a stereotypical manner. As the biceps work varied with flight mode, this demonstrates the importance of calculating muscular work as well as mechanical power when studying muscle function as the role of a muscle may vary relative to the task being performed, even if the net mechanical power output does not differ significantly. *In vitro* analysis of muscular performance can be problematic in some species, such as humans. Birds are clearly a good vertebrate model for these types of muscle physiological questions due to their; homology of form, available knowledge of *in vivo* muscle action across a range of locomotive tasks, ease of obtaining and housing certain species, such as pigeon and chickens, and, in some cases, the size of muscle may be sufficient for analysis of both mechanical performance and efficiency. Combining studies of the mechanical function of muscles and muscular efficiency of muscles during different locomotive tasks should be a focus of future research and the use of birds could help to achieve this goal as muscle efficiency could

potentially be measured simultaneously with muscle work. This could be done by measuring heat production during muscular contraction with metal-film thermopiles (Woledge et al., 1985) or analysing oxygen consumption using polarographic respirometry (Harwood et al., 2002). The function of other intrinsic wing muscles, such as the humerotriceps, should also be examined.

References

Alerstam, T., Rosen, M., Backman, J., Ericson, P. G. P. and Hellgren, O. (2007). Flight speeds among bird species: Allometric and phylogenetic effects. *Plos Biology* **5**, 1656-1662.

Alexander, D. E. (2002). Nature's Flyers: Birds, Insects, and the Biomechanics of Flight. Baltimore: The John Hopkins University Press.

Alexander, R. M. (2003). Principles of animal locomotion. New Jersey, US: Princeton University Press.

Alexander, R. M. (2005). Models and the scaling of energy costs for locomotion. *Journal of Experimental Biology* **208**, 1645-1652.

Altringham, J. D. (1996). Bats: Biology and Behaviour. Oxford: Oxford University Press.

Altshuler, D. L. and Dudley, R. (2003). Kinematics of hovering hummingbird flight along simulated and natural elevational gradients. *Journal of Experimental Biology* **206**, 3139-3147.

Altshuler, D. L., Dudley, R., Heredia, S. M. and McGuire, J. A. (2010a). Allometry of hummingbird lifting performance. *Journal of Experimental Biology* **213**, 725-734.

Altshuler, D. L., Welch, K. C., Cho, B. H., Welch, D. B., Lin, A. F., Dickson, W. B. and Dickinson, M. H. (2010b). Neuromuscular control of wingbeat kinematics in Anna's hummingbirds (Calypte anna). *Journal of Experimental Biology* **213**, 2507-2514.

Askew, G. N. and Ellerby, D. J. (2007). The mechanical power requirements of avian flight. *Biology Letters* **3**, 445-448.

Askew, G. N. and Marsh, R. L. (1997). The effects of length trajectory on the mechanical power output of mouse skeletal muscles. *Journal of Experimental Biology* **200**, 3119-3131.

Askew, G. N. and Marsh, R. L. (1998). Optimal shortening velocity (V/Vmax) of skeletal muscle during cyclical contractions: length-force effects and velocity-dependent activation and deactivation. *Journal of Experimental Biology* **201**, 1527-40.

Askew, G. N. and Marsh, R. L. (2001). The mechanical power output of the pectoralis muscle of blue-breasted quail (Coturnix chinensis): the in vivo length cycle and its implications for muscle performance. *Journal of Experimental Biology* **204**, 3587-3600.

Askew, G. N. and Marsh, R. L. (2002). Muscle designed for maximum short-term power output: Quail flight muscle. *Journal of Experimental Biology* **205**, 2153-2160.

Askew, G. N., Marsh, R. L. and Ellington, C. P. (2001). The mechanical power output of the flight muscles of blue-breasted quail (Coturnix chinensis) during take-off. *Journal of Experimental Biology* **204**, 3601-3619.

Bednekoff, P. A. and Houston, A. I. (1994). Dynamic-Models Of Mass-Dependent Predation, Risk-Sensitive Foraging, And Premigratory Fattening In Birds. *Ecology* **75**, 1131-1140.

Berg, A. M. and Biewener, A. A. (2008). Kinematics and power requirements of ascending and descending flight in the pigeon (Columba livia). *Journal of Experimental Biology* **211**, 1120-1130.

Berg, A. M. and Biewener, A. A. (2010). Wing and body kinematics of takeoff and landing flight in the pigeon (Columba livia). *Journal of Experimental Biology* **213**, 1651-1658.

Biewener, A. A. (1998). Muscle function in vivo: A comparison of muscles used for elastic energy savings versus muscles used to generate mechanical power. *American Zoologist* **38**, 703-717.

Biewener, A. A. (2011). Muscle function in avian flight: achieving power and control. *Philosophical Transactions of the Royal Society B-Biological Sciences* **366**, 1496-1506.

Biewener, A. A., Dial, K. P. and Goslow, G. E. (1992). Pectoralis muscle force and power during flight in the starling. *Journal of Experimental Biology* **164**, 1-18.

Brewer, M. L. and Hertel, F. (2007). Wing morphology and flight behavior of pelecaniform seabirds. *Journal Of Morphology* **268**, 866-877.

Burns, J. and Ydenberg, R. (2002). The effects of wing loading and gender on the escape flights of least sandpipers (Calidris minutilla) and western sandpipers (Calidris mauri). *Behavioral Ecology and Sociobiology* **52**, 128-136.

Carr, J. A., Ellerby, D. J. and Marsh, R. L. (2011). Differential segmental strain during active lengthening in a large biarticular thigh muscle during running. *The Journal of experimental biology* **214**, 3386-3395.

Carruthers, A., Thomas, A. and Taylor, G. (2008). Flow control in the wings of a Steppe eagle Aquila nipalensis: Automatic aeroelastic devices. *Comparative Biochemistry And Physiology A-Molecular & Integrative Physiology* **150**, S76-S77.

Carruthers, A. C., Thomas, A. L. R. and Taylor, G. K. (2007). Automatic aeroelastic devices in the wings of a steppe eagle Aquila nipalensis. *Journal of Experimental Biology* **210**, 4136-4149.

Chai, P. (1997). Hummingbird hovering energetics during moult of primary flight feathers. *Journal of Experimental Biology* **200**, 1527-1536.

Chai, P., Altshuler, D. L., Stephens, D. B. and Dillon, M. E. (1999). Maximal horizontal flight performance of hummingbirds: Effects of body mass and molt. *Physiological And Biochemical Zoology* **72**, 145-155.

Crandell, K. E. and Tobalske, B. W. (2011). Aerodynamics of tip-reversal upstroke in a revolving pigeon wing. *Journal of Experimental Biology* **214**, 1867-1873.

Dial, K. P. (1992). Activity patterns of the wing muscles of the pigeon (Columba livia) during different modes of flight. *Journal of Experimental Zoology* **262**, 357-373.

Dial, K. P. and Biewener, A. A. (1993). Pectoralis muscle force and power output during different modes of flight in pigeons (*Columbia livia*). *Journal of Experimental Biology* **176**, 31-54.

Dial, K. P., Biewener, A. A., Tobalske, B. W. and Warrick, D. R. (1997). Mechanical power output of bird flight. *Nature* **390**, 67-70.

Dial, K. P., Goslow, G. E. and Jenkins, F. A. (1991). The functional anatomy of the shoulder in the European starling (*Sturnus vulagaris*) *Journal Of Morphology* **207**, 327-344.

Dietz, M. W., Piersma, T., Hedenstrom, A. and Brugge, M. (2007). Intraspecific variation in avian pectoral muscle mass: constraints on maintaining manoeuvrability with increasing body mass. *Functional Ecology* **21**, 317-326.

Dillon, M. E. and Dudley, R. (2004). Allometry of maximum vertical force production during hovering flight of neotropical orchid bees (Apidae: Euglossini). *Journal of Experimental Biology* **207**, 417-425.

Dudley, R. (2002). Mechanisms and implications of animal flight maneuverability. *Integrative And Comparative Biology* **42**, 135-140.

Earls, K. D. (2000). Kinematics and mechanics of ground take-off in the starling Sturnis vulgaris and the quail Coturnix coturnix. *Journal of Experimental Biology* **203**, 725-739.

Ellerby, D. J. and Askew, G. N. (2007). Modulation of flight muscle power output in budgerigars Melopsittacus undulatus and zebra finches Taeniopygia guttata: in vitro muscle performance. *Journal of Experimental Biology* **210**, 3780-3788.

Ellington, C. P. (1984a). The Aerodynamics of Hovering Insect Flight. III. Kinematics. *Philosophical Transactions of the Royal Society of London. B, Biological Sciences* **305**, 41-78.

Ellington, C. P. (1984b). The Aerodynamics of Hovering Insect Flight. VI. Lift and Power Requirements. *Philosophical Transactions of the Royal Society of London. B, Biological Sciences* **305**, 145-181.

Ellington, C. P. (1991). Limitations on Animal Flight Performance. *Journal of Experimental Biology* **160**, 71-91.

Emrich, M. A., Clare, E. L., Symondson, W. O., Koenig, S. E. and Fenton, M. B. (2013). Resource partitioning by insectivorous bats in Jamaica. *Molecular Ecology* **23**, 3648-3656.

Felsenstein, J. (1985). Phylogenies and the comparative method. *American Naturalist* **125**, 1-15.

Fernandez, G. and Lank, D. B. (2007). Variation in the wing morphology of Western Sandpipers (Calidris mauri) in relation to sex, age class, and annual cycle. *Auk* **124**, 1037-1046.

Fernandez, M. J., Springthorpe, D. and Hedrick, T. L. (2012). Neuromuscular and biomechanical compensation for wing asymmetry in insect hovering flight. *Journal of Experimental Biology* **215**, 3631-3638.

Forstmeier, W. and Kessler, A. (2001). Morphology and foraging behaviour of Siberian Phylloscopus warblers. *Journal of Avian Biology* **32**, 127-138.

Gardiner, J. D. and Nudds, R. L. (2011). No apparent ecological trend to the flight-initiating jump performance of five bat species. *The Journal of Experimental Biology* **214**, 2182-2188.

Garland, T., Harvey, P. H. and Ives, A. R. (1992). Procedures for the analysis comparative data using phylogenetically independent contrasts. *Systematic Biology* **41**, 18-32.

Girgenrath, M. and Marsh, R. (1997). In vivo performance of trunk muscles in tree frogs during calling. *Journal of Experimental Biology* **200**, 3101-3108.

Gosler, A. G., Greenwood, J. J. D. and Perrins, C. (1995). Predation risk and the cost of being fat. *Nature* **377**, 621-623.

Harwood, C. L., Young, I. S. and Altringham, J. D. (2002). How the efficiency of rainbow trout (Oncorhynchus mykiss) ventricular muscle changes with cycle frequency. *Journal of Experimental Biology* **205**, 697-706.

Hatze, H. (1988). High-precision three-dimensional photogrammetric calibration and object space reconstruction using a modified DLT-approach. *Journal of Biomechanics* **21**, 533-538.

Hedenstrom, A. (2002). Aerodynamics, evolution and ecology of avian flight. *Trends In Ecology & Evolution* **17**, 415-422.

Hedenstrom, A. (2003). Flying with holey wings. *Journal of Avian Biology* **34**, 324-327.

Hedenstrom, A. (2008). Power and metabolic scope of bird flight: a phylogenetic analysis of biomechanical predictions. *Journal of Comparative Physiology a-Neuroethology Sensory Neural and Behavioral Physiology* **194**, 685-691.

Hedenström, A. (1998). The Relationship between wing area and raggedness during molt in the willow warbler and other passerines (La Relación Entre el Área del Ala y la Desaliñez Durante la Muda de Phylloscopus trochilus y de Otras Paserinas). *Journal of Field Ornithology* **69**, 103-108.

Hedenström, A., Johansson, L. C., Wolf, M., von Busse, R., Winter, Y. and Spedding, G. R. (2007). Bat Flight Generates Complex Aerodynamic Tracks. *Science* **316**, 894-897.

Hedenstrom, A. and Sunada, S. (1999). On the aerodynamics of moult gaps in birds. *Journal of Experimental Biology* **202**, 67-76.

Hedrick, T. L. (2008). Software techniques for two- and three-dimensional kinematic measurements of biological and biomimetic systems. *Bioinspiration & Biomimetics* **3**.

Hedrick, T. L. and Biewener, A. A. (2007). Low speed maneuvering flight of the rose-breasted cockatoo (Eolophus roseicapillus). I. Kinematic and neuromuscular control of turning. *Journal of Experimental Biology* **210**, 1897-1911.

Hedrick, T. L., Usherwood, J. R. and Biewener, A. A. (2004). Wing inertia and whole-body acceleration: an analysis of instantaneous aerodynamic force production in cockatiels (Nymphicus hollandicus) flying across a range of speeds. *Journal of Experimental Biology* **207**, 1689-1702.

Heers, A. M., Tobalske, B. W. and Dial, K. P. (2011). Ontogeny of lift and drag production in ground birds. *J Exp Biol* **214**, 717-725.

Holt, N. C. and Askew, G. N. (2012). Locomotion on a slope in leaf-cutter ants: metabolic energy use, behavioural adaptations and the implications for route selection on hilly terrain. *The Journal of experimental biology* **215**, 2545-2550.

Hoppeler, H. and Flück, M. (2002). Normal mammalian skeletal muscle and its phenotypic plasticity. *Journal of Experimental Biology* **205**, 2143-2152.

Iriarte-Diaz, J., Riskin, D. K., Breuer, K. S. and Swartz, S. M. (2012). Kinematic Plasticity during Flight in Fruit Bats: Individual Variability in Response to Loading. *Plos One* **7**.

Iriarte-Diaz, J., Riskin, D. K., Willis, D. J., Breuer, K. S. and Swartz, S. M. (2011). Whole-body kinematics of a fruit bat reveal the influence of wing inertia on body accelerations. *Journal of Experimental Biology* **214**, 1546-1553.

Iriarte-Diaz, J. and Swartz, S. M. (2008). Kinematics of slow turn maneuvering in the fruit bat Cynopterus brachyotis. *Journal of Experimental Biology* **211**, 3478-3489.

Jackson, B. E. (2009). The allometry of bird flight performance. In *Division of Biological Sciences*, vol. Doctor of Philosophy, pp. 111. Missoula, Montana, USA: Montana.

Jackson, B. E. and Dial, K. P. (2011). Scaling of mechanical power output during burst escape flight in the Corvidae. *Journal of Experimental Biology* **214**, 452-461.

Jenni, L. and Winkler, R. (1994). Moult and Ageing of European Passerines. London: Academic Press.

Josephson, R. K. (1985). Mechanical power output from striated muscle during cyclic contraction. *Journal of Experimental Biology* **114**, 493-512.

Josephson, R. K. (1993). Contraction dynamics and power output of skeletal muscle. *Annual Review of Physiology* **55**, 527-546.

Kaboli, M., Aliabadian, M., Guillaumet, A., Roselaar, C. S. and Prodon, R. (2007). Ecomorphology of the wheatears (genus Oenanthe). *Ibis* **149**, 792-805.

Krams, I. (2002). Mass-dependent take-off ability in wintering great tits (Parus major): comparison of top-ranked adult males and subordinate juvenile females. *Behavioral Ecology and Sociobiology* **51**, 345-349.

Kullberg, C. (1998). Does diurnal variation in body mass affect take-off ability in wintering willow tits? *Animal Behaviour* **56**, 227-233.

Kullberg, C., Fransson, T. and Jakobsson, S. (1996). Impaired predator evasion in fat blackcaps (Sylvia atricapilla). *Proceedings of the Royal Society of London Series B-Biological Sciences* **263**, 1671-1675.

Kullberg, C., Houston, D. C. and Metcalfe, N. B. (2002). Impaired flight ability - a cost of reproduction in female blue tits. *Behavioral Ecology* **13**, 575-579.

Kullberg, C., Jakobsson, S. and Fransson, T. (1998). Predator-induced take-off strategy in great tits (Parus major). *Proceedings of the Royal Society of London Series B-Biological Sciences* **265**, 1659-1664.

Lee, S. J., Witter, M. S., Cuthill, I. C. and Goldsmith, A. R. (1996). Reduction in escape performance as a cost of reproduction in gravid starlings, Sturnus vulgaris. *Proceedings of the Royal Society of London Series B-Biological Sciences* **263**, 619-623.

Lehmann, F. O. and Dickinson, M. H. (2001). The production of elevated flight force compromises manoeuvrability in the fruit fly Drosophila melanogaster. *Journal of Experimental Biology* **204**, 627-635.

Lilliendahl, K. (1997). The effect of predator presence on body mass in captive greenfinches. *Animal Behaviour* **53**, 75-81.

Lind, J. (2001). Escape right in moulting tree sparrows (Passer montanus). *Functional Ecology* **15**, 29-35.

Lind, J., Fransson, T., Jakobsson, S. and Kullberg, C. (1999). Reduced Take-Off Ability in Robins (Erithacus rubecula) Due to Migratory Fuel Load. *Behavioral Ecology and Sociobiology* **46**, 65-70.

Lind, J., Hollen, L., Smedberg, E., Svensson, U., Vallin, A. and Jakobsson, S. (2003). Detection distance influences escape behaviour in two parids, Parus major and P. caeruleus. *Journal of Avian Biology* **34**, 233-236.

Lind, J. and Jakobsson, S. (2001). Body building and concurrent mass loss: flight adaptations in tree sparrows. *Proceedings Of The Royal Society Of London Series B-Biological Sciences* **268**, 1915-1919.

Maddison, W. and Maddison, D. (2007). Mesquite: a modular system for evolutionary analyses. Version 1.11, 2006.

Maddison, W. and Maddison, D. (2010). Mesquite: a modular system for evolutionary analysis. Version 2.6. 2009. *Mesquite website. Available at mesquiteproject. org/mesquite/mesquite. html. Accessed March* **23**.

Marchetti, K., Price, T. and Richman, A. (1995). Correlates of wing morphology with foraging behavior and migration distance in the genus Phylloscopus. *Journal of Avian Biology* **26**, 177-181.

Marsh, R. L. (1984). Adaptations of the gray catbird Dumetella carolinensis to long-distance migration - Flight-muscle hypertrophy associated with elevated body mass. *Physiological Zoology* **57**, 105-117.

Marsh, R. L. (1999). How muscles deal with real-world loads: The influence of length trajectory on muscle performance. *Journal of Experimental Biology* **202**, 3377-3385.

Marsh, R. L., Olson, J. M. and Guzik, S. K. (1992). Mechanical performance of scallop adductor muscle during swimming. *Nature* **357**, 411-413.

Midford, P., Garland Jr, T. and Maddison, W. (2005). PDAP package of Mesquite. Version 1.07. *Website http://www.mesquiteproject.org/pdap_mesquite/index.html [accessed 25 September 2007]*.

Morris, C. R. and Askew, G. N. (2010a). Comparison between mechanical power requirements of flight estimated using an aerodynamic model and in vitro muscle performance in the cockatiel (Nymphicus hollandicus). *Journal of Experimental Biology* **213**, 2781-2787.

Morris, C. R. and Askew, G. N. (2010b). The mechanical power output of the pectoralis muscle of cockatiel (Nymphicus hollandicus): the in vivo muscle length trajectory and activity patterns and their implications for power modulation. *Journal of Experimental Biology* **213**, 2770-2780.

Muijres, F. T., Johansson, L. C., Winter, Y. and Hedenstrom, A. (2011). Comparative aerodynamic performance of flapping flight in two bat species using time-resolved wake visualization. *Journal of the Royal Society Interface* **8**, 1418-1428.

Nam, H. Y., Choi, C. Y., Park, J. G., Hong, G. P., Won, I. J., Kim, S. J., Bing, G. C. and Chae, H. Y. (2011). Protandrous migration and variation in morphological characters in Emberiza buntings at an East Asian stopover site. *Ibis* **153**, 494-501.

Norberg, U. M. (1990). Vertebrate Flight: mechanics, physiology, morphology, ecology and evolution. Berlin: Springer-Verlag.

Norberg, U. M. (1995). How a long tail and changes in mass and wing shape affect the cost for flight in animals. *Functional Ecology* **9**, 48-54.

Norberg, U. M. and Rayner, J. M. V. (1987). Ecological morphology and flight in bats (Mammalia, Chiroptera)- wing adaptations flight performance foraging strategy and echolocation. *Philosophical Transactions of the Royal Society of London B Biological Sciences* **316**, 335-427.

Norberg, U. M. L. (2002). Structure, form, and function of flight in engineering and the living world. *Journal Of Morphology* **252**, 52-81.

Park, K. J., Rosen, M. and Hedenstrom, A. (2001). Flight kinematics of the barn swallow (Hirundo rustica) over a wide range of speeds in a wind tunnel. *Journal of Experimental Biology* **204**, 2741-2750.

Pennycuick, C., Klaassen, M., Kvist, A., Lindstr, Ouml, M and Aring. (1996). Wingbeat frequency and the body drag anomaly: wind-tunnel observations on a thrush

nightingale (Luscinia luscinia) and a teal (Anas crecca). *Journal of Experimental Biology* **199**, 2757-65.

Pennycuick, C. J. (1990). Predicting Wingbeat Frequency and Wavelength of Birds. *Journal of Experimental Biology* **150**, 171-185.

Pennycuick, C. J. (2001). Speeds and wingbeat frequencies of migrating birds compared with calculated benchmarks. *Journal of Experimental Biology* **204**, 3283-3294.

Pennycuick, C. J. (2008). Modelling the Flying Bird. Massachusetts: Academic Press, Elsevier.

Pennycuick, C. J., Fuller, M. R. and McAllister, L. (1989). Climbing Performance of Harris' Hawks (Parabuteo Unicinctus) with Added Load: Implications for Muscle Mechanics and for Radiotracking. *Journal of Experimental Biology* **142**, 17-29.

Pennycuick, C. J., Heine, C. E., Kirkpatrick, S. J. and Fuller, M. R. (1992). The Profile Drag of a Hawk'S Wing, Measured by Wake Sampling in a Wind Tunnel. *Journal of Experimental Biology* **165**, 1-19.

Perez-Tris, J. and Telleria, J. L. (2001). Age-related variation in wing shape of migratory and sedentary Blackcaps Sylvia atricapilla. *Journal of Avian Biology* **32**, 207-213.

Peterson, R., Mountfort, G. and Hollom, P. A. D. (2004). Birds of Britain and Europe. London: Harper Collins.

Provini, P., Tobalske, B. W., Crandell, K. E. and Abourachid, A. (2012). Transition from leg to wing forces during take-off in birds. *The Journal of Experimental Biology* **215**, 4115-4124.

Rayner, J. M. (1999). Estimating power curves of flying vertebrates. *Journal of Experimental Biology* **202**, 3449-3461.

Rayner, J. M. V. (1979). A New Approach to Animal Flight Mechanics. *Journal of Experimental Biology* **80**, 17-54.

Rayner, J. M. V. (1994). Dynamics of the vortex wakes of flying and swimming vertebrates. In *Symposia of the Society for Experimental Biology: Biological Fluid Dynamics*, vol. 49 eds. C. P. Ellington and T. J. Pedley), pp. 131-155. University of Leeds, UK: The Company of Biologists Ltd.

Rayner, J. M. V. (1995). Flight mechanics and constraints on flight performance. *Israel Journal of Zoology* **41**, 321-342.

Rayner, J. M. V. and Swaddle, J. P. (2000). Aerodynamics and behaviour of moult and take-off in birds. In *Biomechanics in Animal Behaviour*, eds. D. P and B. R. W), pp. 125-157. Oxford, UK: Bios.

Riskin, D. K., Bergou, A., Breuer, K. S. and Swartz, S. M. (2012). Upstroke wing flexion and the inertial cost of bat flight. *Proceedings of the Royal Society B: Biological Sciences*.

Robertson, A. M. B. and Biewener, A. A. (2012). Muscle function during takeoff and landing flight in the pigeon (Columba livia). *The Journal of experimental biology* **215**, 4104-4114.

Senar, J. C., Domenech, J. and Uribe, F. (2002a). Great tits (Parus major) reduce body mass in response to wing area reduction: a field experiment. *Behavioral Ecology* **13**, 725-727.

Senar, J. C., Domènech, J. and Uribe, F. (2002b). Great tits (Parus major) reduce body mass in response to wing area reduction: a field experiment. *Behavioral Ecology* **13**, 725-727.

Shang, J. K., Combes, S. A., Finio, B. M. and Wood, R. J. (2009). Artificial insect wings of diverse morphology for flapping-wing micro air vehicles. In *Bioinspiration & Biomimetics*, vol. 4, pp. 036002 (6pp).

Sibley, C. and Ahlquist, J. Phylogeny and classification of birds, 1990. *Yale University, New Haven, CT*.

Slikas, B., Sheldon, F. H. and Gill, F. B. (1996). Phylogeny of Titmice (Paridae): I. Estimate of Relationships among Subgenera Based on DNA-DNA Hybridization. *Journal of Avian Biology* **27**, 70-82.

Sokoloff, A. J., Gray-Chickering, J., Harry, J. D., Poore, S. O. and Goslow, G. E. (2001). The function of the supracoracoideus muscle during takeoff in the European starling (Sturnus vulgaris): Maxheinz Sy revisited. New Haven: Peabody Museum Natural Historyyale Univ.

Spedding, G. and McArthur, J. (2010). Span efficiencies of wings at low Reynolds numbers. *Journal of Aircraft* **47**, 120-128.

Svensson, L. (1992). {Identification Guide to European Passerines}.

Swaddle, J. P., Williams, E. V. and Rayner, J. M. V. (1999). The effect of simulated flight feather moult on escape take-off performance in starlings. *Journal of Avian Biology* **30**, 351-358.

Swaddle, J. P. and Witter, M. S. (1997). The effects of molt on the flight performance, body mass, and behavior of European starlings (Sturnus vulgaris): An experimental approach. *Canadian Journal of Zoology* **75**, 1135-1146.

Swartz, S. M. and Biewener, A. (1992). Shape and Scaling. In *Biomechanics-Structures and Systems: A Practical Approach*, (ed. A. Biewener), pp. 21-43. Oxford: Oxford University Press.

Swartz, S. M., Breuer, K. S. and Willis, D. J. (2008). Aeromechanics in aeroecology: flight biology in the aerosphere. *Integrative And Comparative Biology* **48**, 85-98.

Swoap, S. J., Johnson, T. P., Josephson, R. K. and Bennett, A. F. (1993). Temperature, muscle power output and limitations on burst locomotor performance of the lizard Dipsosaurus dorsalis. *The Journal of experimental biology* **174**, 185-197.

Taylor, G. K., Nudds, R. L. and Thomas, A. L. R. (2003). Flying and swimming animals cruise at a Strouhal number tuned for high power efficiency. *Nature* **425**, 707-711.

Telleria, J. L. and Carbonell, R. (1999). Morphometric variation of five Iberian Blackcap Sylvia atricapilla populations. *Journal of Avian Biology* **30**, 63-71.

Tian, X. D., Iriarte-Diaz, J., Middleton, K., Galvao, R., Israeli, E., Roemer, A., Sullivan, A., Song, A., Swartz, S. and Breuer, K. (2006). Direct measurements of the kinematics and dynamics of bat flight. *Bioinspiration & Biomimetics* **1**, S10-S18.

Tobalske, B. W. (1996). Scaling of muscle composition, wing morphology, and intermittent flight behavior in woodpeckers. *Auk* **113**, 151-177.

Tobalske, B. W. (2000). Biomechanics and physiology of gait selection in flying birds. *Physiological And Biochemical Zoology* **73**, 736-750.

Tobalske, B. W. (2007). Biomechanics of bird flight. *Journal of Experimental Biology* **210**, 3135-3146.

Tobalske, B. W., Altshuler, D. L. and Powers, D. R. (2004). Take-off mechanics in hummingbirds (Trochilidae). *Journal of Experimental Biology* **207**, 1345-1352.

Tobalske, B. W. and Biewener, A. A. (2008). Contractile properties of the pigeon supracoracoideus during different modes of flight. *Journal of Experimental Biology* **211**, 170-179.

Tobalske, B. W., Biewener, A. A., Warrick, D. R., Hedrick, T. L. and Powers, D. R. (2010). Effects of flight speed upon muscle activity in hummingbirds. *Journal of Experimental Biology* **213**, 2515-2523.

Tobalske, B. W. and Dial, K. P. (2000). Effects of body size on take-off flight performance in the Phasianidae (Aves). *Journal of Experimental Biology* **203**, 3319-3332.

Triggs, B., McLauchlan, P. F., Hartley, R. I. and Fitzgibbon, A. W. (2000). Bundle adjustment—a modern synthesis. In *Vision algorithms: theory and practice*, pp. 298-372: Springer.

Trizila, P., Kang, C. K., Aono, H., Shyy, W. and Visbal, M. (2011). Low-Reynolds-Number Aerodynamics of a Flapping Rigid Flat Plate. *Aiaa Journal* **49**, 806-823.

Tucker, V. A. and Heine, C. (1990). Aerodynamics of gliding flight in a harris hawk, Parabuteo unicinctus. *Journal of Experimental Biology* **149**, 469-489.

Usherwood, J. R. (2009a). The aerodynamic forces and pressure distribution of a revolving pigeon wing. *Experiments in Fluids* **46**, 991-1003.

Usherwood, J. R. (2009b). Inertia may limit efficiency of slow flapping flight, but mayflies show a strategy for reducing the power requirements of loiter. *Bioinspiration & Biomimetics* **4**, Article No.: 015003.

Usherwood, J. R., Hedrick, T. L. and Biewener, A. A. (2003). The aerodynamics of avian take-off from direct pressure measurements in Canada geese (Branta canadensis). *Journal of Experimental Biology* **206**, 4051-4056.

van den Hout, P. J., Mathot, K. J., Maas, L. R. M. and Piersma, T. (2010). Predator escape tactics in birds: linking ecology and aerodynamics. *Behavioral Ecology* **21**, 16-25.

Vanhooydonck, B., Herrel, A., Gabela, A. and Podos, J. (2009). Wing shape variation in the medium ground finch (Geospiza fortis): an ecomorphological approach. *Biological Journal Of The Linnean Society* **98**, 129-138.

Wakeling, J. M. and Ellington, C. P. (1997a). Dragonfly .3. Lift and power requirements. *Journal of Experimental Biology* **200**, 583-600.

Wakeling, J. M. and Ellington, C. P. (1997b). Dragonfly flight .2. Velocities, accelerations and kinematics of flapping flight. *Journal of Experimental Biology* **200**, 557-582.

Warrick, D. R. (1998). The turning- and linear-maneuvering performance of birds: the cost of efficiency for coursing insectivores. *Canadian Journal Of Zoology-Revue Canadienne De Zoologie* **76**, 1063-1079.

Williams, E. V. and Swaddle, J. P. (2003). Moult, Flight Performance and Wingbeat Kinematics during Take-Off in European Starlings Sturnus vulgaris. *Journal of Avian Biology* **34**, 371-378.

Williamson, M. R., Dial, K. P. and Biewener, A. A. (2001). Pectoralis muscle performance during ascending and slow level flight in mallards (Anas platyrhynchos). *Journal of Experimental Biology* **204**, 495-507.

Winkler, H. and Preleuthner, M. (1999). The ecomorphology of Neotropical frugivores. *Acta Ornithologica (Warsaw)* **34**, 141-148.

Witter, M. S. and Cuthill, I. C. (1993). The ecological costs of avian fat storage *Philosophical Transactions of the Royal Society of London Series B-Biological Sciences* **340**, 73-92.

Witter, M. S., Cuthill, I. C. and Bonser, R. H. C. (1994). Experimental investigations of mass-dependent predation risk in the European starling, Sturnus vulgaris. *Animal Behaviour* **48**, 201-222.

Woledge, R. C., Curtin, N. C. and Homsher, E. (1985). Energetic aspects of muscle contraction. London: Academic Press.

Zhang, L., Liang, B., Parsons, S., Wei, L. and Zhang, S. (2007). Morphology, echolocation and foraging behaviour in two sympatric sibling species of bat (Tylonycteris pachypus and Tylonycteris robustula) (Chiroptera : Vespertilionidae). *Journal of Zoology* **271**, 344-351.

Zimmer, C., Boos, M., Petit, O. and Robin, J. P. (2010). Body mass variations in disturbed mallards Anas platyrhynchos fit to the mass-dependent starvation-predation risk trade-off. *Journal of Avian Biology* **41**, 637-644.

Zimmer, C., Boos, M., Poulin, N., Gosler, A., Petit, O. and Robin, J.-P. (2011). Evidence of the Trade-Off between Starvation and Predation Risks in Ducks. *Plos One* **6**, 11.